

Carbon TerraVault II

Class VI Permit Application

Narrative Report

4-25-2022

Submitted to:

U.S. Environmental Protection Agency Region 9

San Francisco, CA

Prepared by:



27200 Tourney Road, Suite 200
Santa Clarita, CA 91355
(888) 848-4754

Table of Contents

1.0 Project Background and Contact Information	1
2.0 Site Characterization.....	3
2.1 Regional Geology, Hydrogeology, and Local Structural Geology [40 CFR 146.82(a)(3)(vi)] .	3
2.1.1 Field History	3
2.1.2 Geology Overview	4
2.1.3 Geological Sequence	9
2.2 Maps and Cross Sections of the AoR [40 CFR 146.82(a)(2), 146.82(a)(3)(i)]	10
2.2.1 Data	10
2.2.2 Stratigraphy.....	14
2.2.3 Map of the Area of Review	18
2.3 Faults and Fractures [40 CFR 146.82(a)(3)(ii)]	20
2.3.1 Overview	20
2.4 Injection and Confining Zone Details [40 CFR 146.82(a)(3)(iii)]	21
2.4.1 Mineralogy	21
2.4.2 Porosity and Permeability.....	23
2.4.3 Confining Zone Capillary Pressure	28
2.4.4 Depth and Thickness	28
2.4.5 Structure Maps	29
2.4.6 Isopach Maps	29
2.5 Geomechanical and Petrophysical Information [40 CFR 146.82(a)(3)(iv)]	30
2.5.1 Caprock Ductility	30
2.5.2 Stress Field	32
2.6 Seismic History [40 CFR 146.82(a)(3)(v)]	36
2.7 Hydrologic and Hydrogeologic Information [40 CFR 146.82(a)(3)(vi), 146.82(a)(5)]	39
2.7.1 Hydrologic Information.....	40
2.7.2 Base of Fresh Water and Base of USDWs	41
2.7.3 Formations with USDWs	44
2.7.4 Geologic Cross Sections Illustrating Formations with USDWs.....	46
2.7.5 Principal Aquifers	48
2.7.6 Potentiometric Maps	49

2.7.7 Water Supply and Groundwater Monitoring Wells.....	53
2.8 Geochemistry [40 CFR 146.82(a)(6)].....	54
2.8.1 Formation Geochemistry	54
2.8.2 Fluid Geochemistry	54
2.8.3 Fluid-Rock Reactions.....	57
2.9 Other Information (Including Surface Air and/or Soil Gas Data, if Applicable)	58
2.10 Site Suitability [40 CFR 146.83]	58
3.0 AoR and Corrective Action	60
4.0 Financial Responsibility.....	60
5.0 Injection and Monitoring Well Construction	60
5.1 Proposed Stimulation Program [40 CFR 146.82(a)(9)]	61
5.2 Construction Procedures [40 CFR 146.82(a)(12)]	61
5.2.1 Casing and Cementing	62
6.0 Pre-Operational Logging and Testing.....	62
7.0 Well Operation	62
7.1 Operational Procedures [40 CFR 146.82(a)(10)].....	63
7.2 Proposed Carbon Dioxide Stream [40 CFR 146.82(a)(7)(iii) and (iv)]	64
8.0 Testing and Monitoring.....	64
9.0 Injection Well Plugging	64
10.0 Post-Injection Site Care (PISC) and Site Closure	65
11.0 Emergency and Remedial Response	65
12.0 Injection Depth Waiver and Aquifer Exemption Expansion	66
13.0 References.....	66

Class VI Permit Application Narrative
40 CFR 146.82(a)
CTV II

1.0 Project Background and Contact Information

Carbon TerraVault Holdings LLC (CTV), a wholly owned subsidiary of California Resources Corporation (CRC), proposes to construct and operate two CO₂ geologic sequestration wells at Carbon TerraVault II (CTV II), near the [REDACTED], located in San Joaquin County, California. This application was prepared in accordance with the U.S. Environmental Protection Agency's (EPA's) Class VI, in Title 40 of the Code of Federal Regulations (40 CFR 146.81). CTV is not requesting an injection depth waiver or aquifer exemption expansion.

CTV forecasts the potential CO₂ stored in the [REDACTED] at [REDACTED] million tonnes annually for [REDACTED] years. The anthropogenic CO₂ will be sourced from direct air capture and other CO₂ sources in the CTV II area.

The Carbon TerraVault II (CTV II) storage site is located in the Sacramento Valley, [REDACTED] miles southeast of the [REDACTED] near [REDACTED], California (**Figure 2.1-1**) within the [REDACTED] Sacramento Basin. The project will consist of two existing injectors, surface facilities, and monitoring wells. This supporting documentation applies to the two injection wells.

CTV will actively communicate project details and submitted regulatory documents to County and State agencies:

1. Geologic Energy Management Division (CalGEM)
District Deputy
Mark Ghann-Amoah: (661) 322-4031
2. CA Assembly District 13
Assemblyman Carlos Villapudua
31 East Channel Street – Suite 306
Stockton, CA 95202
(209) 948-7479
3. San Joaquin County
District 3 Supervisor –Tom Patti
(209) 468-3113
tpatti@sjgov.org
4. San Joaquin County Community Development
Director – David Kwong
1810 East Hazelton Avenue
Stockton, CA 95205
(209) 468-3121

5. San Joaquin Council of Governments
Executive Director – Diane Nguyen
555 East Weber Avenue
Stockton, CA 95202
(209) 235-0600
6. Region 9 Environmental Protection Agency
75 Hawthorne Street
San Francisco, CA 94105
(415) 947-8000

2.0 Site Characterization

2.1 Regional Geology, Hydrogeology, and Local Structural Geology [40 CFR 146.82(a)(3)(vi)]

2.1.1 [REDACTED]



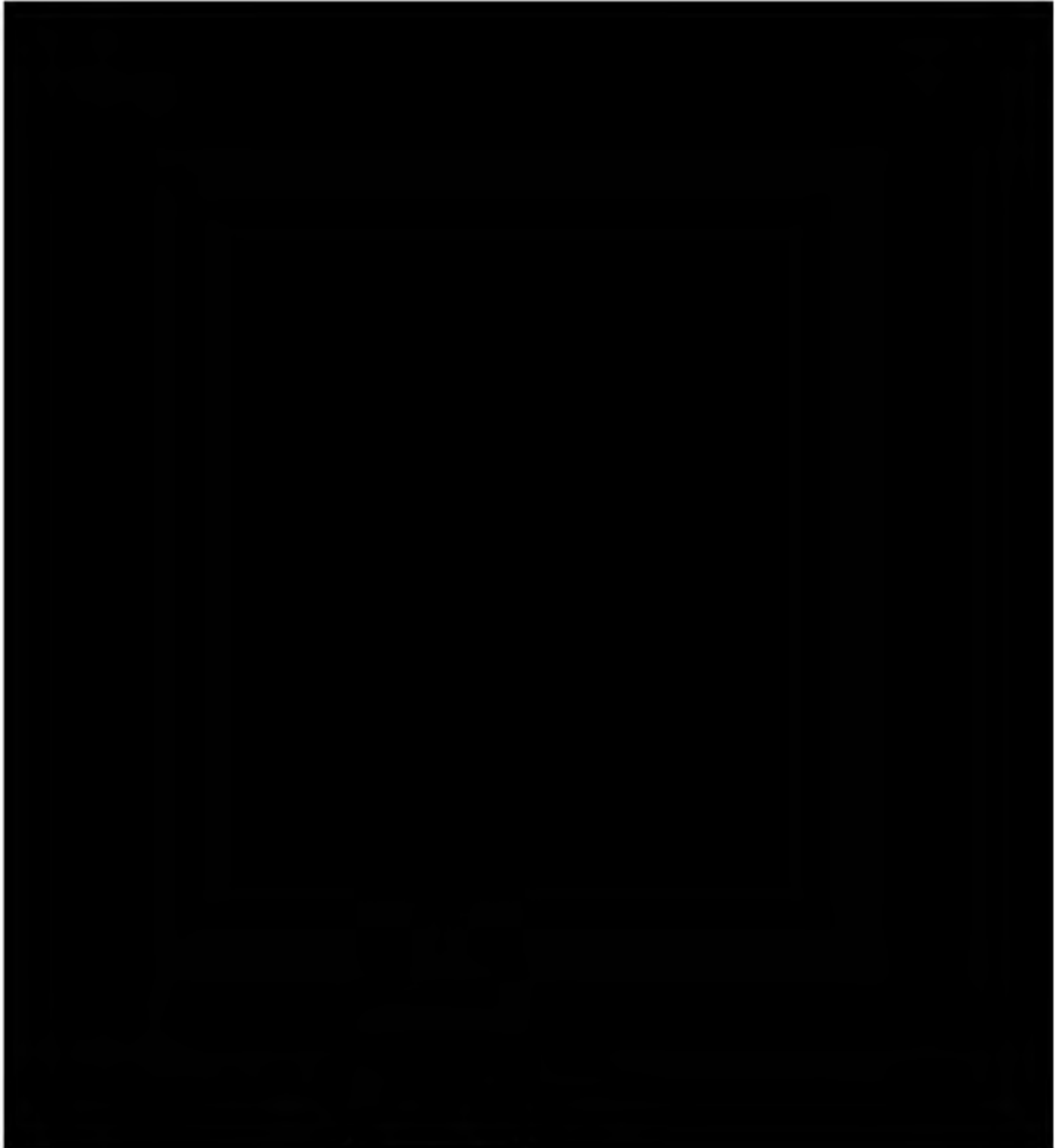


Figure 2.1-1. Location map of the [REDACTED] with the proposed injection AoR in relation to the Sacramento Basin.

2.1.2 Geology Overview

The [REDACTED] lies within the Sacramento Basin in northern California (**Figure 2.1-2**). The Sacramento Basin is the northern, asymmetric sub-basin of the larger, Great Valley Forearc. This portion of the basin, that contains a steep western flank and a broad, shallow eastern flank, spans approximately 240 miles in length and 60 miles wide (Magoon 1995).

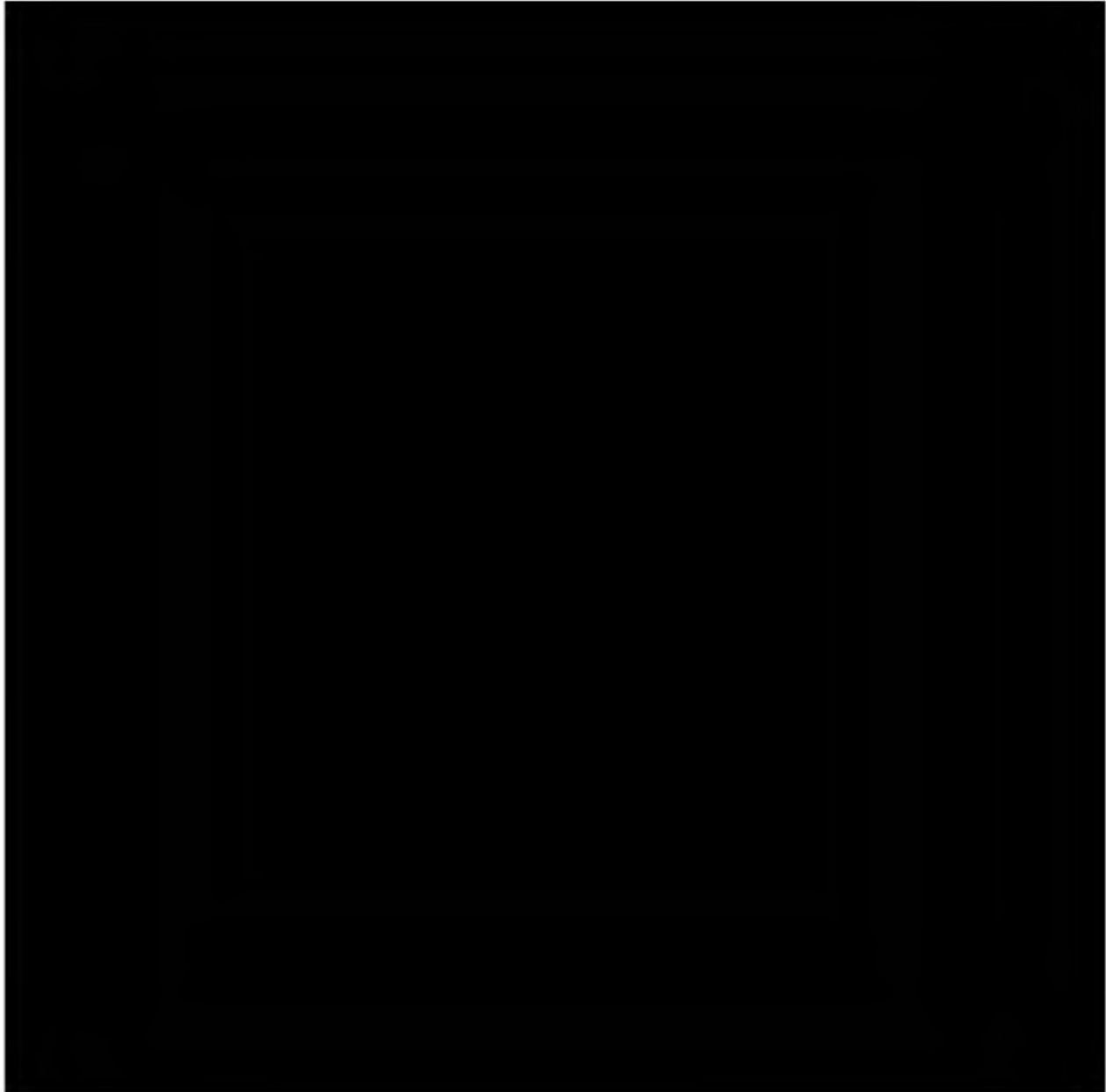


Figure 2.1-2. Location map of California modified from (Beyer, 1988) & (Sullivan, 2012). The Sacramento Basin regional study area is outlined by a dashed black line. B – Bakersfield; F – Fresno; R – Redding.

2.1.2.1 Basin Structure

The Great Valley was developed during mid to late Mesozoic time. The advent of this development occurred under convergent-margin conditions via eastward, Farallon Plate subduction, of oceanic crust beneath the western edge of North America (Beyer 1988). The convergent, continental margin, that characterized central California during the Late Jurassic through Oligocene time, was later replaced by a transform-margin tectonic system. This occurred as a result of the northward migration of the Mendocino Triple Junction (from Baja California to its present location off the coast of Oregon), located along California's coast (**Figure 2.1-3**). Following this migrational event was the progressive cessation of both subduction and arc volcanism as the progradation of a transform fault system moved in as the primary tectonic environment (Graham 1984). The major current day fault, the San Andreas, intersects most of

the Franciscan subduction complex, which consists of the exterior region of the extinct convergent-margin system (Graham 1984).



2.1-3. Migrational position of the Mendocino triple junction (Connection point of the Gorda, North American and Pacific plates) on the west and migrational position of Sierran arc volcanism in the east (Graham, 1984). Figure indicates space-time relations of major continental-margin tectonic events in California during Miocene.

2.1.2.2 Basin Stratigraphy

The structural trough that developed subsequent to these tectonic events, that became named the Great Valley, became a depocenter for eroded sediment and thereby currently contains a thick infilled sequence of sedimentary rocks. These sedimentary formations range in age from Jurassic to Holocene. The first deposits occurred as an ancient seaway and through time were built up by the erosion of the surrounding structures. The basin is constrained on the west by the Coast Range Thrust, on the north by the Klamath Mountains, on the east by the Cascade Range and Sierra Nevada and the south by the Stockton Arch Fault (**Figure 2.1-2**). The west, Coastal Range boundary was created by uplifted rocks of the Franciscan Assemblage (**Figure 2.1-3**). The Sierra Nevadas, that make up the eastern boundary, are a result of a chain of ancient volcanos.

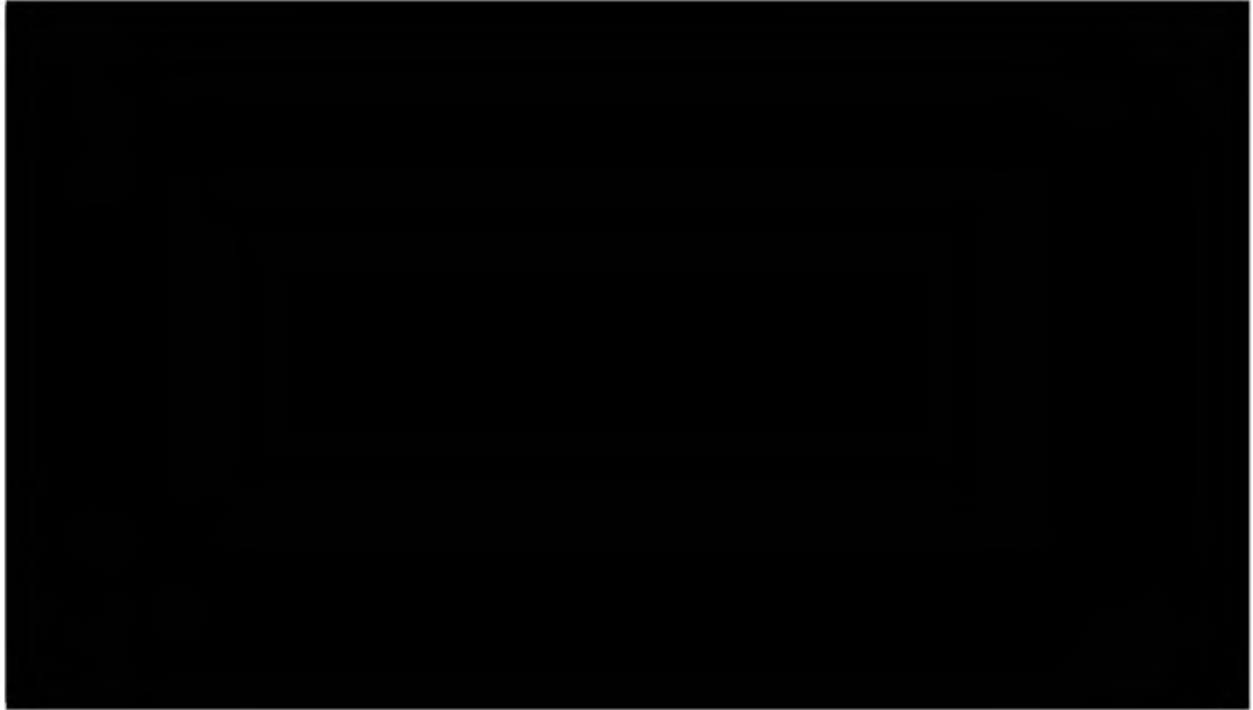
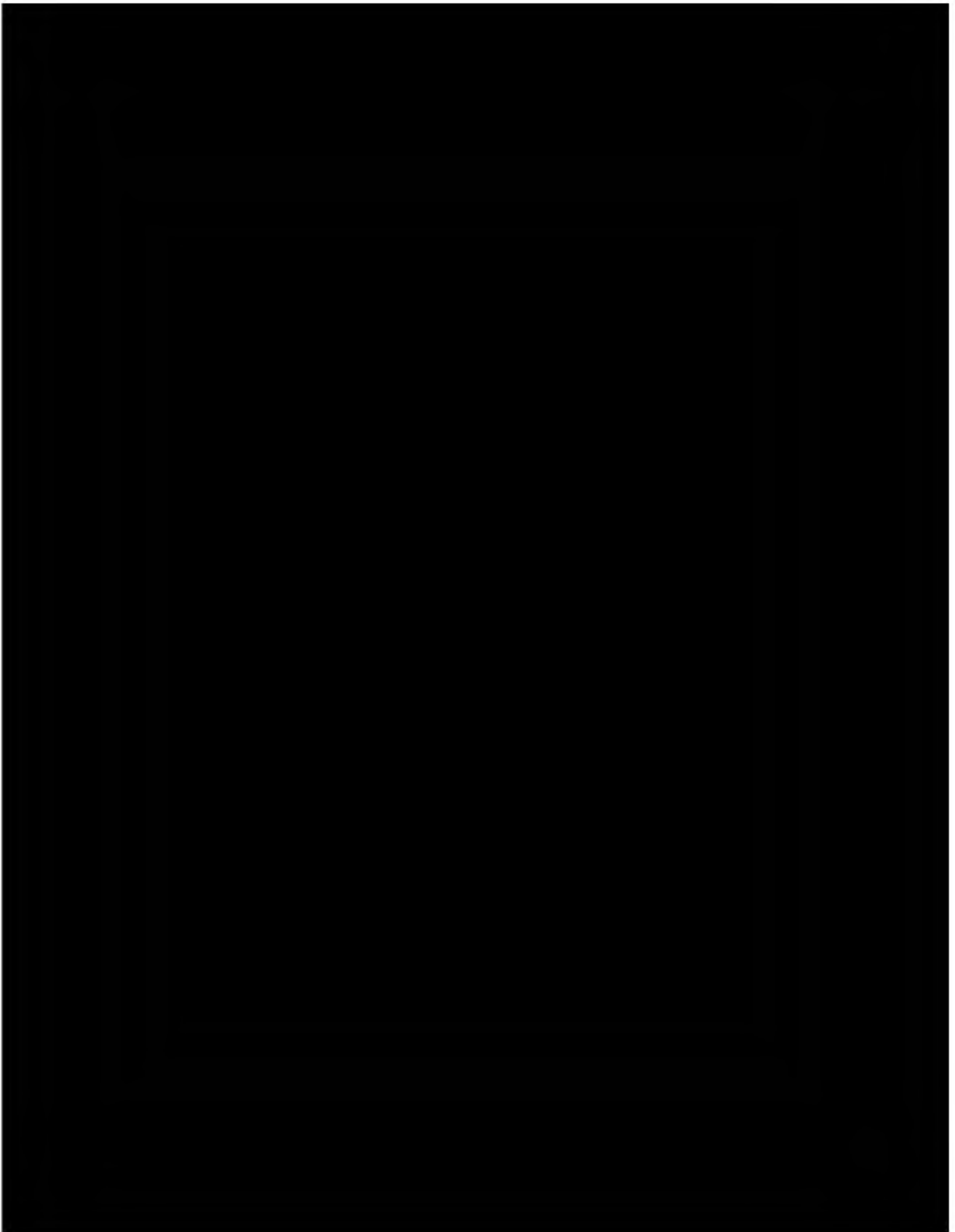


Figure 2.1-4. Schematic W-E cross-section of California, highlighting the Sacramento Basin, as a continental margin during late Mesozoic. The oceanic Farallon plate was forced below the west coast of the North American continental plate.

Basin development is broken out into evolutionary stages at the end of each time-period of the arc-trench system, from Jurassic to Neogene, in **Figure 2.1-5**. As previously stated, sediment infill began as an ancient seaway and was later sourced from the erosion of the surrounding structures. Due to the southward tilt of the basin, sedimentation [REDACTED] [REDACTED] sequestration quality sandstones. Sedimentary infill consists of Cretaceous-Paleogene fluvial, deltaic, shelf and slope sediments.



[REDACTED]

2.1.3 Geological Sequence

[REDACTED]



Figure 2.1-6. Schematic northwest to southeast cross section in the Sacramento basin, intersecting the project AoR.

Following its deposition, [REDACTED]

[REDACTED]

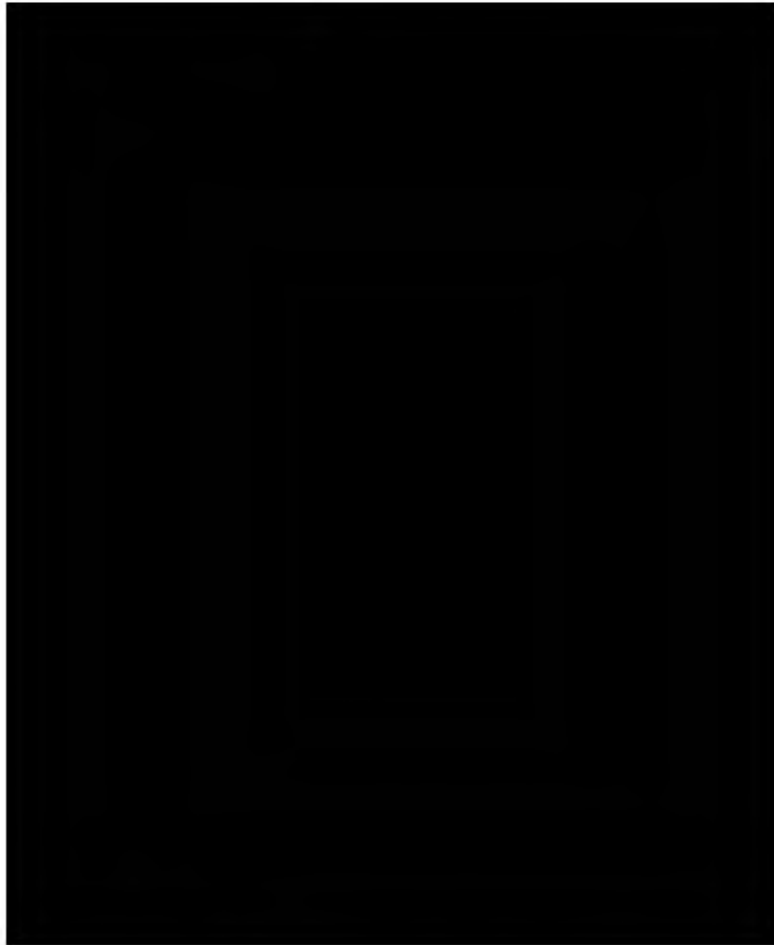


FIGURE 2.1-7. [REDACTED] isopach map for the greater storage project area. Wells shown as blue dots on the map penetrate the [REDACTED] and have open-hole logs. Wells with relative permeability or capillary pressure data are shown as magenta circles.

2.2 Maps and Cross Sections of the AoR [40 CFR 146.82(a)(2), 146.82(a)(3)(i)]

2.2.1 Data

[REDACTED]



Figure 2.2-1: [REDACTED]

Well data are used in conjunction with three-dimensional (3D) and two-dimensional (2D) seismic to define the structure and stratigraphy of the injection zone and confining zone (**Figure 2.2-2**). **Figure 2.2-3** shows outlines of the seismic data used and the area of the structural framework that was built from these seismic surveys. The 3D data in this area were merged using industry standard pre-stack time migration in 2013, allowing for a seamless interpretation across them. The 2D data used for this model were tied to this 3D merge in both phase and time to create a standardized datum for mapping purposes. The following layers were mapped across the 2D and 3D data:

- A shallow marker to aid in controlling the structure of the velocity field
- [REDACTED]
- [REDACTED]
- [REDACTED]
- [REDACTED]
- [REDACTED]
- [REDACTED]
- [REDACTED]

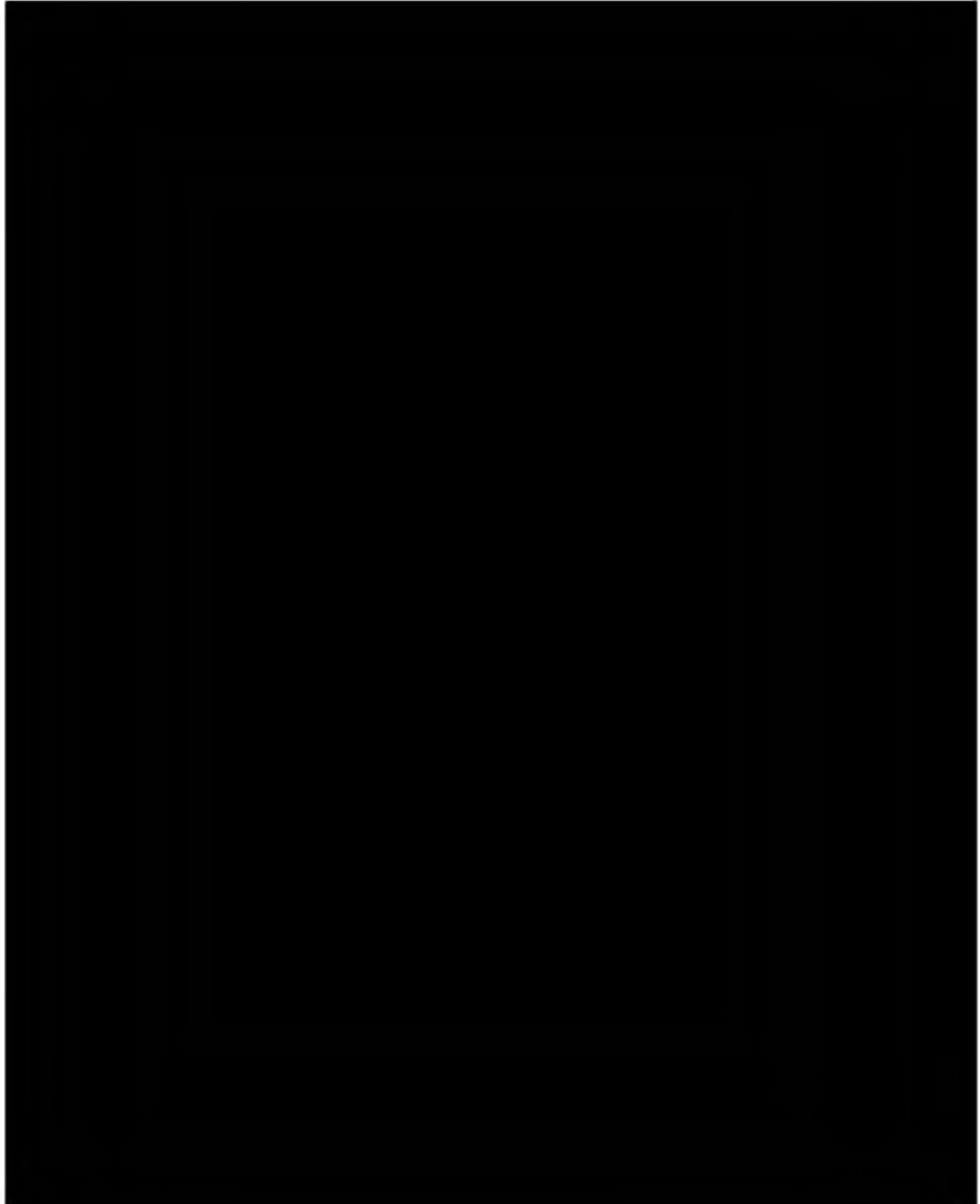


Figure 2.2-2. Type well from the southern edge of the AoR boundary showing average rock properties used in the model for confining and injection zones.



Figure 2.2-3: Summary map and area of seismic data used to build structural model. Both of the 3D surveys were acquired in 1998 and reprocessed in 2013. The 2D seismic were acquired between 1980 and 1985. California gas fields are shown for reference.



Interpretation of these layers began with a series of well ties at well locations shown in **Figure 2.2-3**. These well ties create an accurate relationship between wells which are in depth and the seismic which is in time. The layers listed above were then mapped in time and gridded on a 550 by 550-foot cell basis. Alongside this mapping was the interpretation of any faulting in the area which is discussed further in the Faults and Fracture section of this document.

The gridded time maps and a sub-set of the highest quality well ties and associated velocity data are then used to create a three-dimensional velocity model. This model is guided between well control by the time horizons and is iterated to create an accurate and smooth function. The velocity model is used to convert both the gridded time horizons and interpreted faults into the depth domain. The result is a series of depth grids of the layers listed above which are then used in the next step of this process.

The depth horizons are the basis of a framework which uses conformance relationships to create a series of depth grids that are controlled by formation well tops picked on well logs. The grids are used as structural control between these well tops to incorporate the detailed mapping of the seismic data. These grids incorporate the thickness of zones from well control and the formation strike, dip, and any fault offset from the seismic interpretation. The framework is set up to create the following depth grids for input in to the geologic and plume growth models:

- [redacted]
- [redacted]
- [redacted]
- [redacted]
- [redacted]
- [redacted]
- [redacted]
- [redacted]

- [REDACTED]
- [REDACTED]

2.2.2 Stratigraphy

[REDACTED]

[REDACTED]

[REDACTED]

[REDACTED]

[REDACTED] Of these formations the regional upper seal rock that partitions the reservoir consists of the [REDACTED] These combined formations create an average thickness of ~ 2,240 ft. throughout the AoR. [REDACTED]

[REDACTED]

[REDACTED]

[REDACTED]

[REDACTED]

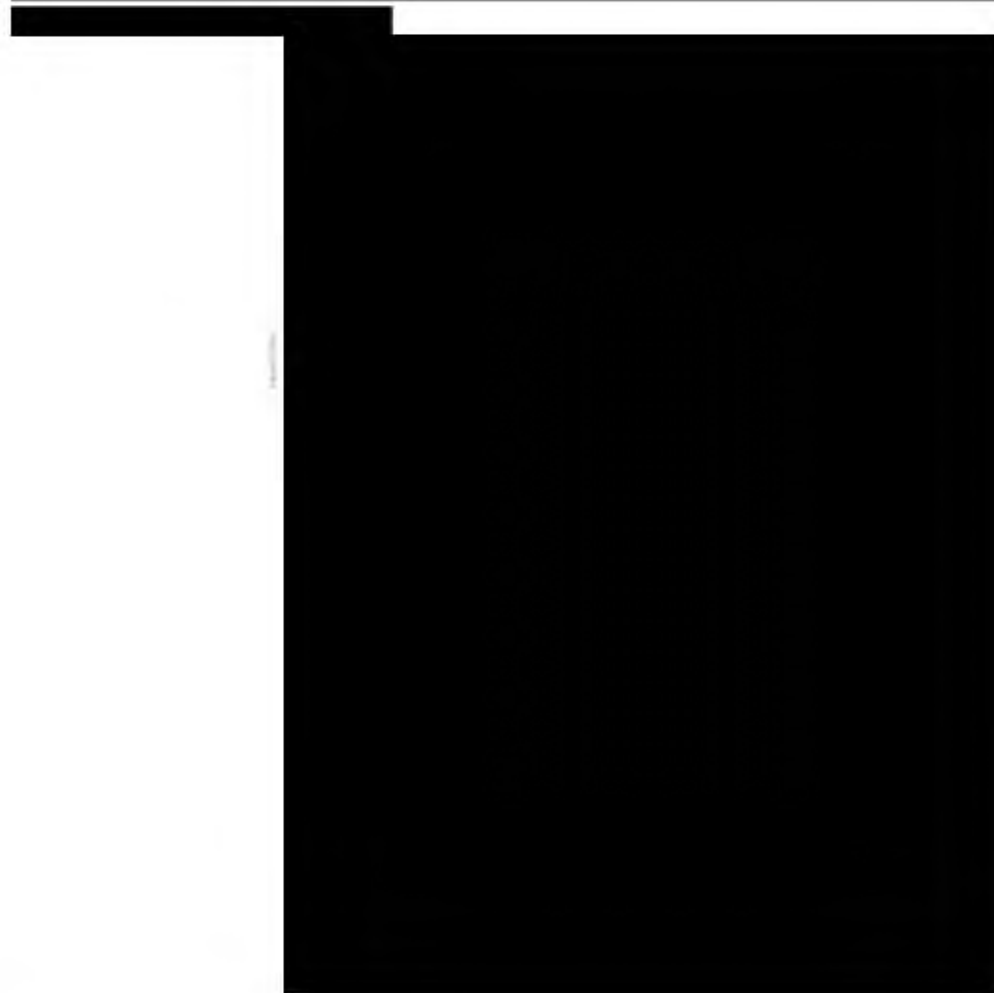


Figure 2.2-4. Cross section showing stratigraphy and lateral continuity of major formations across the project area.

[REDACTED]

The underlying [REDACTED]
[REDACTED] This shale has an average permeability of 0.04mD and porosity of 14.7% (as defined in section 2.4.2). Due to the sparse well penetrations and subsequent lack of log data, this formation has been primarily mapped using seismic data as stated above.

2.2.2.2 [REDACTED]

Within the project area, [REDACTED]
[REDACTED]
[REDACTED]
[REDACTED]

[REDACTED] These deposits were part of a large deep-sea fan system that were sourced from granitic areas in the Sierra Nevada and fed into the system via submarine canyons and feeder channels (Williamson 1981). This creates a blocky, sand-rich reservoir that extends to as much as 1,500 ft thick in the center of the basin. Along the basin axis this sandy suprafan stacks up due to the high rate of sand supply relative to the size of the basin as well as the depositional nature of the fans at basin margins (Williamson 1981). [REDACTED] [REDACTED]

[REDACTED]
[REDACTED]
[REDACTED]
[REDACTED]
[REDACTED]
[REDACTED]



Figure 2.2-5. [REDACTED]

[REDACTED]

[REDACTED] The AoR and injectors for this project are shown in

Figure 2.2-6.

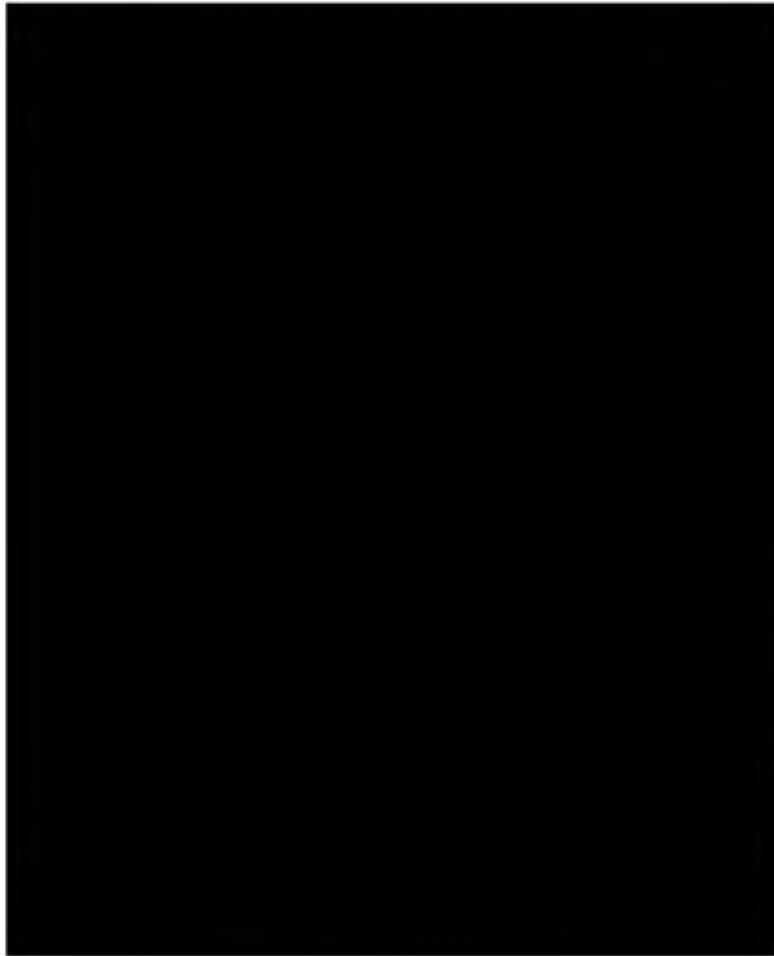


Figure 2.2-6. AoR and injection well location map for the project area. The injection wells are 1,735 ft. apart.

[REDACTED]

[REDACTED]

[REDACTED]

[REDACTED] At the [REDACTED]

[REDACTED] and has a permeability of less than 0.15 mD and 18.5% porosity (as defined in section 2.4.2). [REDACTED]

[REDACTED]

[REDACTED]

[REDACTED]

[REDACTED]

[REDACTED]

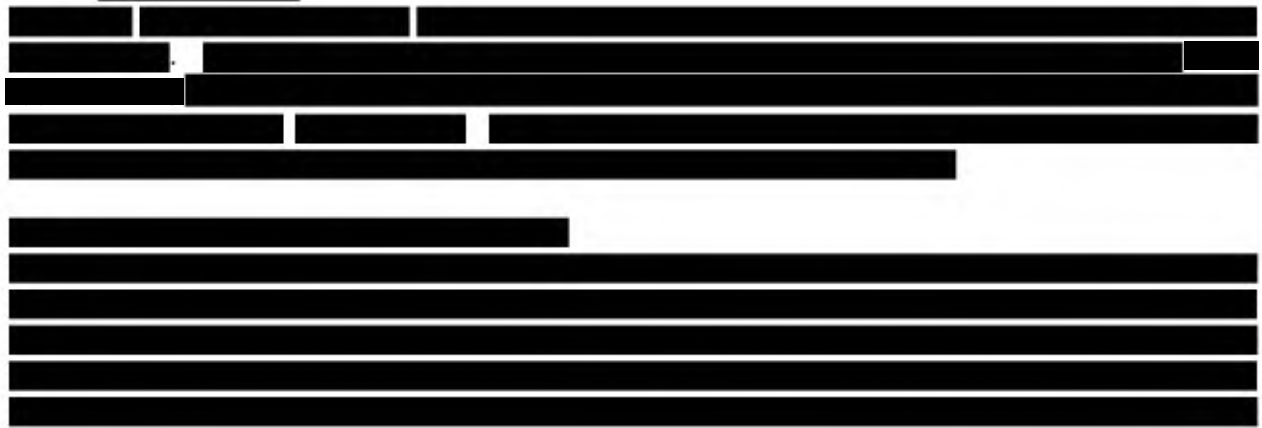
[REDACTED]

[REDACTED]

[REDACTED]

[REDACTED]

2.2.2.8



2.2.3 Map of the Area of Review

As required by 40 CFR 146.82(a)(2), **Figure 2.2-7** shows surface bodies of water, surface features, transportation infrastructure, political boundaries, and cities. Major water bodies in the area are

This figure does not show the surface trace of known and suspected faults because there are no known surface faults in the AoR. There are also no known mines or quarries in the AoR. **Figure 2.2-8** indicates the locations of State- or EPA-approved subsurface cleanup sites. This cleanup site information was obtained from the State Water Resources Control Board's GeoTracker database, which contains records for sites that impact, or have the potential to impact, groundwater quality. Water wells within and adjacent the AoR are discussed in Section 2.7.7 of this document.



Figure 2.2-7. Surface Features and the AoR

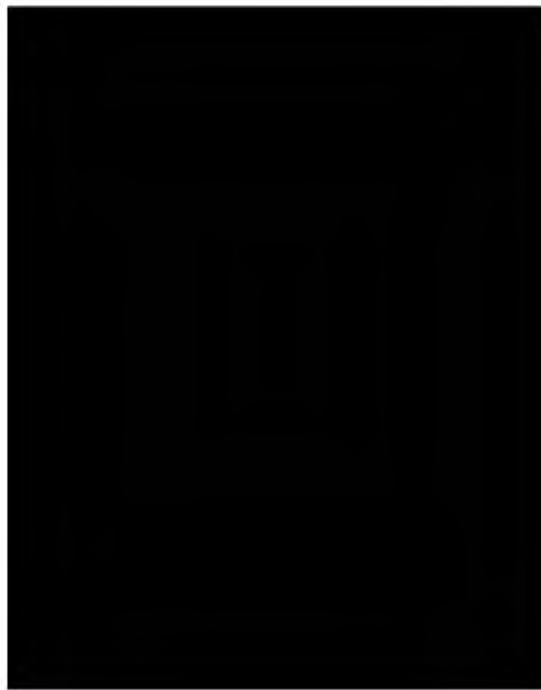


Figure 2.2-8. State or EPA Subsurface Cleanup Sites

2.3 Faults and Fractures [40 CFR 146.82(a)(3)(ii)]

2.3.1 Overview

[REDACTED]

The 3D seismic data described in the prior section were used together with well control to define the fault planes within the geologic model boundary. This geologic model is a subset of the larger structural framework that was built using the seismic and well data. [REDACTED]

[REDACTED]

[REDACTED] of the [REDACTED] which may be [REDACTED] and the planned injection [REDACTED] is not discussed further in this report.

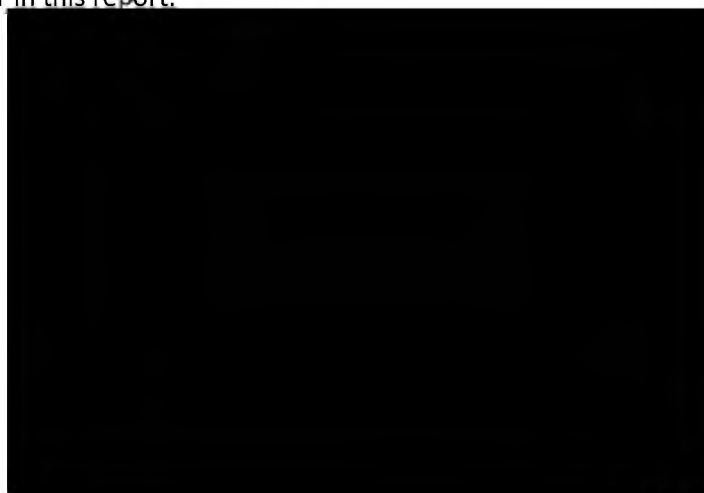


Figure 2.3-1. [REDACTED] The [REDACTED] is [REDACTED] in cross-section. Yellow line highlights the cross-section shown in **Figure 2.3-2**

[REDACTED]



Figure 2.3-2. Structural cross section across the geologic model. Well [REDACTED] is shown with SP log (negative values to left) for correlation and geologic packages. Geologic surfaces developed from seismic interpretation. The [REDACTED] is cut-off by the Base [REDACTED]

[REDACTED]

[REDACTED]

2.4 Injection and Confining Zone Details [40 CFR 146.82(a)(3)(iii)]

2.4.1 Mineralogy

No quantitative mineralogy information exists within the AoR boundary. Mineralogy data will be acquired across all the zones of interest as part of pre-operational testing. Several wells outside the AoR have mineralogy over the respective formations of interest, and that data is presented below.

[REDACTED]

[REDACTED]

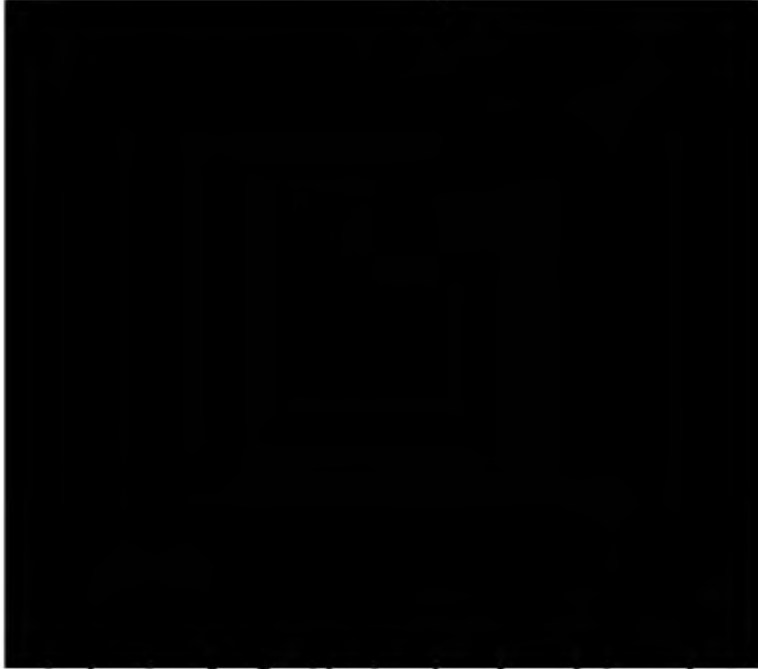


Figure 2.4-1. Map showing location of wells with mineralogy data relative to the AoR.

Table 2.4-1: Formation mineralogy from X-ray diffraction in [REDACTED] and XRD and Fourier transform infrared spectroscopy (FTIR) in the [REDACTED] well.

[REDACTED]

2.4.2 Porosity and Permeability

Wireline log data was acquired with measurements that include but are not limited to spontaneous potential, natural gamma ray, borehole caliper, compressional sonic, resistivity as well as neutron porosity and bulk density.

Formation porosity is determined one of two ways: from bulk density using 2.65 g/cc matrix density as calibrated from core grain density and core porosity data, or from compressional sonic using 55.5 $\mu\text{sec}/\text{ft}$ matrix slowness and the Raymer-Hunt equation.

Volume of clay is determined by spontaneous potential and is calibrated to core data.

Log-derived permeability is determined by applying a core-based transform that utilizes capillary pressure porosity and permeability along with clay values from XRD or FTIR. Core data from two wells with 13 data points was used to develop a permeability transform. An example of the transform from core data is illustrated in **Figure 2.4-2** below.

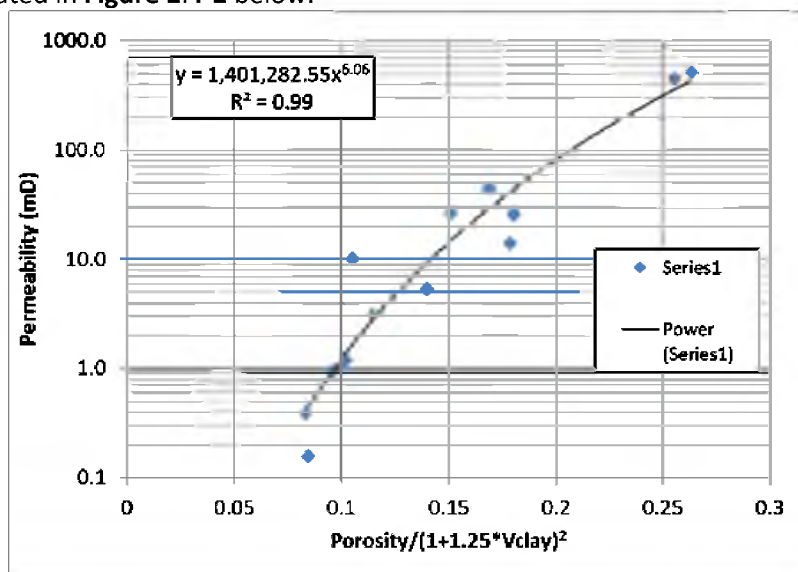
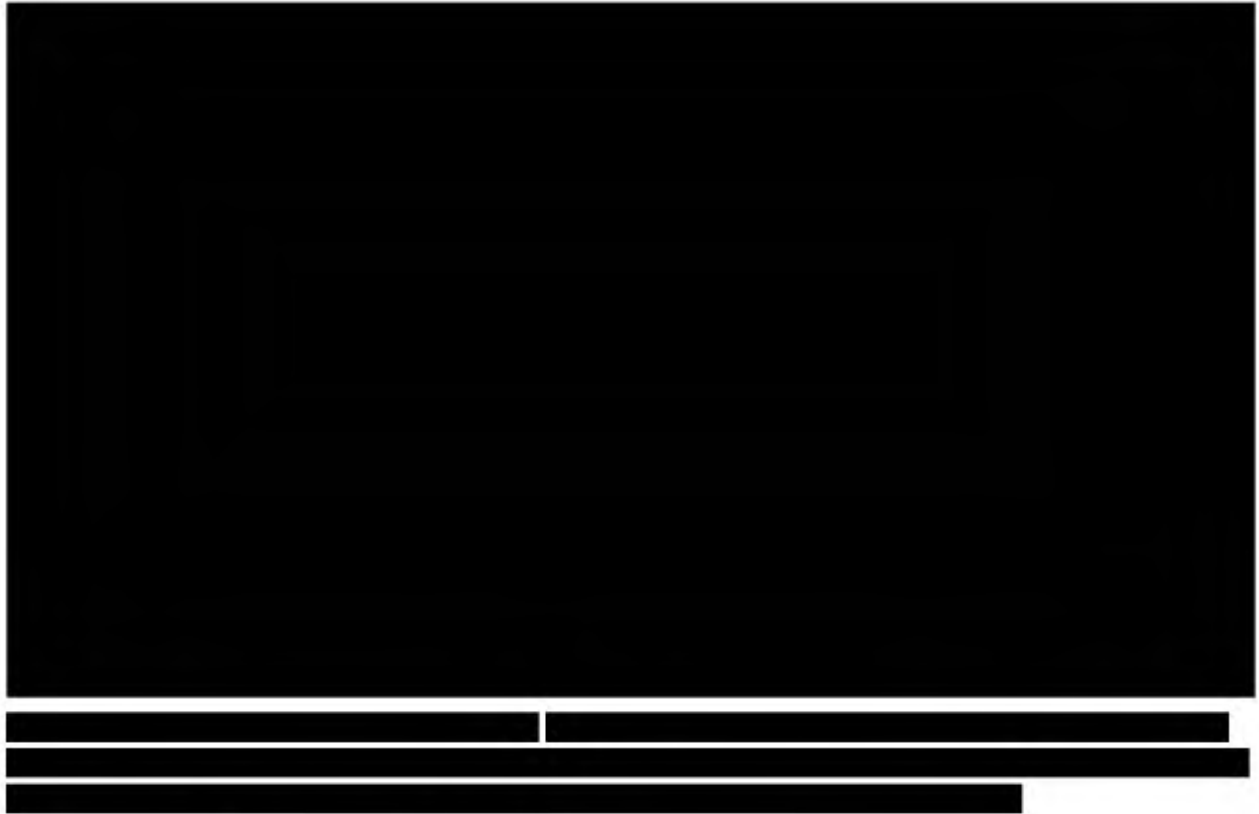


Figure 2.4-2. Permeability transform for Sacramento basin zones.

[REDACTED]

[REDACTED]

[REDACTED]



A log plot for the [REDACTED] is included in **Figure 2.4-5**. Core porosity and permeability are shown in comparison to log calculated porosity and permeability.

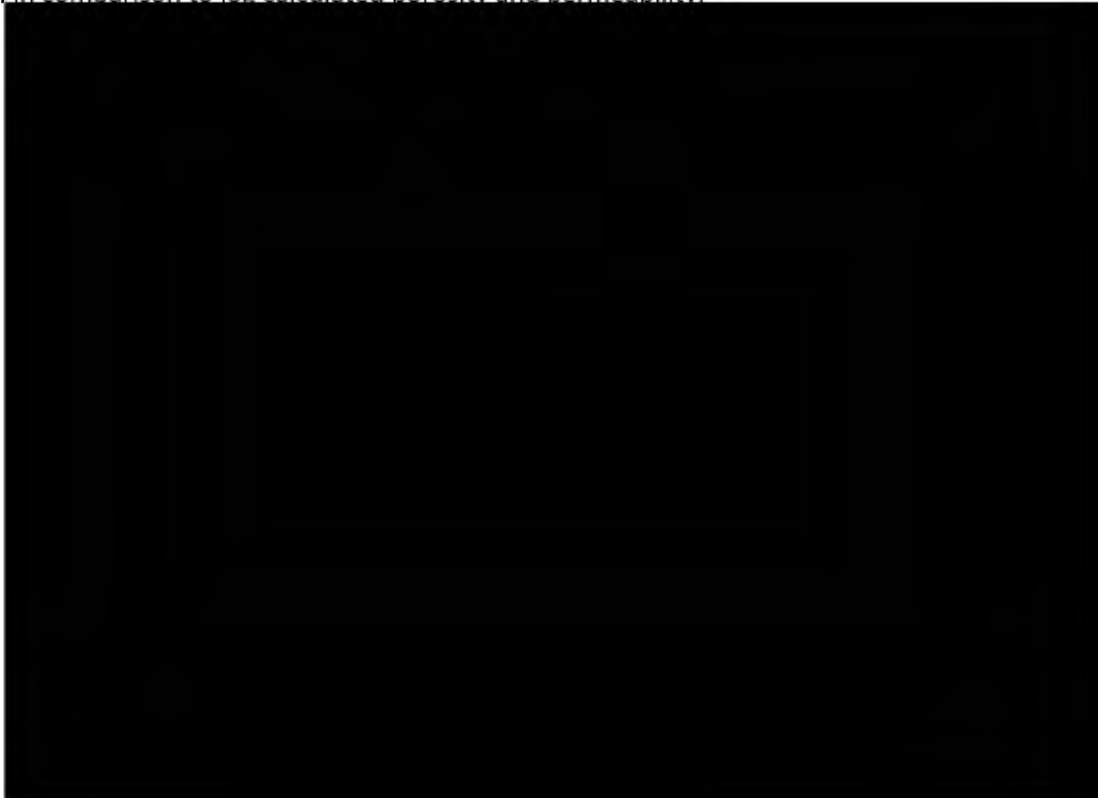


Figure 2.4-5. Log plot for well [REDACTED], showing the log curves used as inputs into calculations of clay volume, porosity and permeability, and their outputs. Core data for porosity and permeability is shown for comparison to the log model. Track 1: Correlation and caliper logs. Track 2: Measured depth. Track 3: Vertical depth and vertical subsea depth. Track 4: Zones. Track 5: Resistivity. Track 6: Compressional sonic and density logs. Track 7: Volume of clay. Track 8: Porosity calculated from log curves and core porosity. Track 9: Permeability calculated using transform and core permeability.



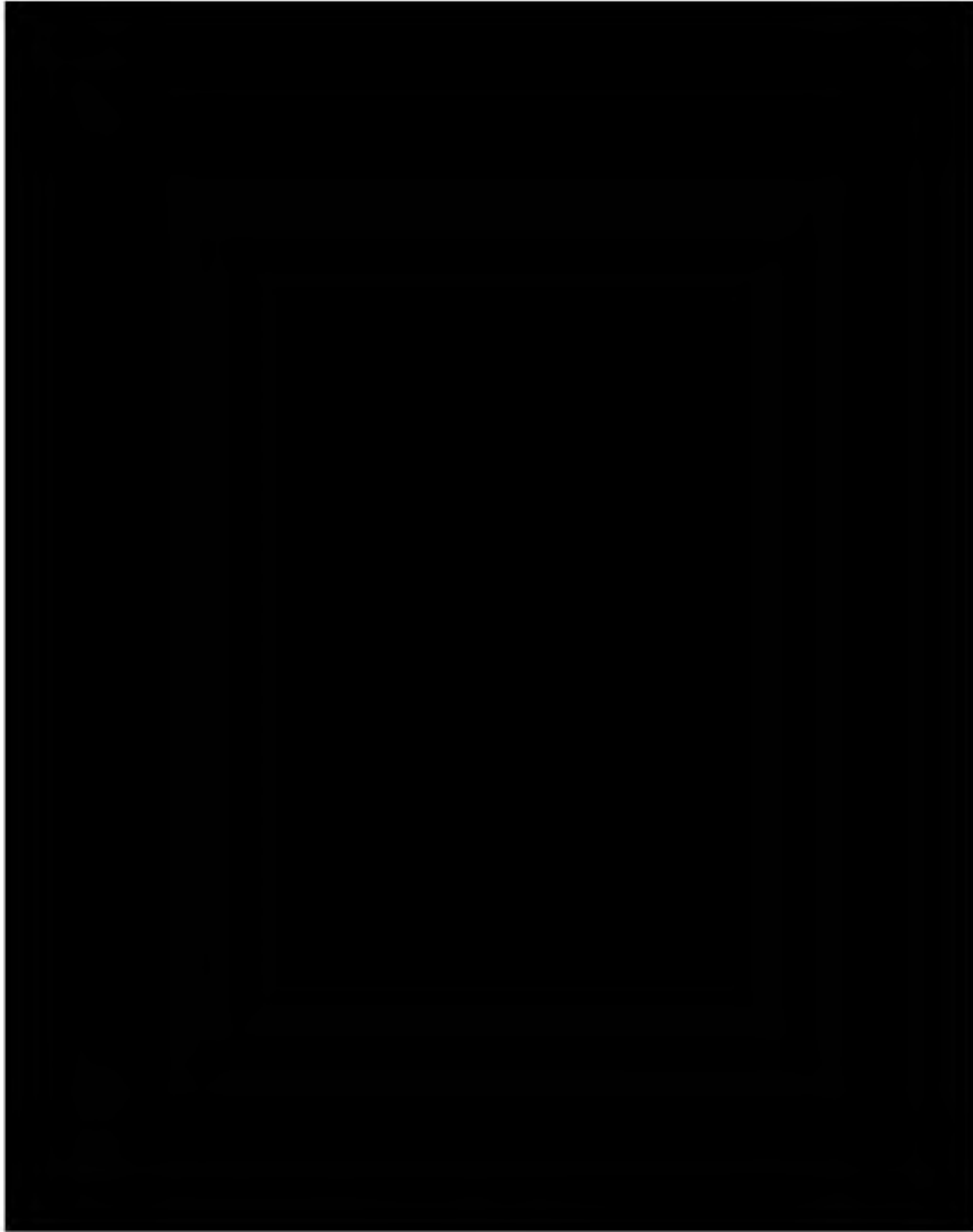


Figure 2.4-6. Map of wells with porosity and permeability data.

[REDACTED]

The average porosity of the upper confining zone is 23.0%, based on 16 wells with porosity logs and 50563 individual logging data points.

The geometric average permeability of the upper confining zone is 0.59 mD, based on 16 wells with porosity logs and 49,662 individual logging data points.

[REDACTED]

The average porosity of the lower confining zone [REDACTED] is 14.7%, based on 13 wells with porosity logs and 2983 individual logging data points.

The geometric average permeability of the lower confining zone [REDACTED] is 0.04 mD, based on 13 wells with porosity logs and 2906 individual logging data points.

2.4.3 Confining Zone Capillary Pressure

Capillary pressure is the difference across the interface of two immiscible fluids. Capillary entry pressure is the minimum pressure required for an injected phase to overcome capillary and interfacial forces and enter the pore space containing the wetting phase.

No capillary pressure data was available for the upper confining zone. This data will be acquired as part of pre-operational testing.

2.4.4 Depth and Thickness

[REDACTED]

[REDACTED]

[REDACTED]

[REDACTED]

Table 2.4-2:

Zone	Property	Low	High	Mean
Upper Confining Zone [REDACTED]	Thickness (feet)	2,158	2,322	2,243
	Depth (feet TVD)	7,208	7,788	7,456
Reservoir [REDACTED]	Thickness (feet)	120	365	256
	Depth (feet TVD)	9,482	9,994	9,727



Figure 2.4-7. [REDACTED]

2.4.5 Structure Maps

Structure maps are provided in order to indicate a depth to reservoir adequate for supercritical-state injection.

2.4.6 Isopach Maps

Spontaneous potential (SP) logs from surrounding gas wells were used to identify sandstones. Negative millivolt deflections on these logs, relative to a baseline response in the enclosing shales, define the sandstones. These logs were baseline shifted to 0mV. Due to the log vintage variability, there is an effect on quality which creates a degree of subjectivity within the gross sand, however this will not have a material impact on the maps.

2.5 Geomechanical and Petrophysical Information [40 CFR 146.82(a)(3)(iv)]

2.5.1 Caprock Ductility

Ductility and the unconfined compressive strength (UCS) of shale are two properties used to describe geomechanical behavior. Ductility refers to how much a rock can be distorted before it fractures, while the UCS is a reference to the resistance of a rock to distortion or fracture. Ductility generally decreases as compressive strength increases.

Ductility and rock strength calculations were performed based on the methodology and equations from Ingram & Urai, 1999 and Ingram et. al., 1997. Brittleness is determined by comparing the log derived unconfined compressive strength (UCS) vs. an empirically derived UCS for a normally consolidated rock (UCS_{NC}).

$$\log UCS = -6.36 + 2.45 \log(0.86V_p - 1172) \quad (1)$$

$$\sigma' = OB_{pres} - P_p \quad (2)$$

$$UCS_{NC} = 0.5\sigma' \quad (3)$$

$$BRI = \frac{UCS}{UCS_{NC}} \quad (4)$$

Units for the UCS equation are UCS in MPa and V_p (compressional velocity) in m/s. OB_{pres} is overburden pressure, P_p is pore pressure, σ' is effective overburden stress, and BRI is brittleness index.

If the value of BRI is less than 2, empirical observation shows that the risk of embrittlement is lessened, and the confining zone is sufficiently ductile to accommodate large amounts of strain without undergoing brittle failure. However, if BRI is greater than 2, the “risk of development of an open fracture network cutting the whole seal depends on more factors than local seal strength and therefore the BRI criterion is likely to be conservative, so that a seal classified as brittle may still retain hydrocarbons” (Ingram & Urai, 1999).

Within the AoR, four wells had compressional sonic and bulk density data over the upper confining zone to calculate ductility, comprising 9633 individual logging data points (see pink squares in **Figure 2.4-1**). 16 wells had compressional sonic data over the upper confining zone to calculate UCS, comprising 59014 individual logging data points (see black circles in **Figure 2.4-1**). The average ductility of the confining zone based on the mean value is 2.0. Additionally, 65% of the shale within the confining layer has a ductility less than 2. The average rock strength of the confining zone, as determined by the log derived UCS equation above, is 4,593 psi.

An example calculation for the well [REDACTED] shown below (**Figure 2.5-1**). UCS_CCS_VP is the UCS based on the compressional velocity, UCS_NC is the UCS for a normally consolidated rock, and BRI is the calculated brittleness using this method. Brittleness less than two (representing ductile rock) is shaded red.



Figure 2.5-1: Unconfined compressive strength and ductility calculations for well [REDACTED]. The upper confining zone ductility is less than two. Track 1: Correlation logs. Track 2: Measured depth. Track 3: Vertical depth and vertical subsea depth. Track 4: Zones. Track 5: Resistivity. Track 6: Density log. Track 7: Density and compressional sonic logs. Track 8: Volume of clay. Track 9: Porosity calculated from sonic and density. Track 10: Water saturation. Track 11: Permeability. Track 12: Caliper. Track 13: Overburden pressure and hydrostatic pore pressure. Track 14: UCS and UCS_NC. Track 15: Brittleness.

[REDACTED]

[REDACTED]

[REDACTED]

[REDACTED]

[REDACTED]

2.5.2 Stress Field

The stress of a rock can be expressed as three principal stresses. Formation fracturing will occur when the pore pressure exceeds the least of the stresses. In this circumstance, fractures will propagate in the direction perpendicular to the least principal stress (**Figure 2.5-2**).



Figure 2.5-2: Stress diagram showing the three principal stresses and the fracturing that will occur perpendicular to the minimum principal stress.

Stress orientations in the Sacramento basin have been studied using both earthquake focal mechanisms and borehole breakouts (Snee and Zoback, 2020, Mount and Suppe, 1992). The azimuth of maximum principal horizontal stress (S_{Hmax}) was estimated at $N40^{\circ}E \pm 10^{\circ}$ by Mount and Suppe, 1992. Data from the World Stress Map 2016 release (Heidbach et al., 2016) shows an average S_{Hmax} azimuth of $N37.4^{\circ}E$ once several far field earthquakes with radically different S_{Hmax} orientations are removed (**Figure 2.5-3**), which is consistent with Mount and Suppe, 1992. The earthquakes in the area indicate a strike-slip/reverse faulting regime.

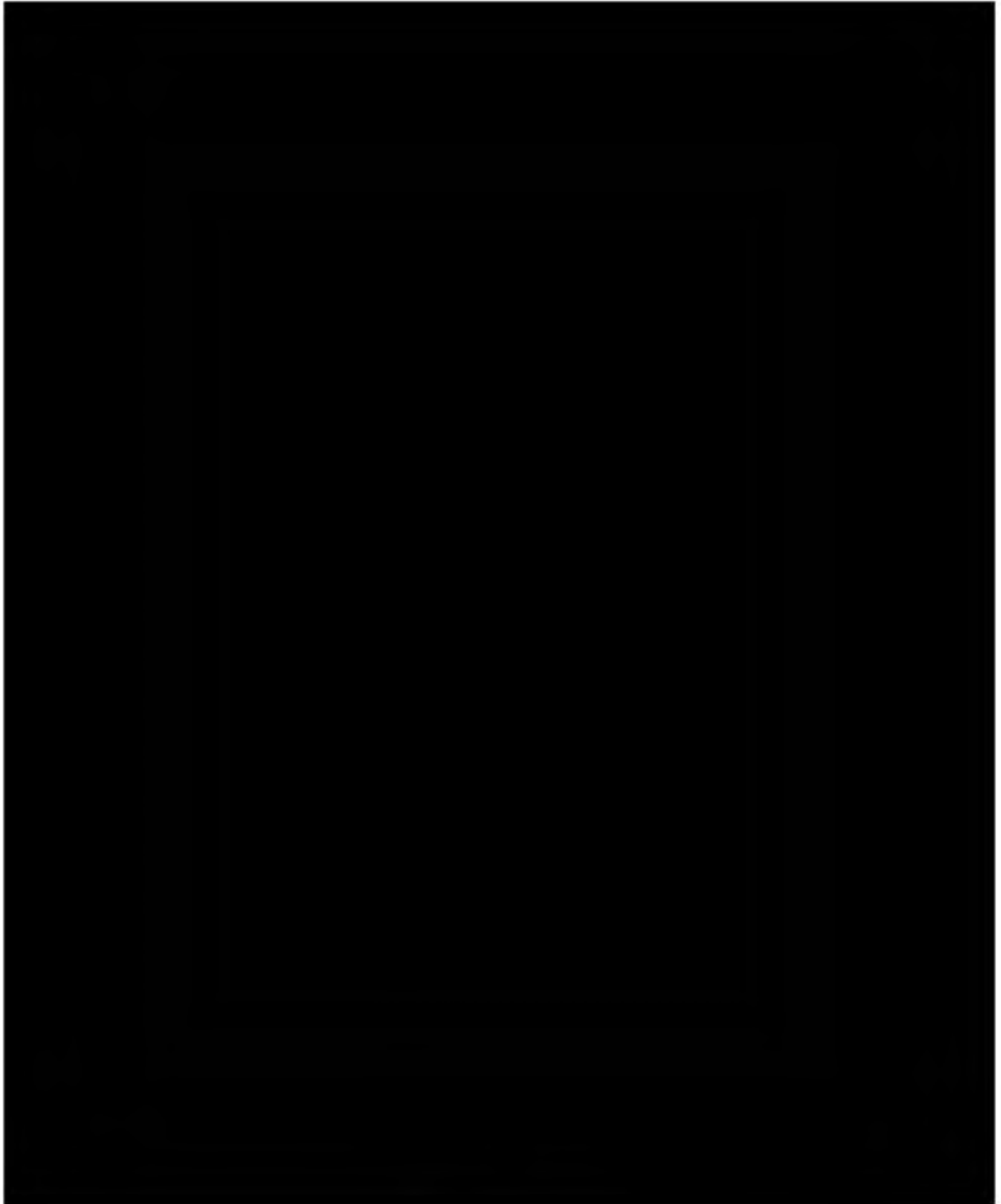


Figure 2.5-3: World Stress Map output showing S_{Hmax} azimuth indicators and earthquake faulting styles

[Redacted text block]

[REDACTED]

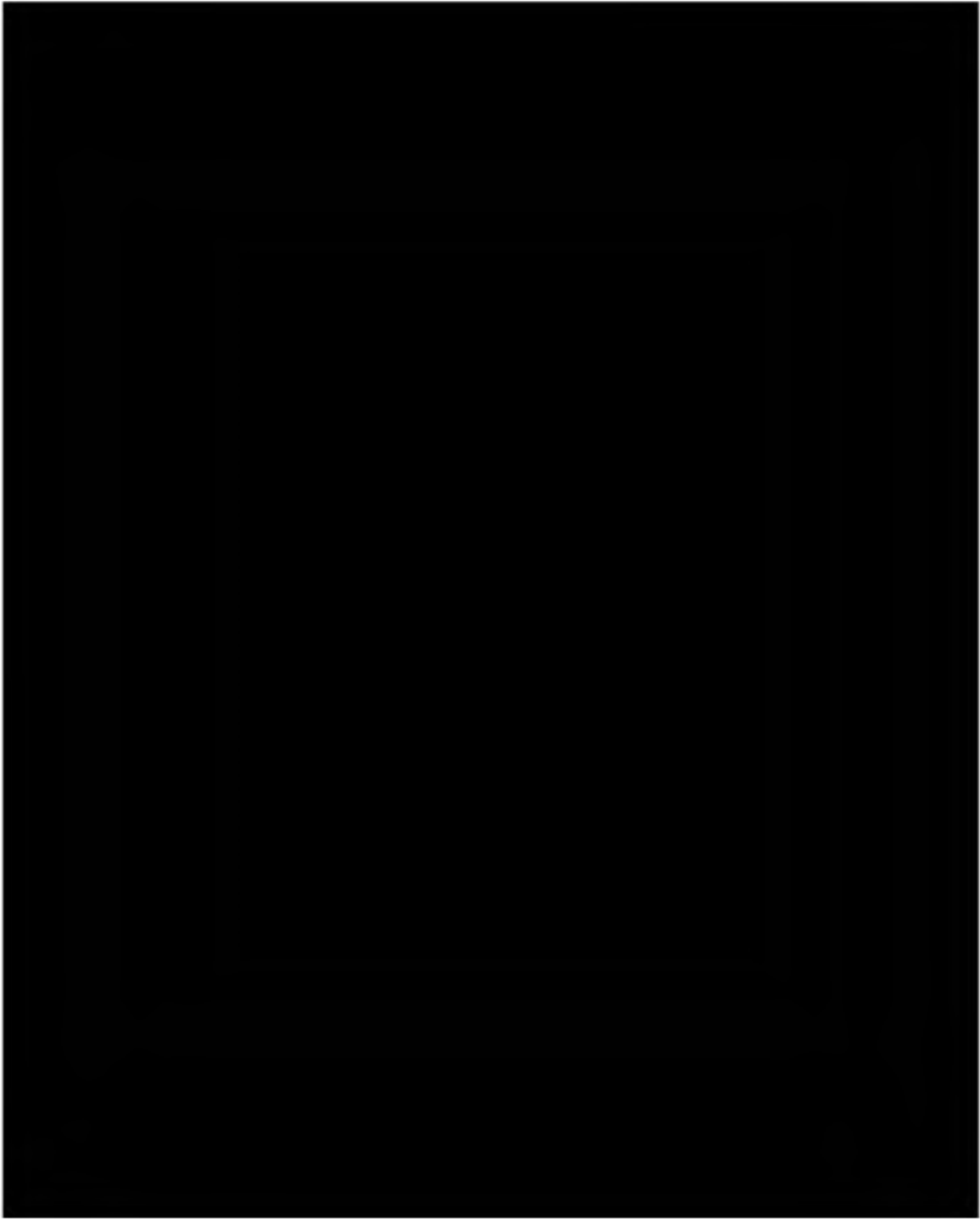


Figure 2.5-4: Location of wells with FIT data.

In the project AoR there is no site-specific fracture pressure or fracture gradient for the upper confining zone. A step rate test will be conducted in the upper confining zone as per the preoperational testing plan.

In [REDACTED]
[REDACTED]

The overburden stress gradient in the reservoir and confining zone is 0.94 psi/ft. No data currently exists for the pore pressure of the confining zone. This will be determined as part of the preoperational testing plan.

2.6 Seismic History [40 CFR 146.82(a)(3)(v)]

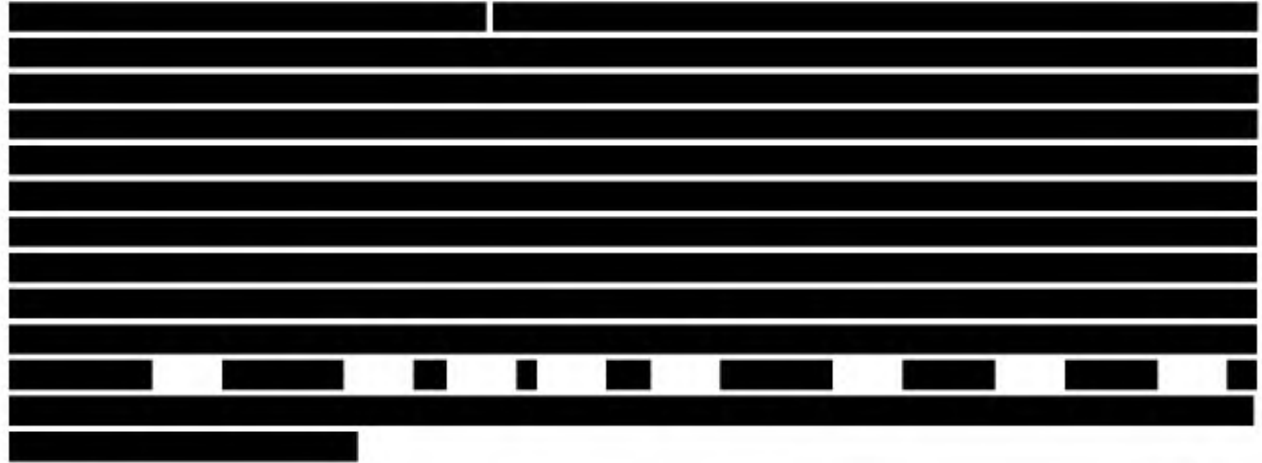


Figure 2.6-1: Fault Activity Map from the California Geologic Survey. [REDACTED]



(<https://maps.conservation.ca.gov/cgs/fam/>)

The seismic interpretation provides an estimation of the time when the [REDACTED] was last actively growing. The United States Geologic Survey (USGS) provides an earthquake catalog tool (<https://earthquake.usgs.gov/earthquakes/search/>) which can be used to search for recent seismicity that could be associated with faults in the area for movement. A search was made for earthquakes in the greater vicinity of the project area from 1850 to modern day with events of a magnitude greater than

three. **Figure 2.6-2** shows the results of this search and **Table 2.6-1** summarizes some of the data taken from them.



Figure 2.6-2. Image is modified from USGS search results. Data from these events are compiled in **Table 2.6-1** in chronological order associated with events 1 through 11 on the map.

[REDACTED]

Table 2.6-1: Data from USGS earthquake catalog for faults in the region of CTV II.

By limiting the

[REDACTED]

Lund-Snee and Zoback (2020) published updated maps for crustal stress estimates across North America. **Figure 2.6-3** shows a modified image from that work highlighting CTV II. This work is in agreement with previous estimates of maximum horizontal stress in the region of approximately N40°E in a strike-slip to reverse stress regime (Mount and Suppe 1992) and is consistent with World Stress map data for the area (Heidbach et al. 2016). [REDACTED]

[REDACTED] Attachment C of this application discusses the seismicity monitoring plan for this injection site.



Figure 2.6-3: Image modified from Lund Snee and Zoback (2020) showing relative stress magnitudes across California. Red star indicates CTV II project site area.

2.6.2 Seismic Hazard Mitigation

[REDACTED]

The following is a summary of CTVs seismic hazard mitigation for CTV II:

The project has a geologic system capable of receiving and containing the volumes of CO₂ proposed to be injected

- [REDACTED]

- [REDACTED]
- There are no faults or fractures identified in the AoR that will impact the confinement of CO₂ injectate. The [REDACTED] has proven to seal hydrocarbons at pressures above which CTV will operate.

Will be operated and monitored in a manner that will limit risk of endangerment to USDWs, including risks associated with induced seismic events

- [REDACTED]
- Injection pressure will be lower than the fracture gradient of the sequestration reservoir with a safety factor (90% of the fracture gradient)
- [REDACTED]
- A seismic monitoring program will be designed to detect events lower than seismic events that can be felt. This will ensure that operations can be modified with early warning events, before a felt seismic event

Will be operated and monitored in a way that in the unlikely event of an induced event, risks will be quickly addressed and mitigated

- Via monitoring and surveillance practices (pressure and seismic monitoring program) CTV personnel will be notified of events that are considered an early warning sign. Early warning signs will be addressed to ensure that more significant events do not occur
- CTV will establish a central control center to ensure that personnel have access to the continuous data being acquired during operations

Minimizing potential for induced seismicity and separating any events from natural to induced

- Pressure will be monitored in each injector and sequestration monitoring well to ensure that pressure does not exceed the fracture pressure of the reservoir or confining zone
- Seismic monitoring program will be installed pre-injection for a period to monitor for any baseline seismicity that is not being resolved by current monitoring programs
- Average depth of prior seismic hazard in the region based on reviewed historical seismicity has been approximately 9.2km. Significantly deeper than the proposed injection zone
- [REDACTED]

2.7 Hydrologic and Hydrogeologic Information [40 CFR 146.82(a)(3)(vi), 146.82(a)(5)]

The California Department of Water Resources has defined 515 groundwater basins and subbasins with the state. The AOR is [REDACTED]

[REDACTED]

[REDACTED]

2.7.1 Hydrologic Information

[REDACTED]

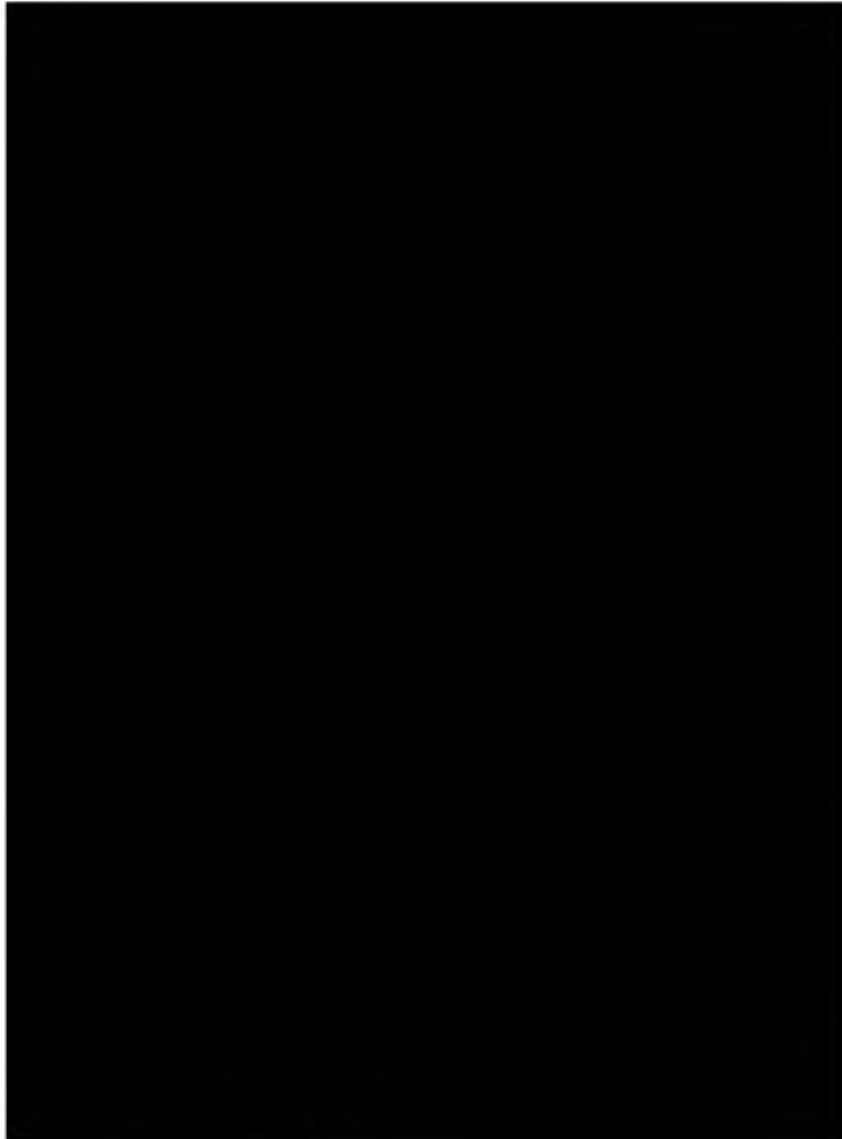


Figure 2.7-1 [REDACTED] Surface Geology, and Cross Section Index Map

2.7.2 Base of Fresh Water and Base of USDWs

The owner or operator of a proposed Class VI injection well must define the general vertical and lateral limits of all USDWs and their positions relative to the injection zone and confining zones. The intent of this information is to demonstrate the relationship between the proposed injection formation and any USDWs, and it will support an understanding of the water resources near the proposed injection wells. A USDW is defined as an aquifer or its portion which supplies any public water system; or which contains a sufficient quantity of ground water to supply a public water system; and currently supplies drinking water for human consumption; or contains fewer than 10,000 mg/l total dissolved solids; and which is not an exempted aquifer.

2.7.2.1 Base of Fresh Water

The base of fresh water (BFW) helps define the aquifers that are used for public water supply. Local water



the geologic history of freshwater sediments from which groundwater is extracted for beneficial uses as defined and regulated under SGMA.



groundwater for five water agencies. The focus of this study was the uppermost 500 feet, where most water wells were completed. Subsequently Luhdorff & Scalmanini (2016) used logs also examined for the nature of geologic units at greater depths to better define the BFW. The top of the geophysical logs tended to be at 800 feet or greater depths. These logs generally show fine-grained geologic units with few sand beds. The depth to base of fresh water was difficult to discern in available geophysical logs because of the lack of sand beds. The elevation of the base of freshwater aquifers determined from logs were plotted on a base map (see **Figure 2.7-2**). Contour lines of one hundred feet were drawn, but are variable based on well control.



Figure 2.7-2 Geologic Map and Base of Fresh Water

2.7.2.2 Base of USDWs

CTV has used geophysical logs to investigate the base of the USDW. The calculation of salinity from logs used by CTV is a four-step process:

- (1) converting measured density or sonic to formation porosity

The equation to convert measured density to porosity is:

$$POR = \frac{(R_{hom} - R_{HOB})}{(R_{hom} - R_{hof})} \quad (5)$$

Parameter definitions for the equation are:

POR is formation porosity

R_{hom} is formation matrix density grams per cubic centimeters (g/cc); 2.65 g/cc is used for sandstones

R_{HOB} is calibrated bulk density taken from well log measurements (g/cc)

R_{hof} is fluid density (g/cc); 1.00 g/cc is used for water-filled porosity

The equation to convert measured sonic slowness to porosity is:

$$POR = -1 \left(\frac{\Delta t_{ma}}{2\Delta t_f} - 1 \right) - \sqrt{\left(\frac{\Delta t_{ma}}{2\Delta t_f} - 1 \right)^2 + \frac{\Delta t_{ma}}{\Delta t_{log}} - 1} \quad (6)$$

Parameter definitions for the equation are:

POR is formation porosity

Δ_{tma} is formation matrix slowness (μs/ft); 55.5 μs/ft is used for sandstones

Δ_{tf} is fluid slowness (μs/ft); 189 μs/ft is used for water-filled porosity

Δ_{tlog} is formation compressional slowness from well log measurements (μs/ft)

- (2) calculation of apparent water resistivity using the Archie equation,

The Archie equation calculates apparent water resistivity. The equation is:

$$R_{wah} = \frac{POR^m R_t}{a} \quad (7)$$

Parameter definitions for the equation are:

R_{wah} is apparent water resistivity (ohmm)

POR is formation porosity

m is the cementation factor; 2 is the standard value

R_t is deep reading resistivity taken from well log measurements (ohmm)

a is the archie constant; 1 is the standard value

- (3) correcting apparent water resistivity to a standard temperature

Apparent water resistivity is corrected from formation temperature to a surface temperature standard of 75 degrees Fahrenheit:

$$R_{wahc} = R_{wah} \frac{TEMP + 6.77}{75 + 6.77} \quad (8)$$

Parameter definitions for the equation are:

R_{wahc} is apparent water resistivity (ohmm), corrected to surface temperature

TEMP is down hole temperature based on temperature gradient (DegF)

- (4) converting temperature corrected apparent water resistivity to salinity.

The following formula was used (Davis 1988):

$$SAL_{a_EPA} = \frac{5500}{Rwahc} \quad (9)$$

Parameter definitions for the equation are:
 SAL_a_EPA is salinity from corrected Rwahc (ppm)

The base of fresh water and the USDW are shown on the geologic Cross Section A-A' (**Figure 2.2-4**) The base of fresh water and based of the lowermost USDW are at a measure depths of approximately 600 ft bgs and 2,400 ft bgs, respectively.

2.7.3 Formations with USDWs



2.7.3.1 Alluvium

The Alluvium (Q) includes sediments deposited in the channels of active streams as well as overbank deposits and terraces of those streams. They consist of unconsolidated silt, sand, and gravel. Sand and gravel zones in the younger alluvium are highly permeable and yield significant



2.7.3.2 Flood Basin and Intertidal Deposits

These sediments consist of peaty mud, clay, silt, sand and organic materials. Stream-channel deposits of coarse sand and gravel are also included in this unit. The flood basin deposits have low permeability and generally yield low quantities of water to wells due to their fine-grained nature. Flood basin deposits generally contain poor quality groundwater with occasional zones of fresh water. The maximum thickness of the unit is about 1,400 feet (DWR 2006).

2.7.3.3 Alluvial Fan Deposits

Along the southern margin of the Subbasin, in the Non-Delta uplands areas of the Subbasin are fan deposits (Qf) from the Coast Ranges. These deposits consist of loosely to moderately compacted sand, silt, and gravel deposited in alluvial fans during the Pliocene and Pleistocene ages. The fan deposits likely interfinger with the Flood Basin Deposits. The thickness of these fans is about 150 feet (DWR 2006).

[REDACTED]

[REDACTED]

[REDACTED]

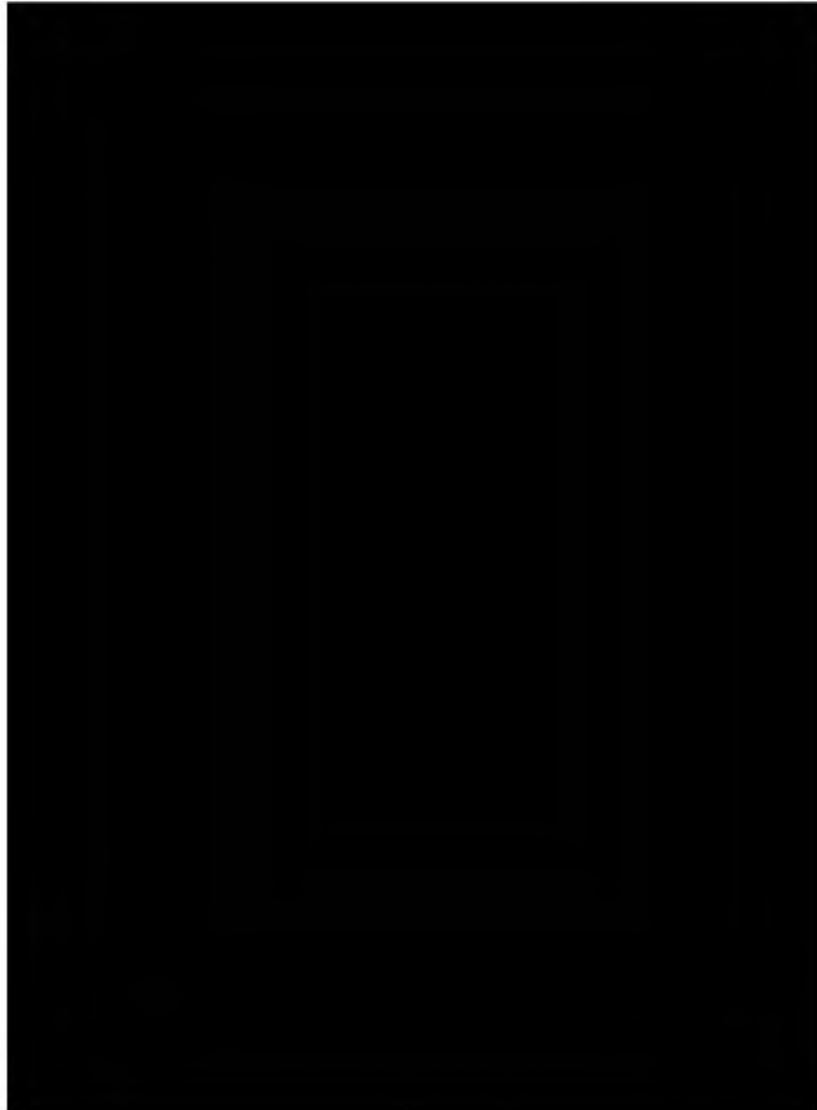


Figure 2.7-3 Estimated Corcoran Clay Thickness and Extent

2.7.3.6 Undifferentiated Non-marine Sediments

The upper Paleogene and Neogene sequence begin with the Valley Springs Formation which represents fluvial deposits that blanket the entire southern Sacramento Basin. The unconformity at the base of the Valley Springs marks a widespread Oligocene regression and separates the more deformed Mesozoic and lower Paleogene strata below from the less deformed uppermost Paleogene and Neogene strata above. These undifferentiated non-marine sediments contain approximately 3,000 - 10,000 milligrams per liter (mg/l) total dissolved solids (TDS) water and is the lowermost USDW in the AoR (**Figure 2.2-4**).

2.7.4 Geologic Cross Sections Illustrating Formations with USDWs

illustrate the relationship of the geologic units. The geologic sections were originally prepared for

[REDACTED]



Geologic Cross Section C-C' (**Figure 2.7-5**) runs [REDACTED]
Delta area. [REDACTED]

[REDACTED] Where the clay location is uncertain, no wells were present that penetrated deep enough to confirm its presence or absence. The base of fresh water varies throughout the Subbasin and is shown on the sections. It is as shallow as -400 feet msl to as much as -2,000 feet msl (GEI 2021).



Figure 2.7-5 Geologic Cross Section C-C'

2.7.5 Principal Aquifers



2.7.5.1 Upper Aquifer

The Upper Aquifer is used by domestic, community water systems, and for agriculture. The Upper aquifer also supports native vegetation where groundwater levels are less than 30 feet bgs (GEI 2021).

The Upper Aquifer is an unconfined to semi-confined aquifer. [REDACTED]



There are multiple coarse-grained sediment layers that make up the unconfined aquifer, however the water levels are generally similar. Generally, the aquifer confinement tends increase with depth becoming semi-confined conditions. There is also typically a downward gradient in the

aquifers (Hotchkiss and Balding 1971) in the non-Delta areas; the gradient ranges from a few feet bgs to as much as 70 feet bgs. The groundwater levels in the Upper Aquifer are usually 10 to 30 feet higher than in the Lower Aquifer. The groundwater levels in the Delta are typically at sea level and artesian flowing wells are common in the center of the islands (Hydrofocus 2015).

The hydraulic characteristics of the unconfined aquifer are highly variable. The USGS estimated horizontal hydraulic conductivity values for organic sediments ranging from 0.0098 ft/d to 133.86 ft/d (Hydrofocus 2015). Wells in the unconfined aquifer produce 6 to 5,300 gpm. The transmissivity of the unconfined aquifers, ranges between 600 to greater than 2,300 gallons per day per foot (gpd/ft). The storativity is about 0.05 (GEI 2021).

Water quality in the Upper Aquifer is mostly transitional, with no single predominate anion. Most water are characterized as sulfate bicarbonate and chloride bicarbonate type (Hotchkiss and Balding 1971). The TDS of these transitional water ranges between 400 to 4,200 mg/L. Nitrate is generally high in the Upper aquifer in the non-Delta portions of the Subbasin. Nitrate is generally low in the Delta portions of the Subbasin (GEI 2021).

2.7.5.2 Lower Aquifer

[REDACTED]

The groundwater levels are generally deeper than water levels in the Upper Aquifer (Hotchkiss and Balding 1971). Groundwater levels in the confined aquifer are about -25 to -75 feet msl. The groundwater levels are normally 60 to 200 feet above the top of the Corcoran Clay.

Wells in the Lower Aquifer produce about 700 to 2,500 gpm. The transmissivity typically ranges from 12,000 to 37,000 gpd/ft, but can be 120,000 gpd/ft. The storage coefficient or storativity has been measured to be 0.0001 (Padre 2004).

Water quality in the Lower Aquifer in the western portions are chloride type water but mostly transitional type of sulfate chloride near the valley margins and sulfate bicarbonate and bicarbonate sulfate near the San Joaquin River (Hotchkiss and Balding 1971). In general, the TDS ranges between 400 and 1,600 mg/L. Nitrate is typically low in the Lower Aquifer. [REDACTED]

[REDACTED]

2.7.6 Potentiometric Maps

[REDACTED]

which have been reported to DWR's CASGEM or Water Data Library systems. To evaluate groundwater levels, the GSP only used wells with known total depths and construction details so

that the wells were assigned to a principal aquifer. To supplement data from these wells, additional monitoring wells were located that were being used for other regulatory programs.

2.7.6.1 Upper Aquifer

Groundwater elevations in the Delta area are typically below sea level because the ground

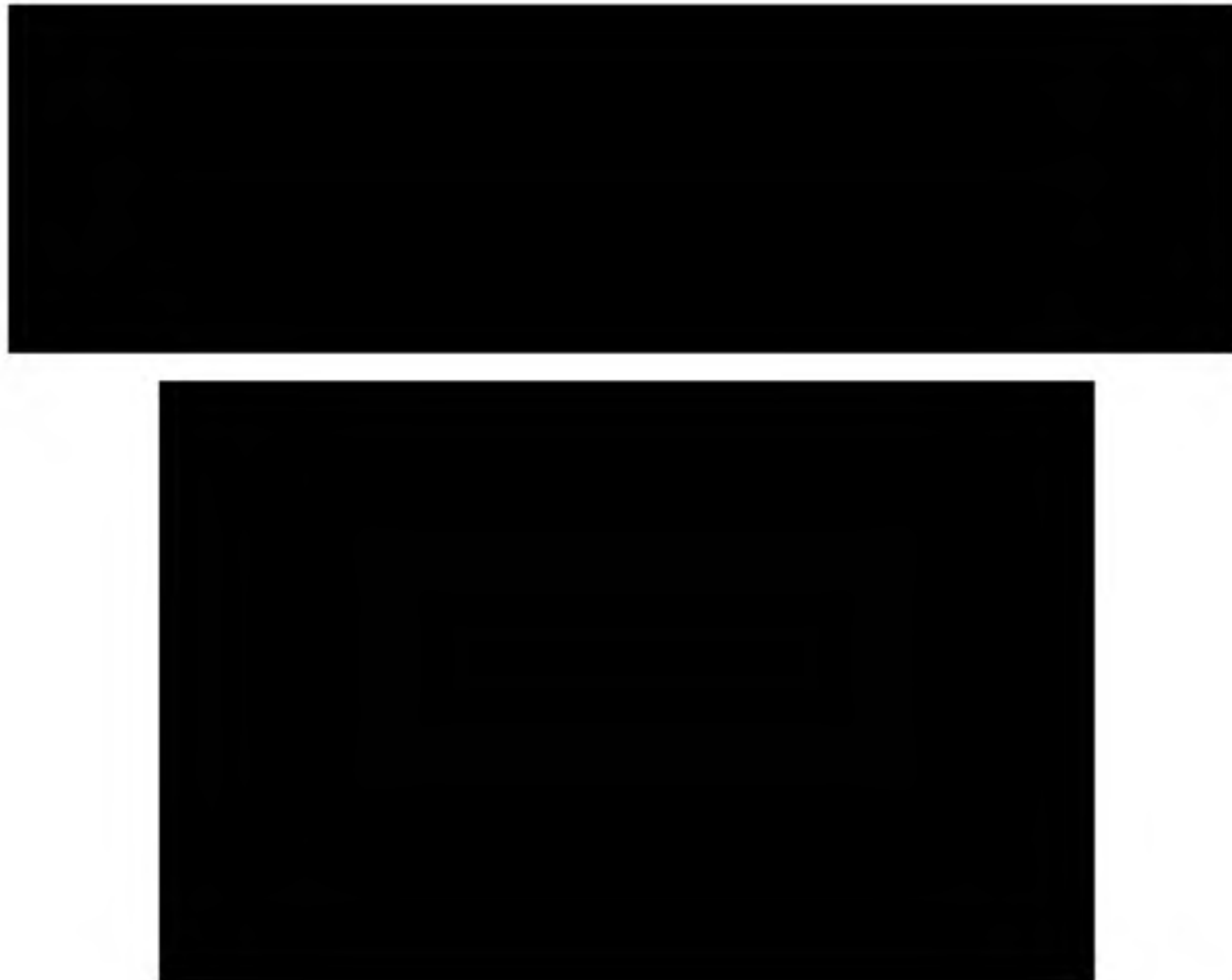
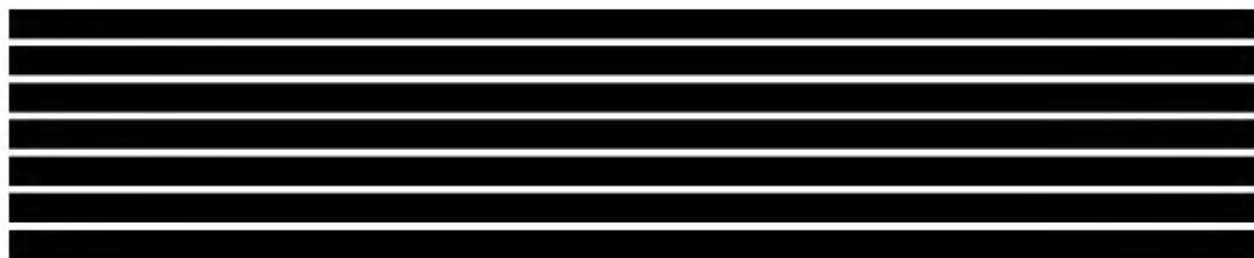


Figure 2.7-6 Principal Aquifer Schematic Profile



are perpendicular to the Stanislaus-San Joaquin County line, suggesting that there is no flow in the Upper Aquifer between the subbasins, other than the areas of the Delta Mendota Subbasin north of the County line, where water apparently flows into and out of both subbasins.

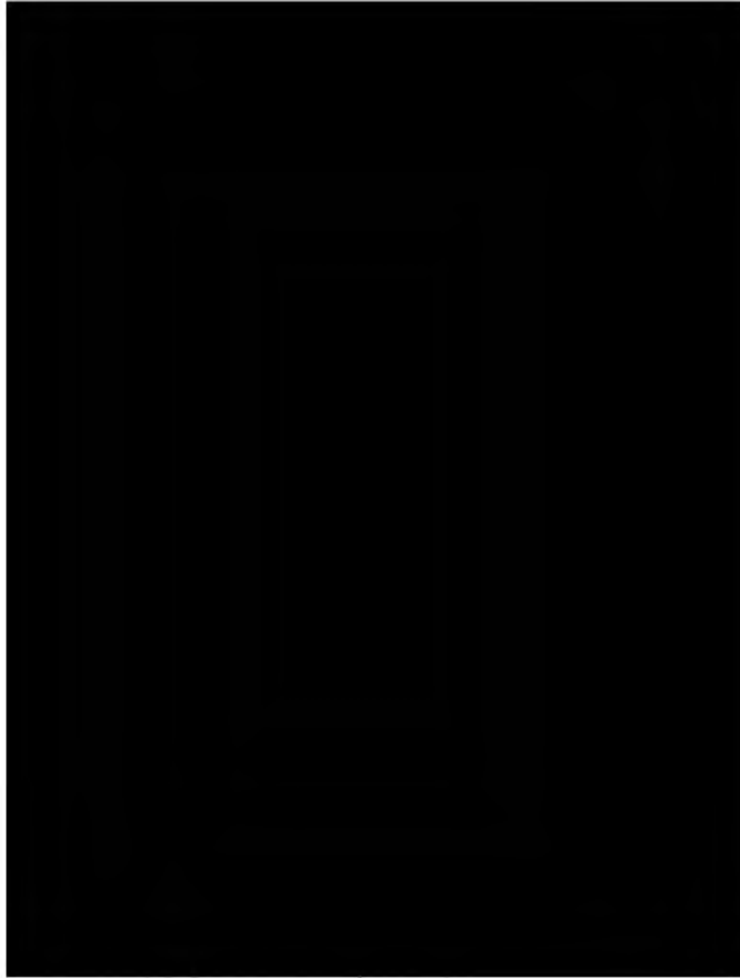


Figure 2.7-7 Upper Aquifer Groundwater Elevations Fall 2019

2.7.6.2 Lower Aquifer

[REDACTED]
at [REDACTED] Groundwater contours for the Lower Aquifer were developed using data from the CASGEM monitoring wells that [REDACTED]

[REDACTED] Groundwater monitoring well data were used from [REDACTED]



Figure 2.7-8 Lower Aquifer Groundwater Elevations Spring 2019

Groundwater elevation contours in the Lower Aquifer imply groundwater is entering the subbasin from the south (Delta Mendota Subbasin) and from the east (Eastern San Joaquin Subbasin). [REDACTED]

[REDACTED]
[REDACTED]
[REDACTED]

The groundwater gradient in Fall 2019 [REDACTED]
[REDACTED] Due to the pumping depression, the gradient increases around the [REDACTED]. The gradient near the western edge

2.7.7 Water Supply and Groundwater Monitoring Wells

The California State Water Resources Control Board Groundwater Ambient Monitoring Assessment Program (GAMA), the Department of Water Resources (DWR), CASGEM, and other public databases were searched to identify any water supply and groundwater monitoring wells within a one-mile radius of the AOR. There are no wells with the AoR. Seven water supply wells were identified within one mile of the AoR. Data provided from public databases indicate that the wells identified are completed much shallower than the proposed injection zone. A map of well locations and table of information are found in **Figure 2.7-9 Water Well Map** and **Table 2.7-1 Water Well Information**, respectively.

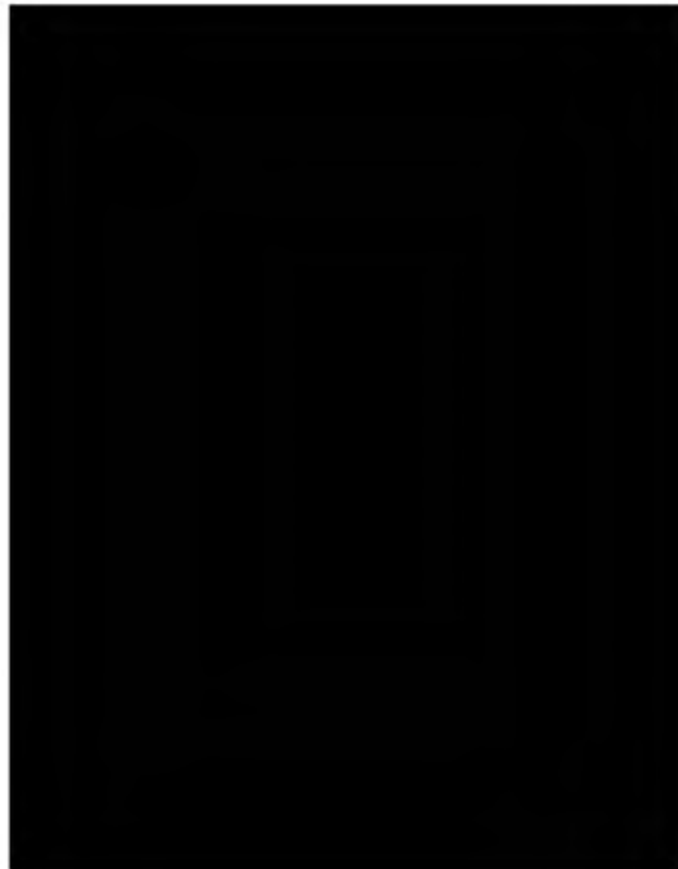


Figure 2.7-9 Water Well Location Map

Groundwater in the Subbasin is used for municipal, industrial, irrigation, domestic, stock watering, frost protection, and other purposes. The number of water wells is based on well logs filed and contained within public records may not reflect the actual number of active wells

because many of the wells contained in files may have been destroyed and others may not have been recorded.





2.8 Geochemistry [40 CFR 146.82(a)(6)]

2.8.1 Formation Geochemistry



2.8.2 Fluid Geochemistry

 The well  was sampled for water in 2015. The measurement of total dissolved solids (TDS) for the sample is 15595 mg/L. The complete water chemistry is shown in **Figure 2.8-1**.

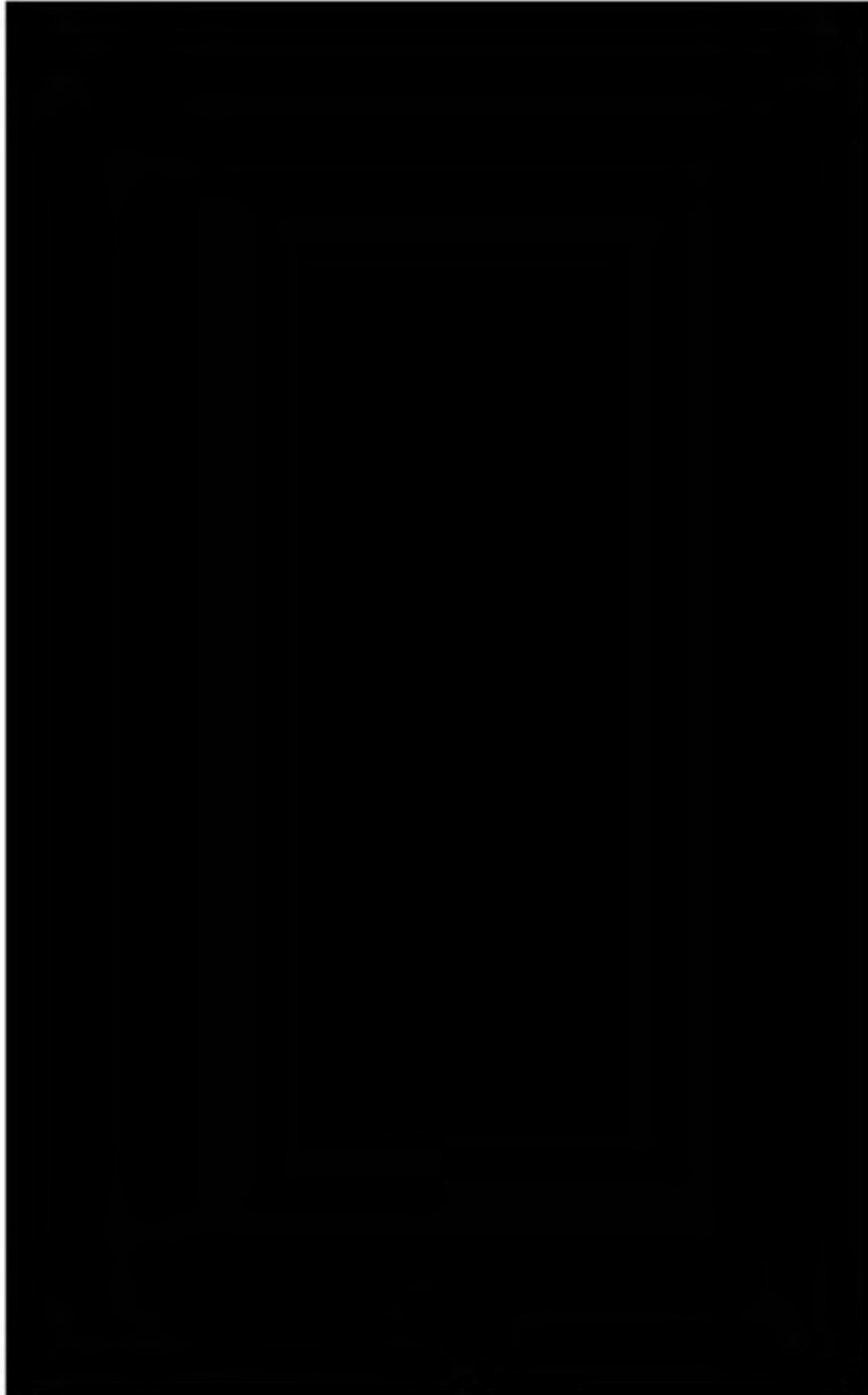
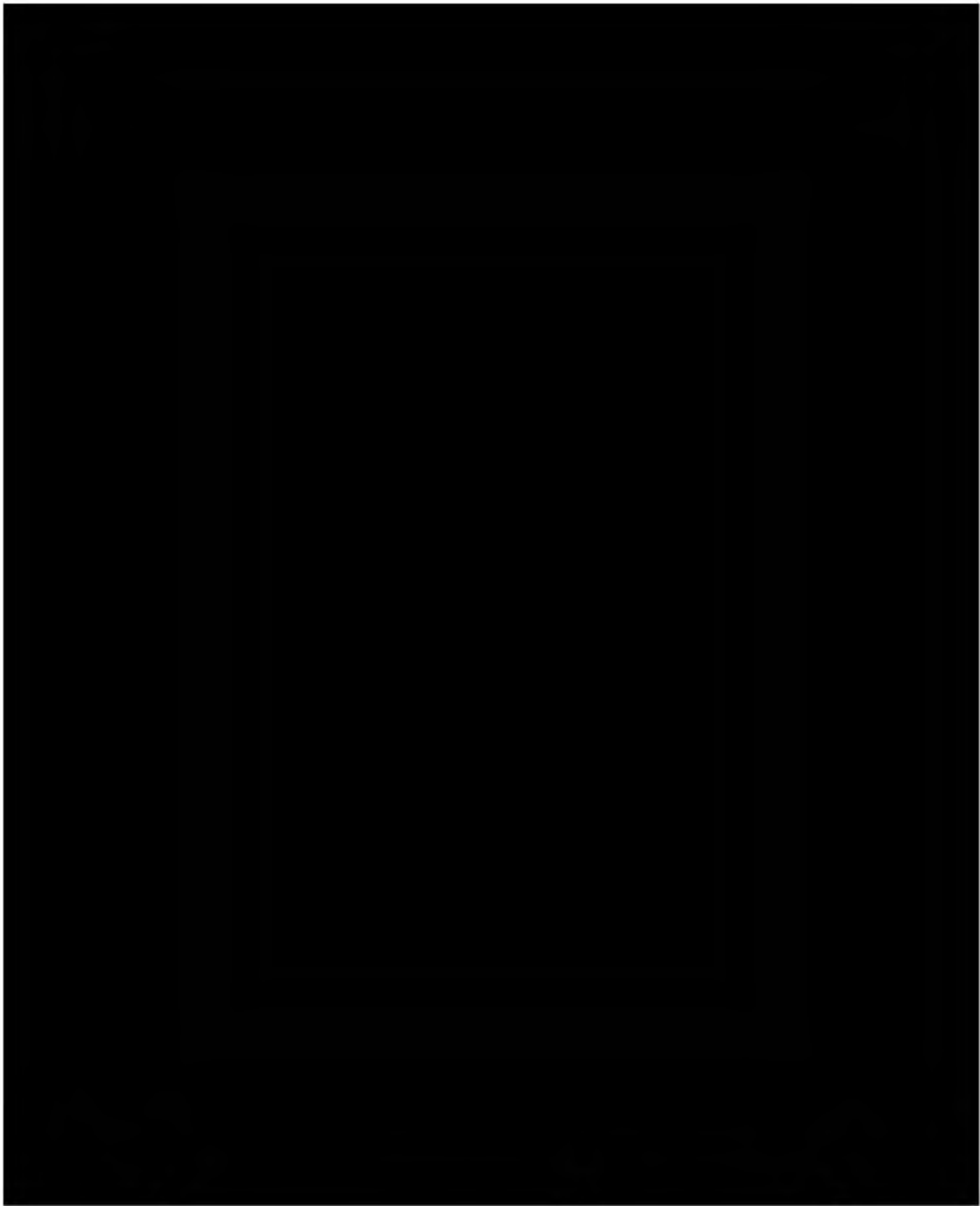


Figure 2.8-1: Water geochemistry for [REDACTED]

[REDACTED]
[REDACTED]



[REDACTED]

The location of the [REDACTED] and the [REDACTED] is shown in Figure 2.8-3.



Figure 2.8-3: Location of wells with geochemistry data.

2.8.3 Fluid-Rock Reactions

[REDACTED]

[REDACTED]

[REDACTED]

[REDACTED]

[REDACTED]

[REDACTED]

[REDACTED]

[REDACTED]

[REDACTED]

[REDACTED]

[REDACTED]

[REDACTED]

2.8.3.2 Upper Confining Zone [REDACTED]

There is no fluid geochemistry analysis for the upper confining zone. The shale will only provide fluid for analysis if stimulated. However, given the low permeability of the rock and the low carbonate content, the upper confining zone is not expected to be impacted by the CO₂ injectate.

2.8.3.2 [REDACTED]

There is no fluid geochemistry analysis for the [REDACTED] The shale will only provide fluid for analysis if stimulated. However, given the low permeability of the rock and the low carbonate content, the [REDACTED] [REDACTED] is not expected to be impacted by the CO₂ injectate.

2.9 Other Information (Including Surface Air and/or Soil Gas Data, if Applicable)

No additional information necessary.

2.10 Site Suitability [40 CFR 146.83]

[REDACTED]
[REDACTED]
[REDACTED]
[REDACTED]
[REDACTED]
[REDACTED]
[REDACTED]

[REDACTED]
[REDACTED]
[REDACTED]
[REDACTED]
[REDACTED]
[REDACTED]
[REDACTED]

Thickness maps and petrophysics demonstrate confinement based on the upper confining intervals laterally continuity, low-permeability, and thickness. [REDACTED]

[REDACTED]
[REDACTED]
[REDACTED]

[REDACTED]
[REDACTED]
[REDACTED]
[REDACTED]



Figure 2.10-1. [REDACTED]

CTV estimates maximum storage for the proposed project is █ MMT of CO₂. This was derived from computational modeling.

3.0 AoR and Corrective Action

CTV's AoR and Corrective Action plan pursuant to 40 CFR 146.82(a)(4), 40 CFR 146.82(a)(13) and 146.84(b), and 40 CFR 146.84(c) describes the process, software, and results to establish the AoR, and the wells that require corrective action.

AoR and Corrective Action GSDT Submissions

GSDT Module: AoR and Corrective Action

Tab(s): All applicable tabs

Please use the checkbox(es) to verify the following information was submitted to the GSDT:

- ☒ Tabulation of all wells within AoR that penetrate confining zone [40 CFR 146.82(a)(4)]
- ☒ AoR and Corrective Action Plan [40 CFR 146.82(a)(13) and 146.84(b)]
- ☒ Computational modeling details [40 CFR 146.84(c)]

4.0 Financial Responsibility

CTV's Financial Responsibility demonstration pursuant to 40 CFR 146.82(a)(14) and 40 CFR 146.85 is met with a line of credit for Injection Well Plugging and Post-Injection Site Care and Site Closure and insurance to cover Emergency and Remedial Responses.

Financial Responsibility GSDT Submissions

GSDT Module: Financial Responsibility Demonstration

Tab(s): Cost Estimate tab and all applicable financial instrument tabs

Please use the checkbox(es) to verify the following information was submitted to the GSDT:

- ☒ Demonstration of financial responsibility [40 CFR 146.82(a)(14) and 146.85]

5.0 Injection and Monitoring Well Construction



Injection and monitoring well construction is addressed in Attachment G: Well Construction and Testing of the application, which includes the well construction approach for all proposed injection and monitoring wells. Appendix C-1: Injection and Monitoring Well Schematics provides casing diagrams, well construction tables, and completion details.

5.1 Proposed Stimulation Program [40 CFR 146.82(a)(9)]

There are no proposed stimulation programs currently.

5.2 Construction Procedures [40 CFR 146.82(a)(12)]

New wells will be drilled during pre-operational testing, and no major drilling and completion issues are anticipated. [REDACTED]

- Well designs will be sufficient to withstand all anticipated load cases including safety factors
- Multiple cemented casing strings will protect shallow USDW-bearing zones from contacting injection fluid
- All casing strings will be cemented in place with volume sufficient to place cement to surface using industry-proven recommended practices for slurry design and placement
- Cement bond logging (CBL) will be used to verify presence of cement in the production casing annulus through and above the confining layer
- Mechanical integrity testing (MIT) will be performed on the tubing and the tubing/casing annulus. This is described in further detail in Attachment G: Construction Details.
- Upper completion design enables monitoring devices to be installed downhole, cased hole logs to be acquired and MIT to be conducted.
- All wellhead equipment and downhole tubulars will be designed to accommodate the dimensions necessary for deployment of monitoring equipment such as wireline-conveyed logging tools and sampling devices.
- Realtime surface monitoring equipment with remote connectivity to a centralized facility and alarms provides continual awareness to potential anomalous injection conditions
- Annular fluid (packer fluid) density and additives to mitigate corrosion provide additional protection against mechanical or chemical failure of production casing and upper completion equipment

Well materials utilized will be compatible with the CO₂ injectate and will limit corrosion.

- Wellhead – stainless steel or other corrosion resistant alloy
- Casing – 13Cr L-80 or other corrosion resistant alloy in specified sections of production string (ie. flow-wetted casing)
- Cement – Portland cement has been used extensively in enhanced oil recovery (EOR) injectors. Data acquired from existing wells supports that the materials are compatible with CO₂ where good cement bond between formation and casing exists.
- Tubing – 13Cr L-80 or other corrosion resistant alloy
- Packer – corrosion resistant alloy and hardened elastomer

Well materials follow the following standards:

- API Spec 6/CT ISO 11960 – Specifications for Casing and Tubing
- API Spec 10A/ISO 10426-1 – Specifications for Cements and Materials for Cementing
- API Spec 11D1/ISO 14310 – Downhole Equipment – Packers and Bridge Plugs

5.2.1 Casing and Cementing

The casing specification in Appendix C-1: Injection and Monitoring Well Schematics are sufficient to meet the requirements of 40 CFR 146.86(b)(1)(iv) and to allow for the safe operation at bottomhole injection conditions that will not exceed the maximum allowable operating pressure (MAOP) of 0.63 psi/ft, specified in the Appendix: Operating Procedures and to be confirmed during pre-operational testing.

[REDACTED]
[REDACTED] Standard cementing and casing best practices are sufficient to ensure successful placement and isolation. Industry standard practices and procedures for designing and placing primary cement in the casing annuli will be utilized to ensure mechanical integrity of cement and casing. Staged cementing is not an anticipated requirement.

Operational parameters acquired throughout the cementing operation will be used to compare modeled versus actual pressure and rate. The presence of circulated cement at surface will also be a primary indicator of effective cement placement. Cement evaluation logging will be conducted to confirm cement placement and isolation.

5.2.2 Tubing and Packer

The information in the tables provided in Appendix C-1: Injection and Monitoring Well Schematics is representative of completion equipment that will be used and meets the requirements at 40 CFR 146.86(c). Tubing and packer selection and specifications will be determined prior to completion or conversion during pre-operational testing.

6.0 Pre-Operational Logging and Testing

CTV has attached a Pre-Operational logging and testing plan pursuant to 40 CFR 146.82(a)(8) and 40 CFR 146.87.

Pre-Operational Logging and Testing GSDT Submissions

GSDT Module: Pre-Operational Testing

Tab(s): Welcome tab

Please use the checkbox(es) to verify the following information was submitted to the GSDT:

☒ Proposed pre-operational testing program [40 CFR 146.82(a)(8) and 146.87]

7.0 Well Operation

CTV has provided detailed operating procedures for each injection well. These procedures are provided for both injectors in the Appendix: Operating Procedures document. Example of operational procedure for planned injector conversion of [REDACTED] is included below.

7.1 Operational Procedures [40 CFR 146.82(a)(10)]

For a target rate of ■ million standard cubic feet per day (mmscf/d), bottom hole and surface pressures have been estimated for the well over the life of the project. These pressures were estimated using results from the reservoir simulation as an input into the multiphase well nodal analysis software – PROSPER by Petroleum Experts Ltd. PROSPER has been used extensively in CO₂ EOR to model CO₂ injection wells. The pressures have been currently calculated assuming a 100% CO₂ stream. Operating conditions will be updated as CTV defines the injection stream and impurities.

At the start of injection, surface and bottom hole injection pressures of 945 psi and 1,533 psi respectively, are required to inject the target rate. As the pressure in the reservoir builds up, increasing surface and bottom hole pressures will be required to maintain injection at the target rate. At the end of injection, the estimated surface and bottom hole pressures required are 1,425 psi and 4,711 psi, respectively.

The expected fracture pressure gradient for the injection zone is estimated to be 0.7 – 0.8 psi/ft, and 0.70 psi/ft is conservatively used for the wellbore performance modelling. Using a 10% safety factor, as per the EPA's guidelines, the maximum allowable BHP is 6,021 psi (calculated at the top perforation). Reservoir fracture gradient will be determined with step-rate testing during pre-operational testing to confirm maximum allowable injection pressure. During injection, the well will be controlled using automation to never exceed the maximum allowable bottomhole injection pressure. The estimated bottom hole pressures over the life of the project are lower than the maximum allowable bottom hole pressure of 6,021 psi.

The expected beginning and ending pressures for injector ■ are summarized in Table 7.1.

Table 7-1: Proposed operational conditions

Parameters/Conditions	Limit or Permitted Value	Unit
Maximum Allowable Pressure	Using 0.70 psi/ft frac gradient with 10% safety factor	
Surface	2,529	psig
Downhole	6,021	psig
Injection Pressure @ Target Rate	Expected range over project	
Surface – Start / End	945 / 1,425	psig
Downhole – Start / End	1,533 / 4,711	psig
Target Injection Rate	■	mmscf/d
Average Injection Volume and/or Mass	■ million	tons
Annulus Pressure @ Target Rate	Expected range over project	
Surface – Start / End	100 / 632	psig
Downhole – Start / End	4,279 / 4,811	psig
Annulus / Injection Tubing Pressure Differential	>100	psig

7.2 Proposed Carbon Dioxide Stream [40 CFR 146.82(a)(7)(iii) and (iv)]

There are currently multiple sources of anthropogenic CO₂ being considered for the project. These include capture from existing and potential future industrial sources in the Sacramento Valley area, as well as Direct Air Capture (DAC). The carbon dioxide stream will consist of a minimum of 95% CO₂ by volume. Other key constituents that will be controlled for corrosion mitigation include water content (<25 lb/mmscf) and oxygen level (<50 ppm).

Corrosiveness of the CO₂ stream is very low as long as the entrained water is kept in solution with the CO₂. This is ensured by the < 25 lb/mmscf injectate specification referred to above. Injectate water solubility will vary with depth and time as temperature and pressures change. The water specification is conservative to ensure water solubility across super-critical operating ranges. CRA tubing will be used in the injection wells to mitigate this potential corrosion impact should free-phase water be present. CTV may optimize the maximum water content specification prior to injection based on technical analysis.

8.0 Testing and Monitoring

CTV's Testing and Monitoring plan pursuant to 40 CFR 146.82 (a) (15) and 40 CFR 146.90 describes the strategies for testing and monitoring to ensure protection of the USDW, injection well mechanical integrity, and plume monitoring.

Testing and Monitoring GSDT Submissions

GSDT Module: Project Plan Submissions

Tab(s): Testing and Monitoring tab

Please use the checkbox(es) to verify the following information was submitted to the GSDT:

☒ Testing and Monitoring Plan [40 CFR 146.82(a)(15) and 146.90]

9.0 Injection Well Plugging

CTV's Injection Well Plugging Plan pursuant to 40 CFR 146.92 describes the process, materials and methodology for injection well plugging.

Injection Well Plugging GSDT Submissions

GSDT Module: Project Plan Submissions

Tab(s): Injection Well Plugging tab

Please use the checkbox(es) to verify the following information was submitted to the GSDT:

☒ Injection Well Plugging Plan [40 CFR 146.82(a)(16) and 146.92(b)]

10.0 Post-Injection Site Care (PISC) and Site Closure

CTV has developed a Post-Injection Site Care and Site Closure plan pursuant to 40 CFR 146.93 (a) to define post-injection testing and monitoring.

At this time CTV is not proposing an alternative PISC timeframe.

PISC and Site Closure GSDT Submissions

GSDT Module: Project Plan Submissions

Tab(s): PISC and Site Closure tab

Please use the checkbox(es) to verify the following information was submitted to the GSDT:

☒ PISC and Site Closure Plan [40 CFR 146.82(a)(17) and 146.93(a)]

GSDT Module: Alternative PISC Timeframe Demonstration

Tab(s): All tabs (only if an alternative PISC timeframe is requested)

Please use the checkbox(es) to verify the following information was submitted to the GSDT:

☐ Alternative PISC timeframe demonstration [40 CFR 146.82(a)(18) and 146.93(c)]

11.0 Emergency and Remedial Response

CTV's Emergency and Remedial Response plan pursuant to 40 CFR 164.94 describes the process and response to emergencies to ensure USDW protection.

Emergency and Remedial Response GSDT Submissions

GSDT Module: Project Plan Submissions

Tab(s): Emergency and Remedial Response tab

Please use the checkbox(es) to verify the following information was submitted to the GSDT:

☒ Emergency and Remedial Response Plan [40 CFR 146.82(a)(19) and 146.94(a)]

12.0 Injection Depth Waiver and Aquifer Exemption Expansion

No depth waiver or Aquifer Exemption expansion is being requested as part of this application.

Injection Depth Waiver and Aquifer Exemption Expansion GSDT Submissions

GSDT Module: Injection Depth Waivers and Aquifer Exemption Expansions

Tab(s): All applicable tabs

Please use the checkbox(es) to verify the following information was submitted to the GSDT:

- ☐ Injection Depth Waiver supplemental report *[40 CFR 146.82(d) and 146.95(a)]*
- ☐ Aquifer exemption expansion request and data *[40 CFR 146.4(d) and 144.7(d)]*

13.0 References

[REDACTED]

[REDACTED]

[REDACTED]

[REDACTED]

[REDACTED]

[REDACTED]

[REDACTED]

[REDACTED]

[REDACTED]

[REDACTED]

[REDACTED]

[REDACTED]

[REDACTED]

[REDACTED]

[REDACTED]

[REDACTED]

[REDACTED]

[REDACTED]

[REDACTED]

[REDACTED]

[REDACTED]

[REDACTED]

[REDACTED]

[REDACTED]

[REDACTED]

NARRATIVE REPORT - FIGURES

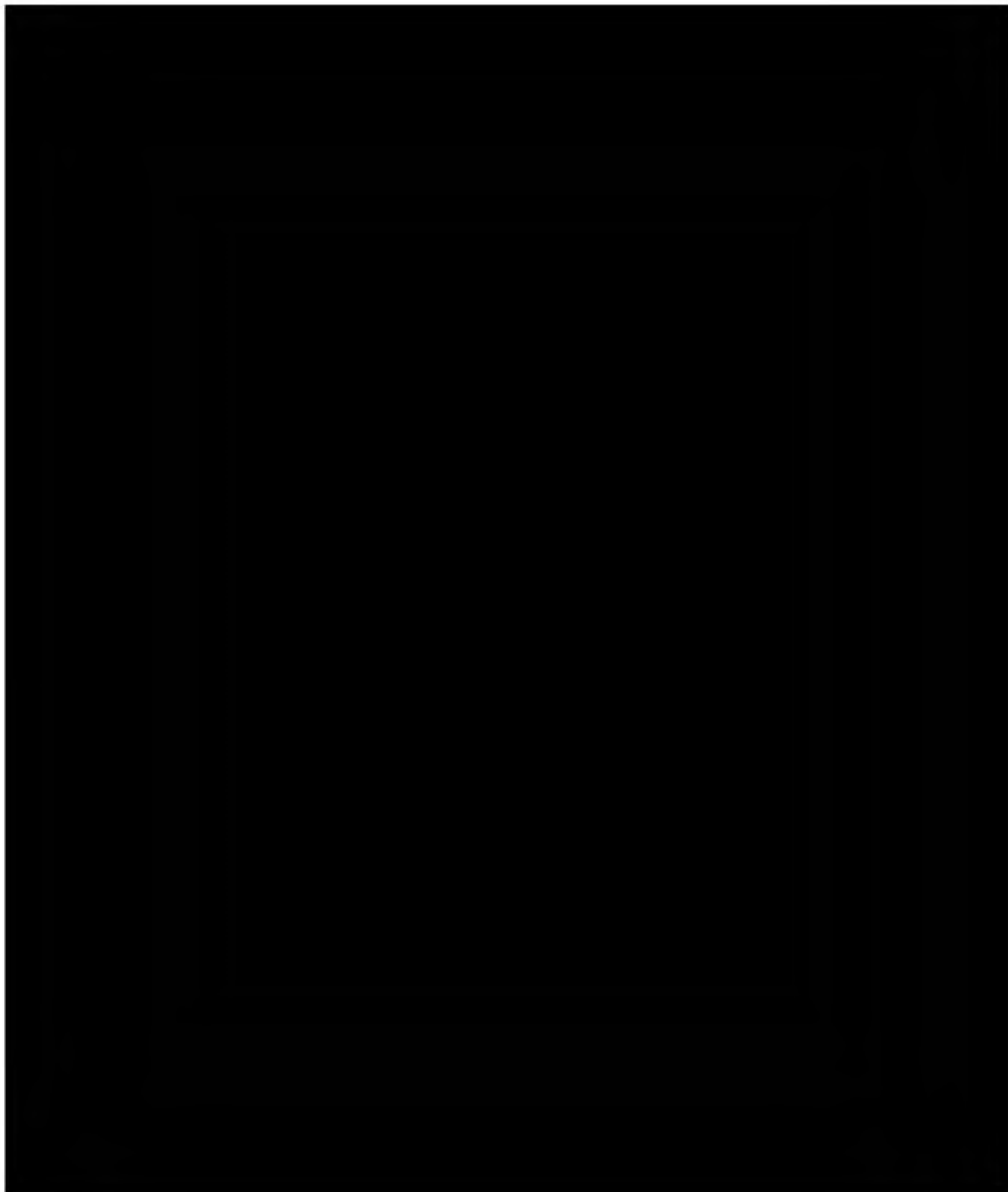


FIGURE 2.1-7. [REDACTED]
[REDACTED] Wells with relative permeability or capillary pressure data are shown as magenta circles.

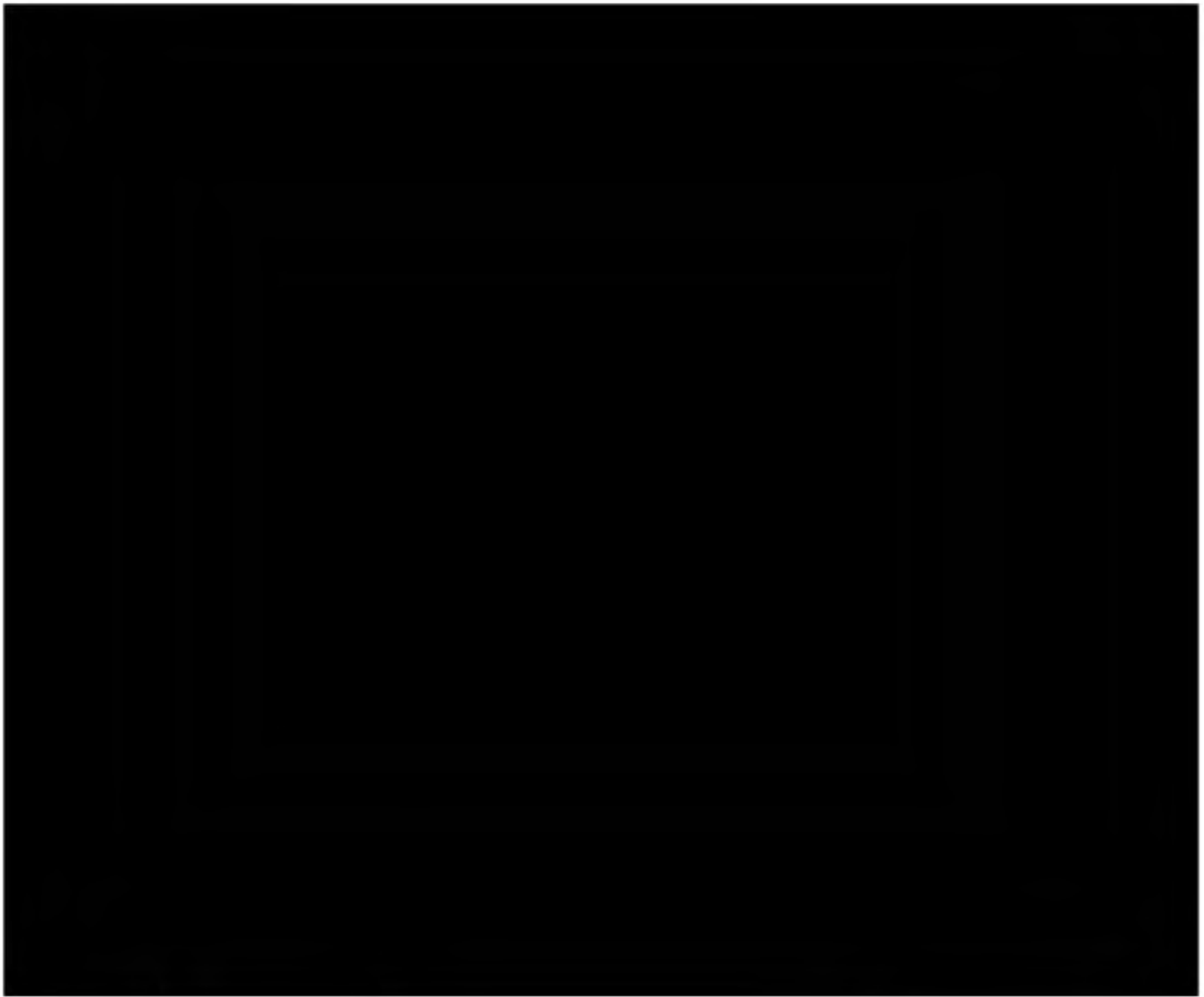


Figure 2.2-1. [REDACTED]

Figure 2.2-2. Type well taken from south of the AoR showing average rock properties used in the model for confining and injection zones.

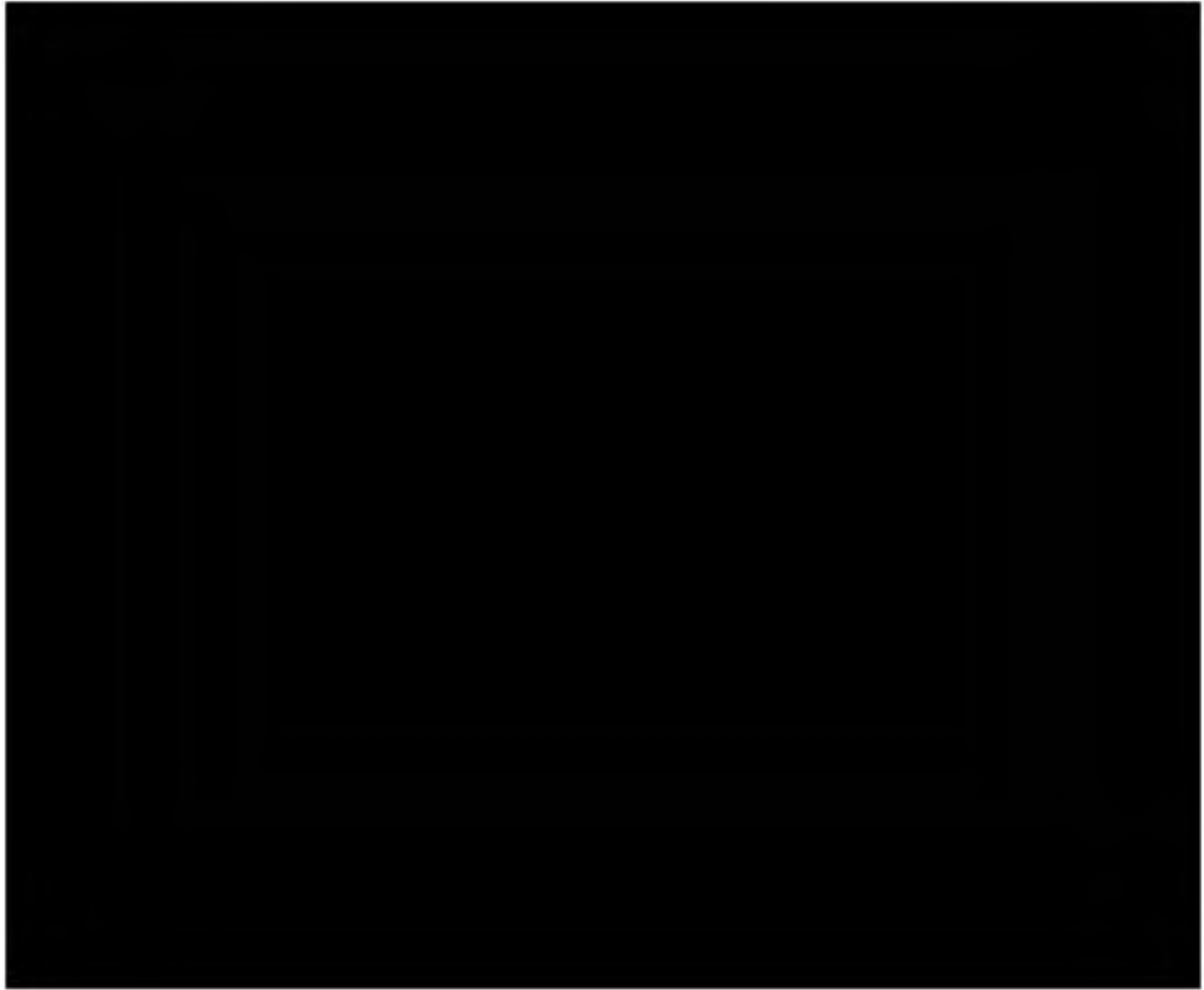


Figure 2.2-3. Summary map and area of seismic data used to build structural model. Both of the 3D surveys were acquired in 1998 and reprocessed in 2013. The 2D seismic were acquired between 1980 and 1985. California gas fields are shown for reference.

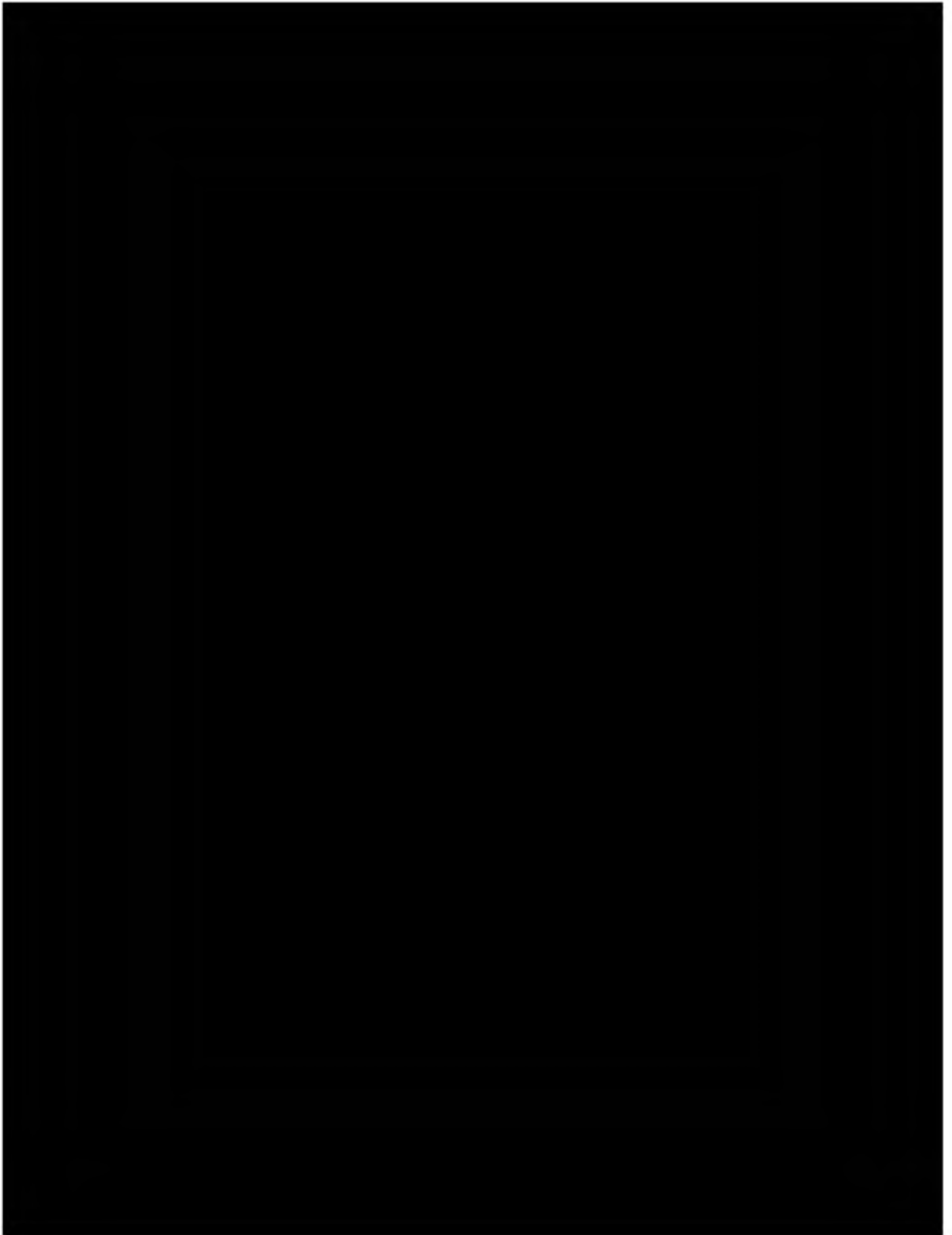


Figure 2.2-4. Cross section showing stratigraphy and lateral continuity of major formations across the project area.

Figure 2.2-5.

[REDACTED]

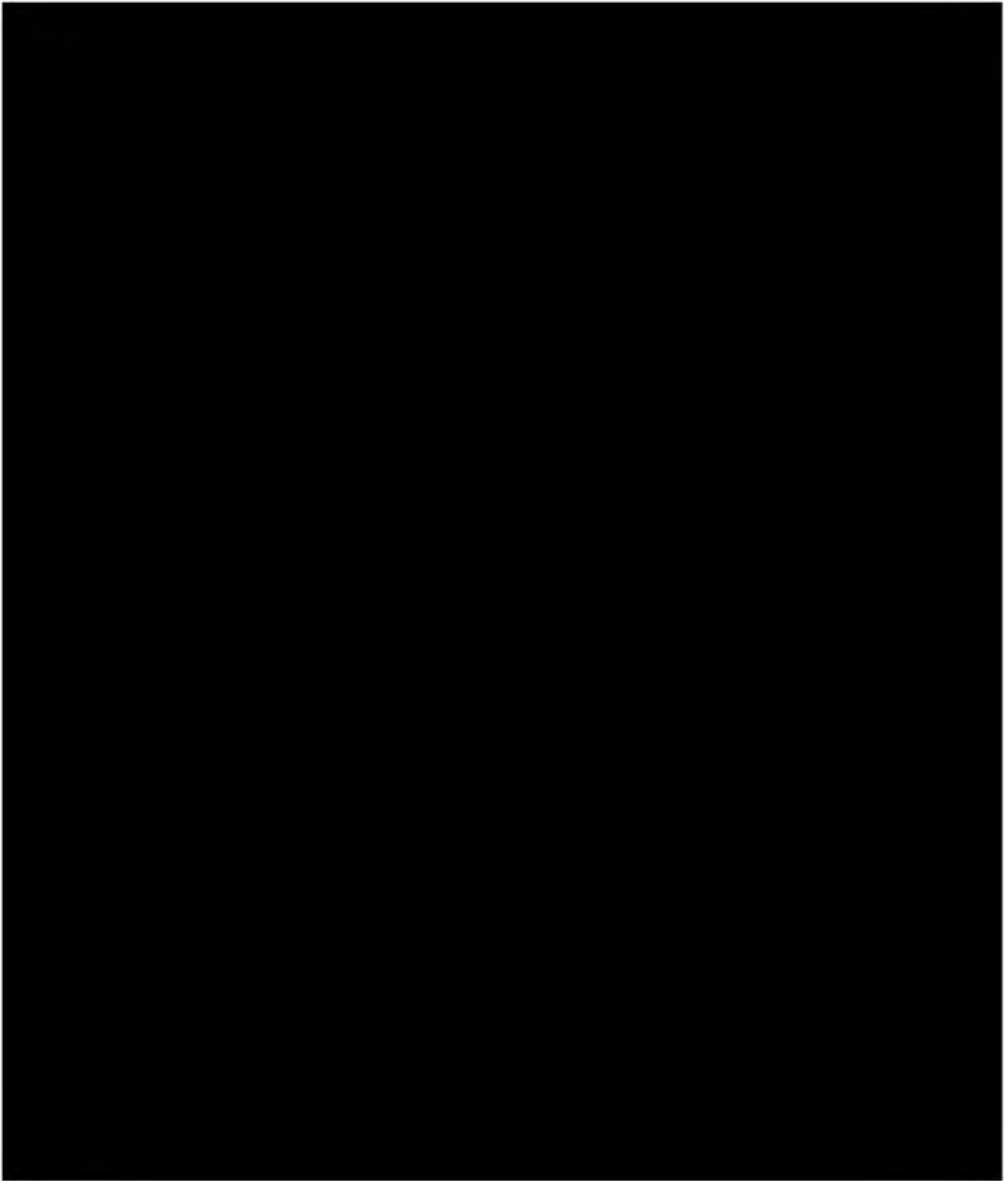


Figure 2.2-6. Injection well location map for the project area. Injection wells are 1,735 ft. apart.

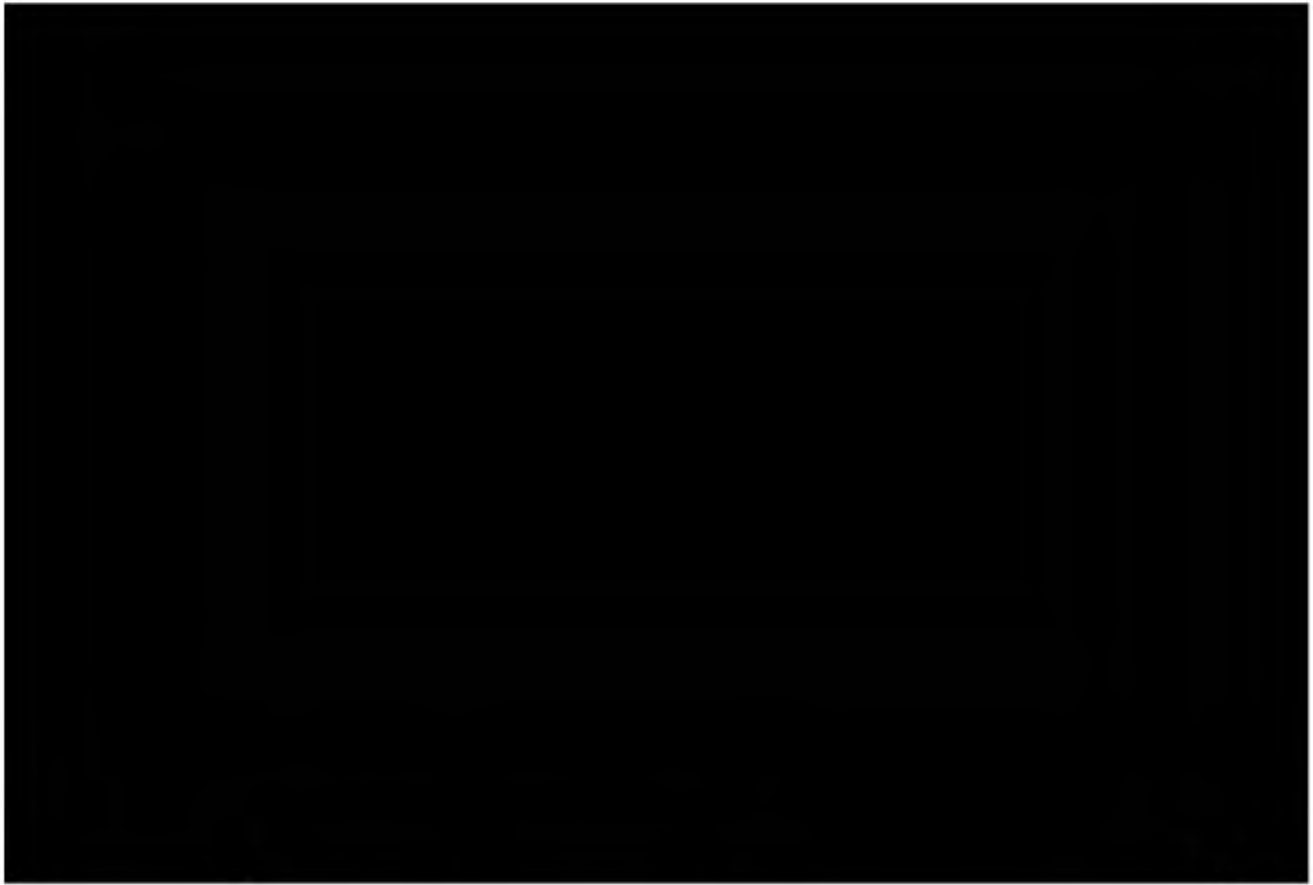


Figure 2.3-1. The [REDACTED] and is dashed into it in cross-section. Yellow line highlights the cross-section shown in **Figure 2.3-2**.



Figure 2.3-2. Structural cross section across the geologic model. Well [REDACTED] is shown with SP log (negative values to left) for correlation and geologic packages. Geologic surfaces developed from seismic interpretation. The [REDACTED] is cut-off by the Base Valley Springs. The interpreted antithetic fault to the east is dashed into the [REDACTED]



Figure 2.4-1. Map showing location of wells with mineralogy data relative to the AoR.

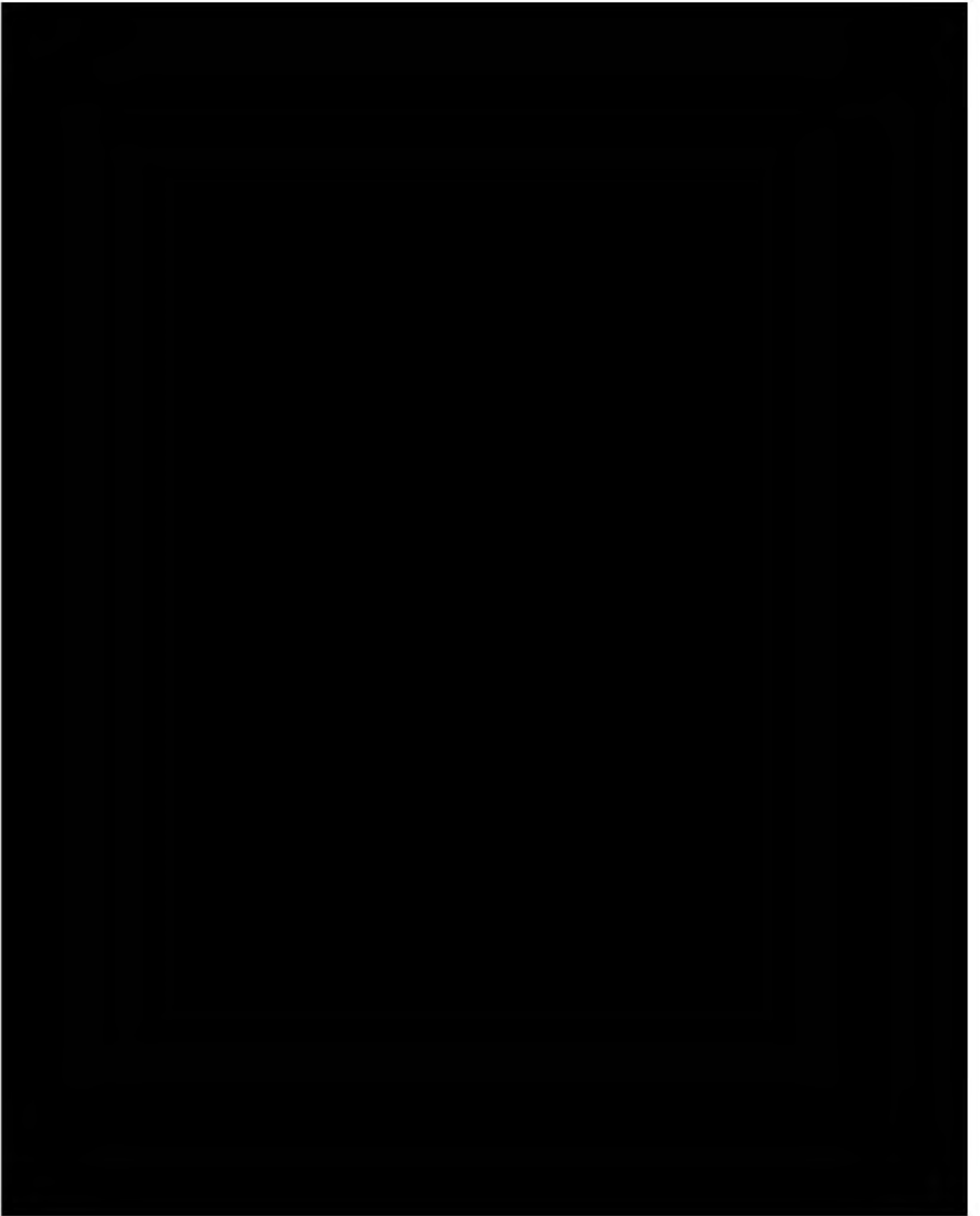
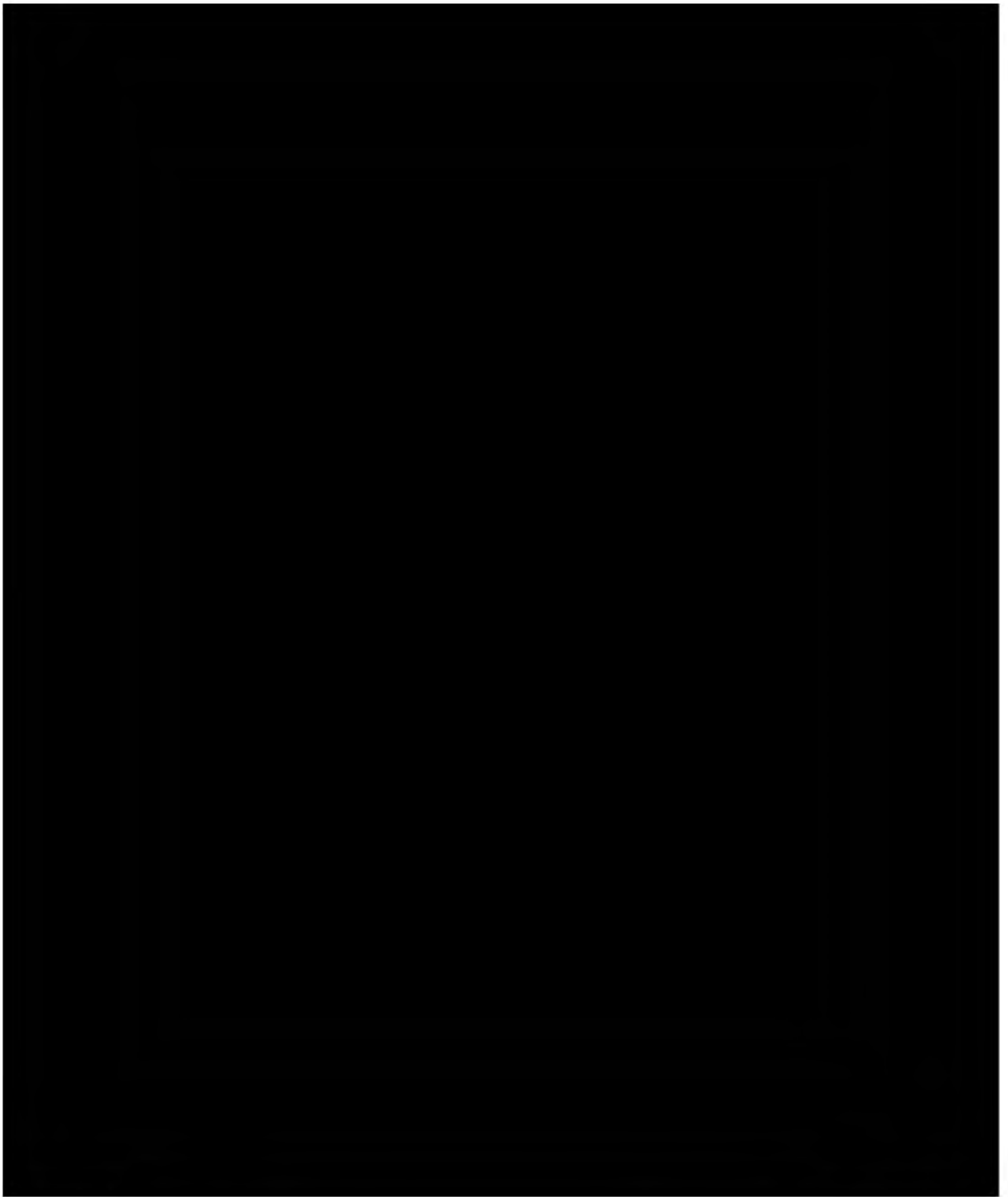


Figure 2.4-6. Map of wells with porosity and permeability data.

[REDACTED]

[REDACTED]



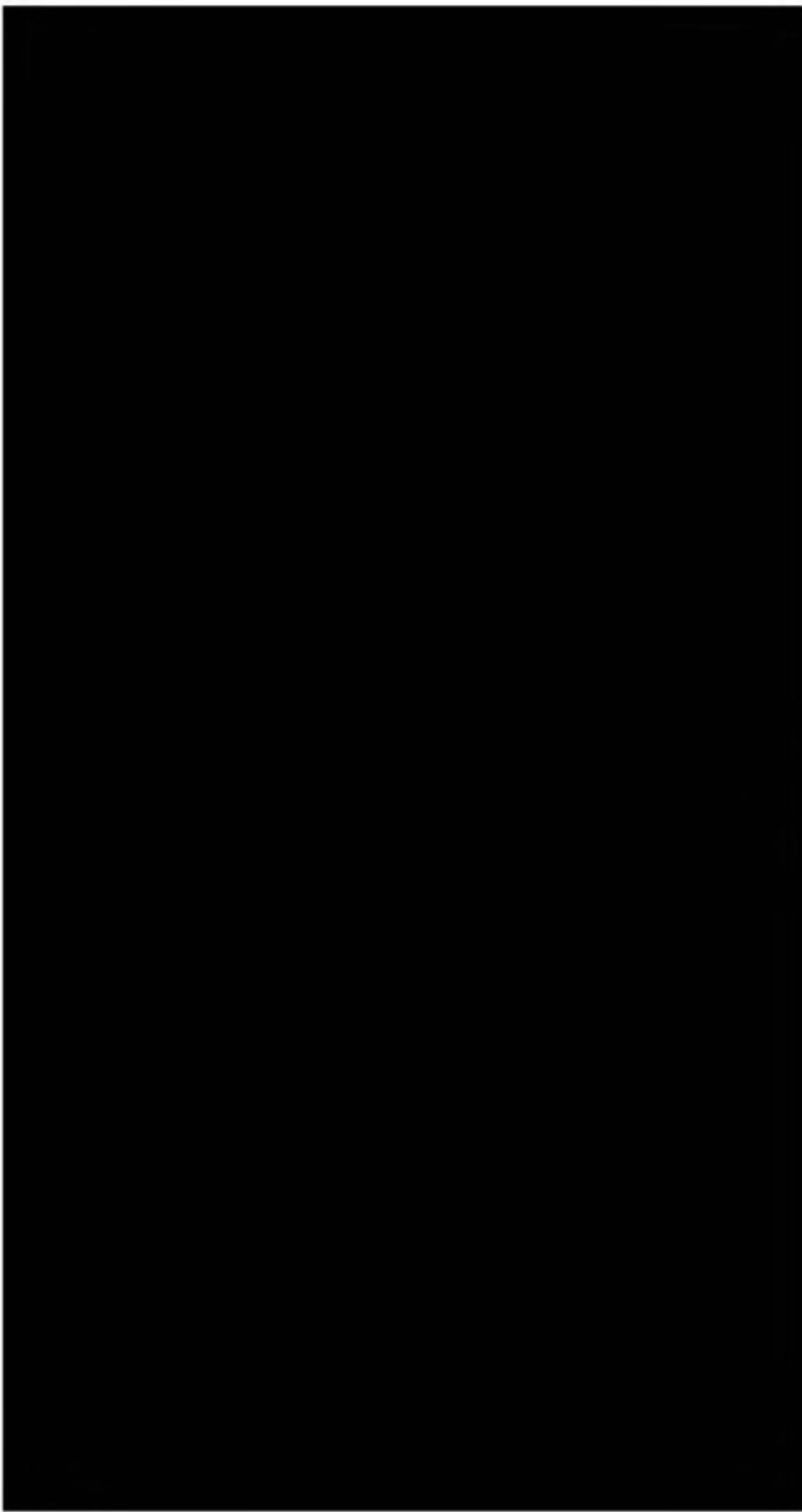


Figure 2.6-1. Fault Activity Map from the California Geologic Survey.

(<https://maps.conservation.ca.gov/cgs/fam/>).

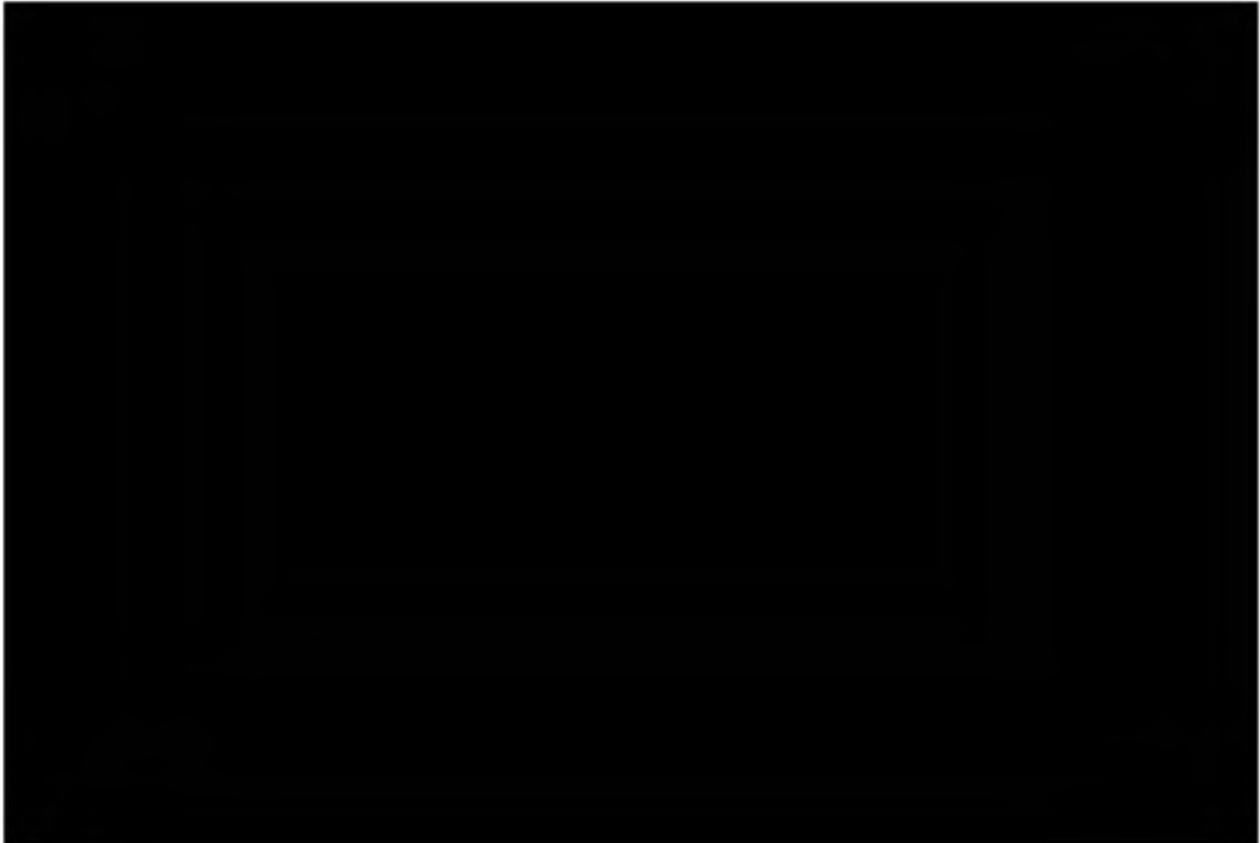


Figure 2.6-2. Image is modified from USGS search results. Data from these events are compiled in **Table 2.6-1** in chronological order associated with events 1 through 11 on the map.

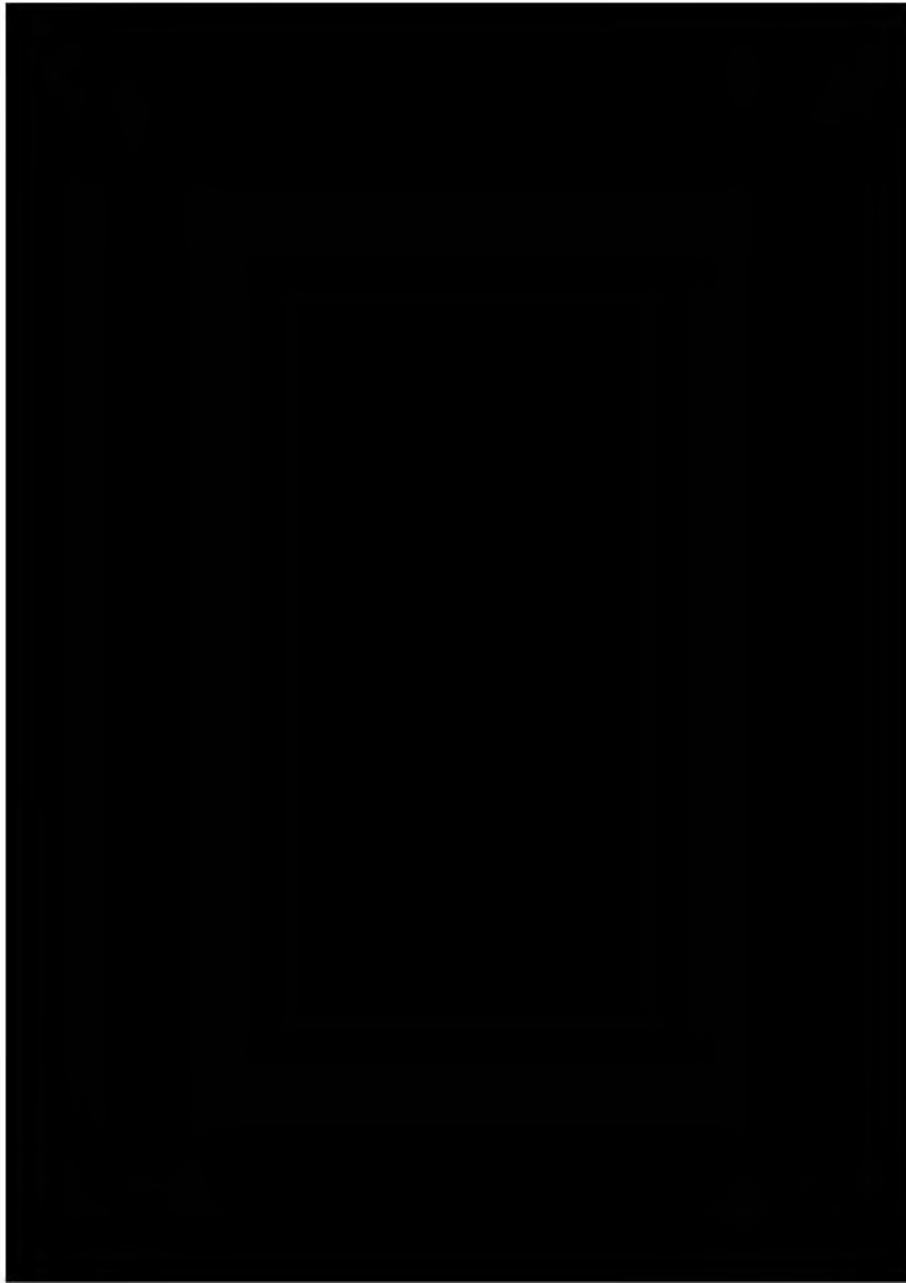


Figure 2.6-3. Image modified from Lund Snee and Zoback (2020) showing relative stress magnitudes across California. Red star indicates CTV II site area.

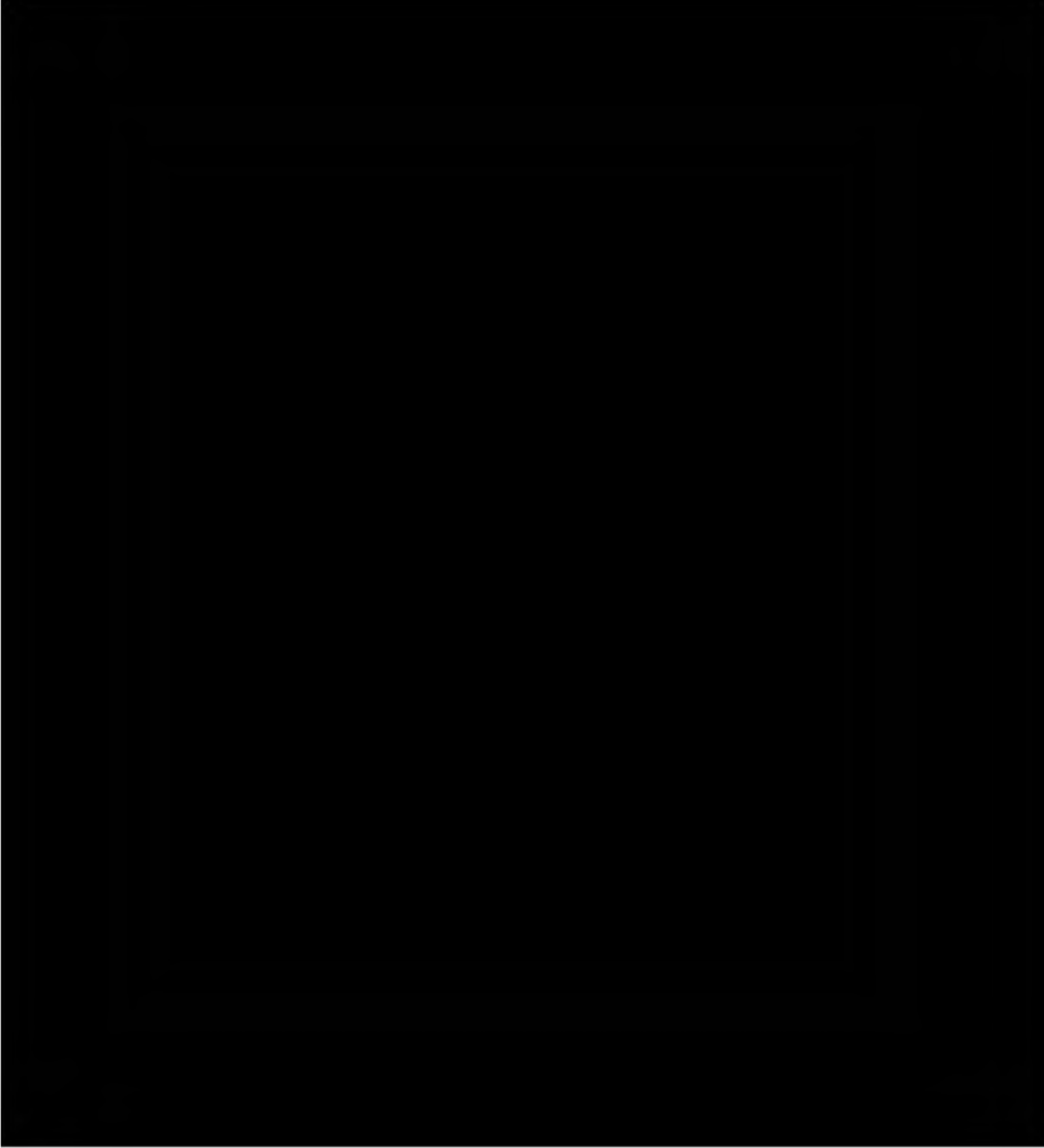


Figure 2.1-1. Location map of the proposed injection AoR (red) in relation to the Sacramento Basin.

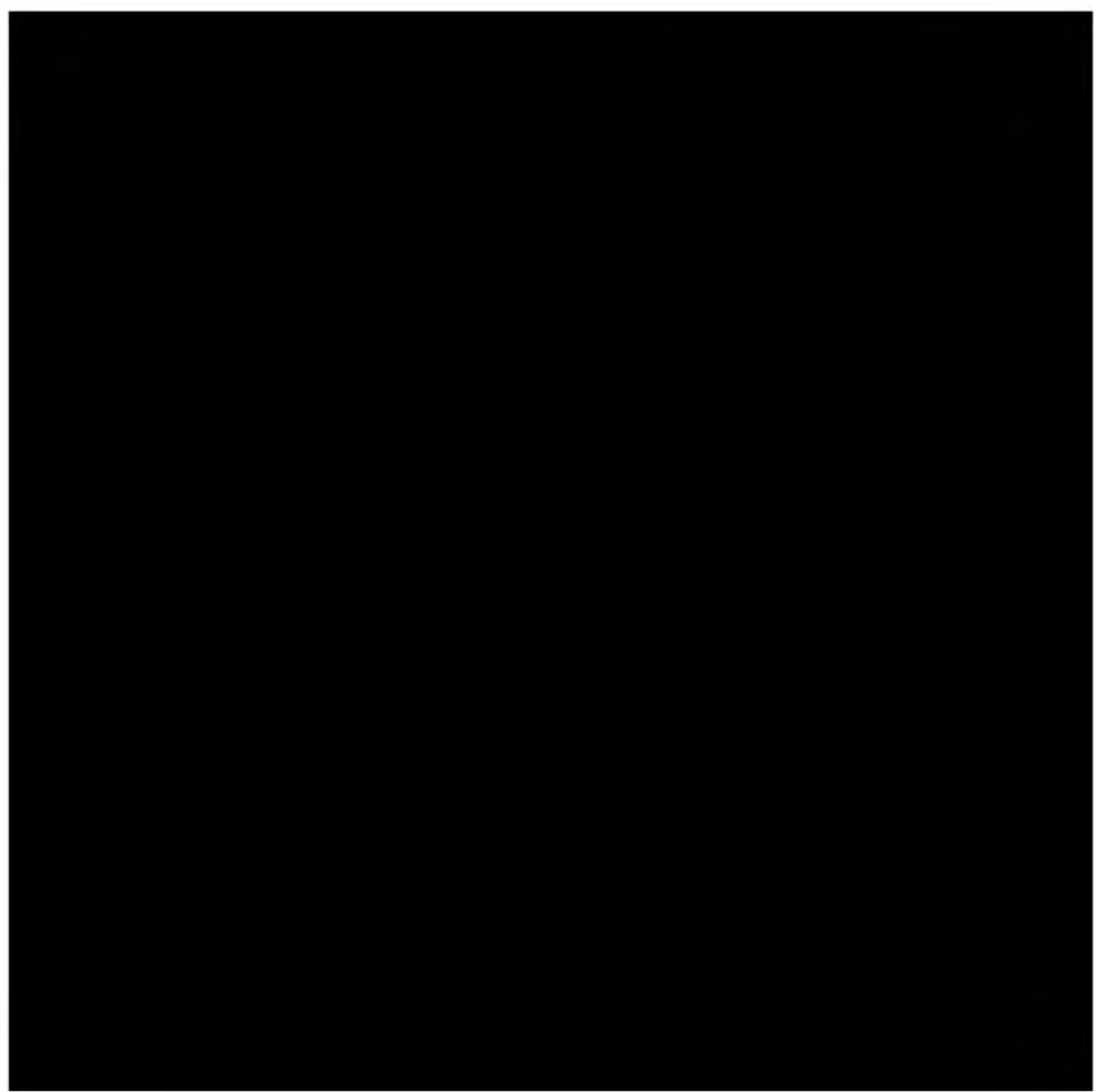


Figure 2.1-2. Location map of California modified from (Beyer, 1988) & (Sullivan, 2012). The Sacramento Basin regional study area is outlined by a dashed black line. B – Bakersfield; F – Fresno; R – Redding.



Figure 2.1-3. Migrational position of the Mendocino triple junction (Connection point of the Gorda, North American and Pacific plates) on the west and migrational position of Sierran arc volcanism in the east (Graham, 1984). Figure indicates space-time relations of major continental-margin tectonic events in California during Miocene.



Figure 2.1-4. Schematic W-E cross-section of California, highlighting the Sacramento Basin, as a continental margin during late Mesozoic. The oceanic Farallon plate was forced below the west coast of the North American continental plate.

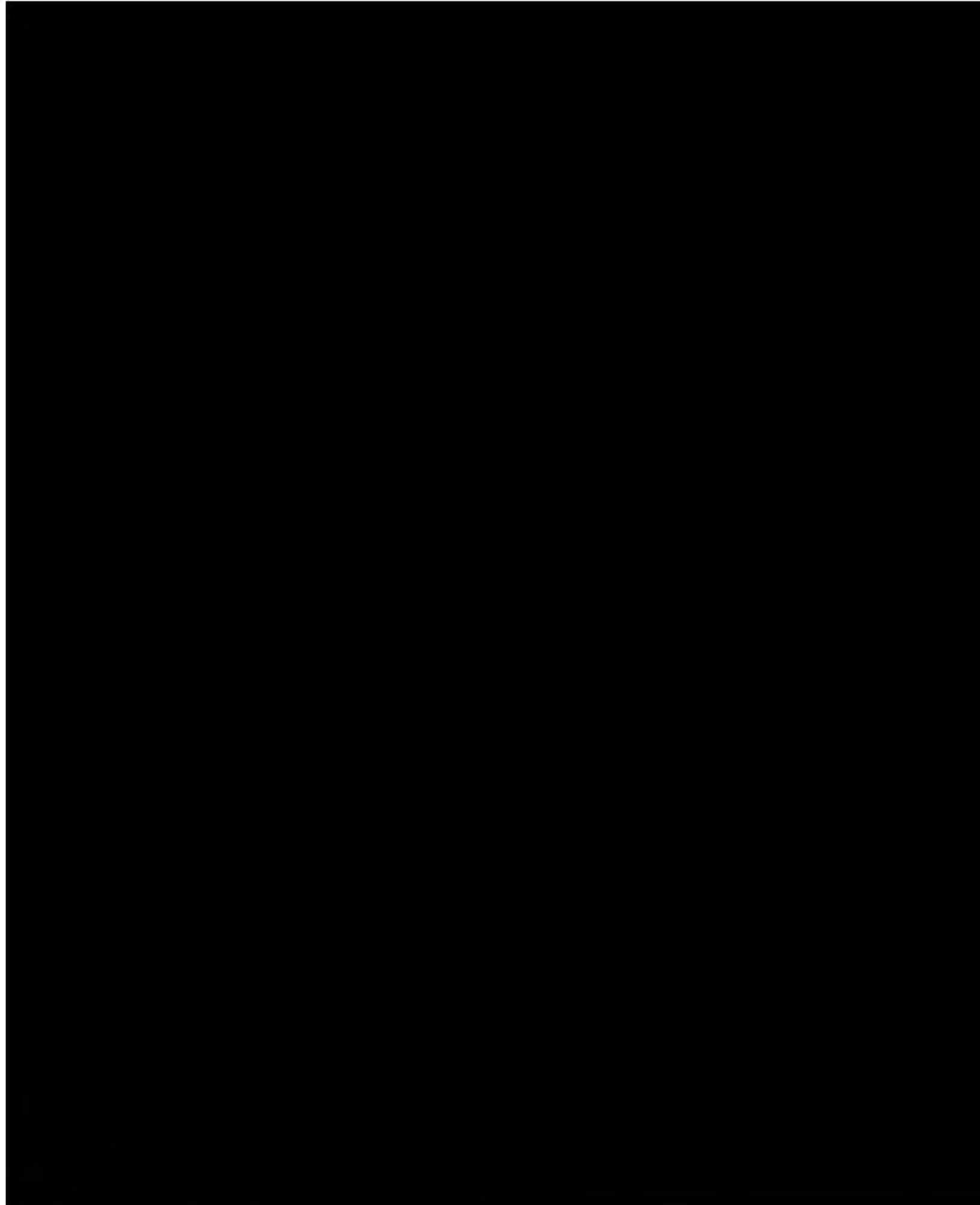


Figure 2.1-5. Evolutionary stages showing the history of the arc-trench system of California from Jurassic (A) to Neogene (E) (modified from Beyer, 1988).

Figure 2.1-6. Schematic northwest to southeast cross section in the Sacramento basin.

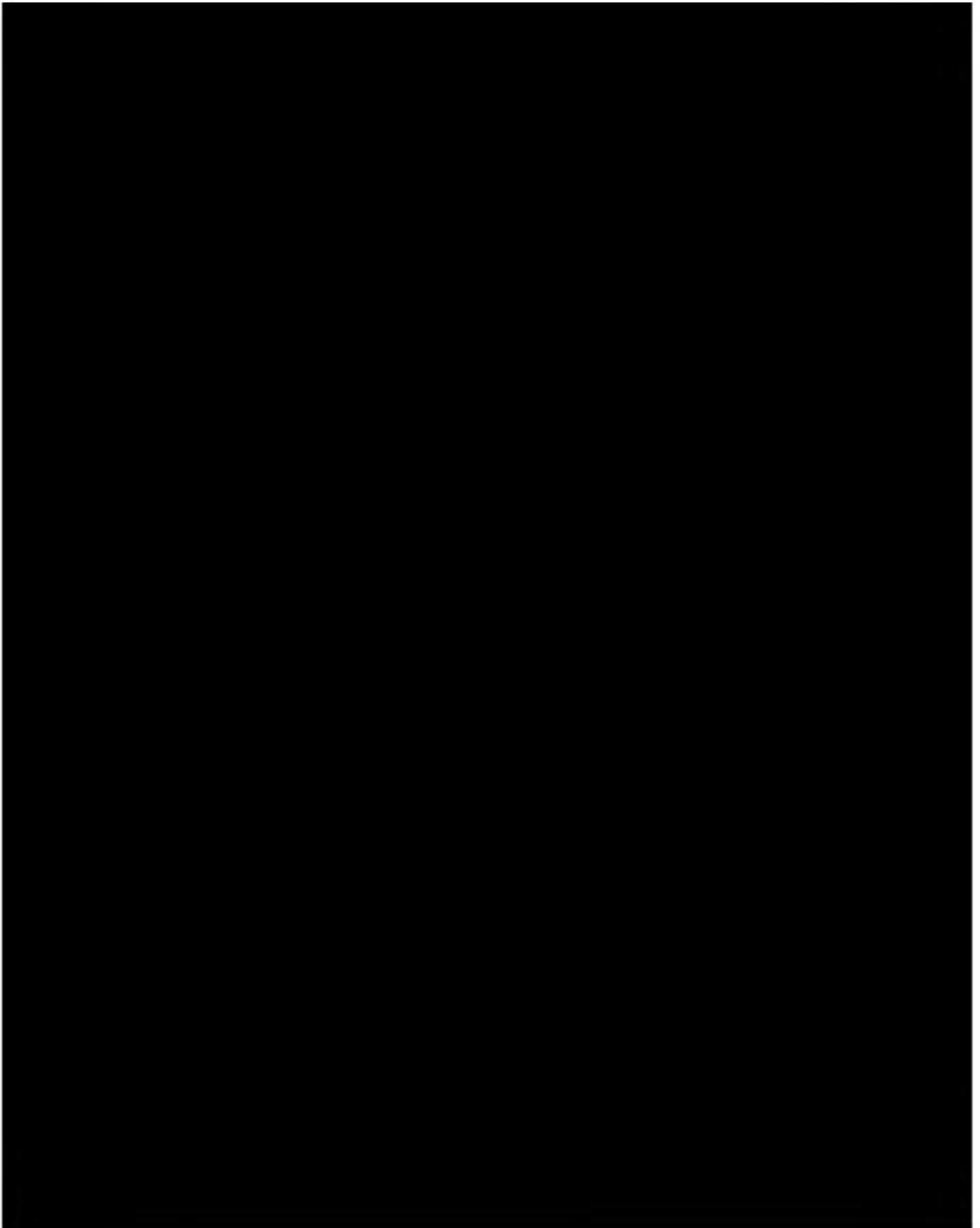


Figure 2.2-7 Surface Features and the AoR

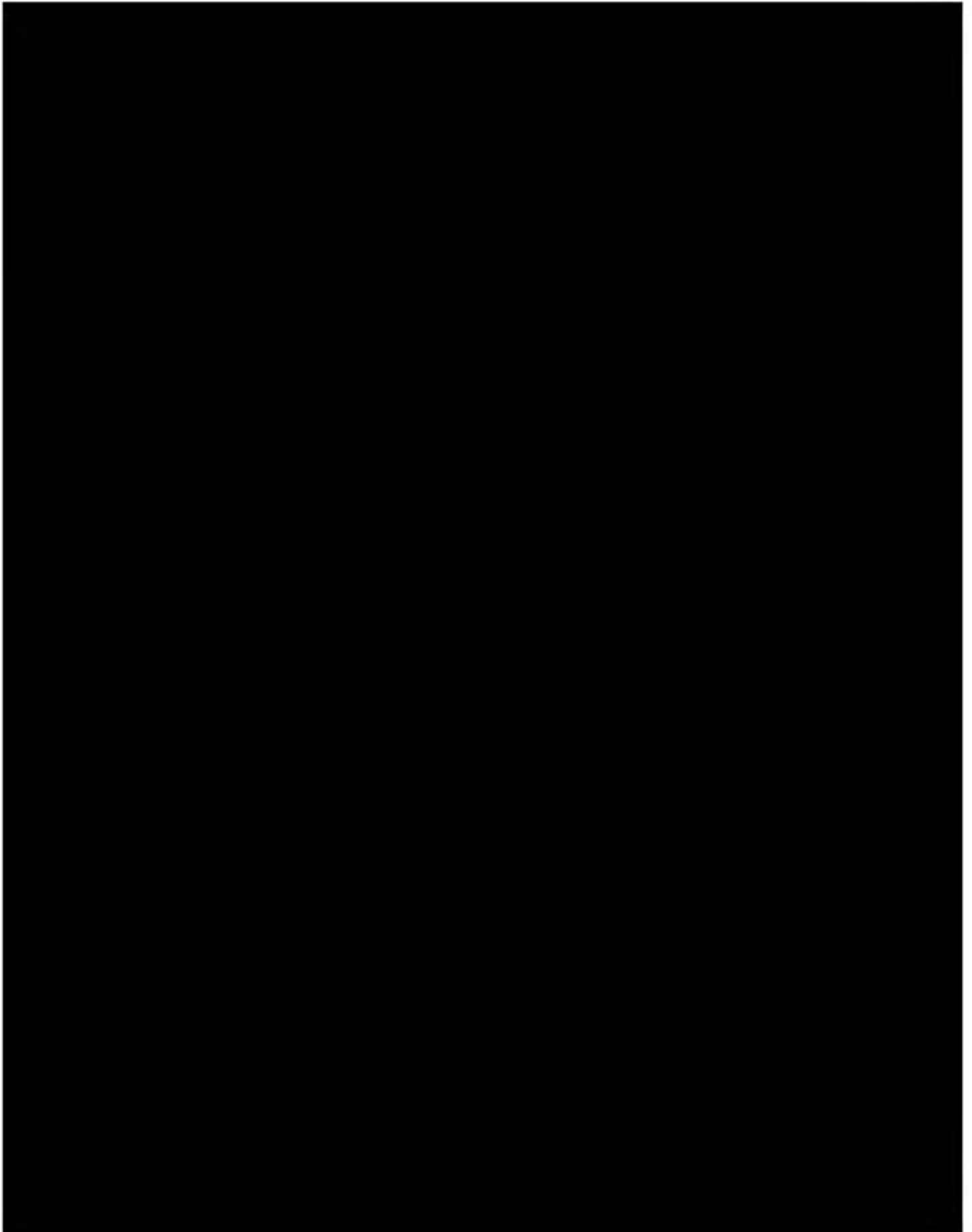


Figure 2.2-8 State and EPA approved Cleanup Sites

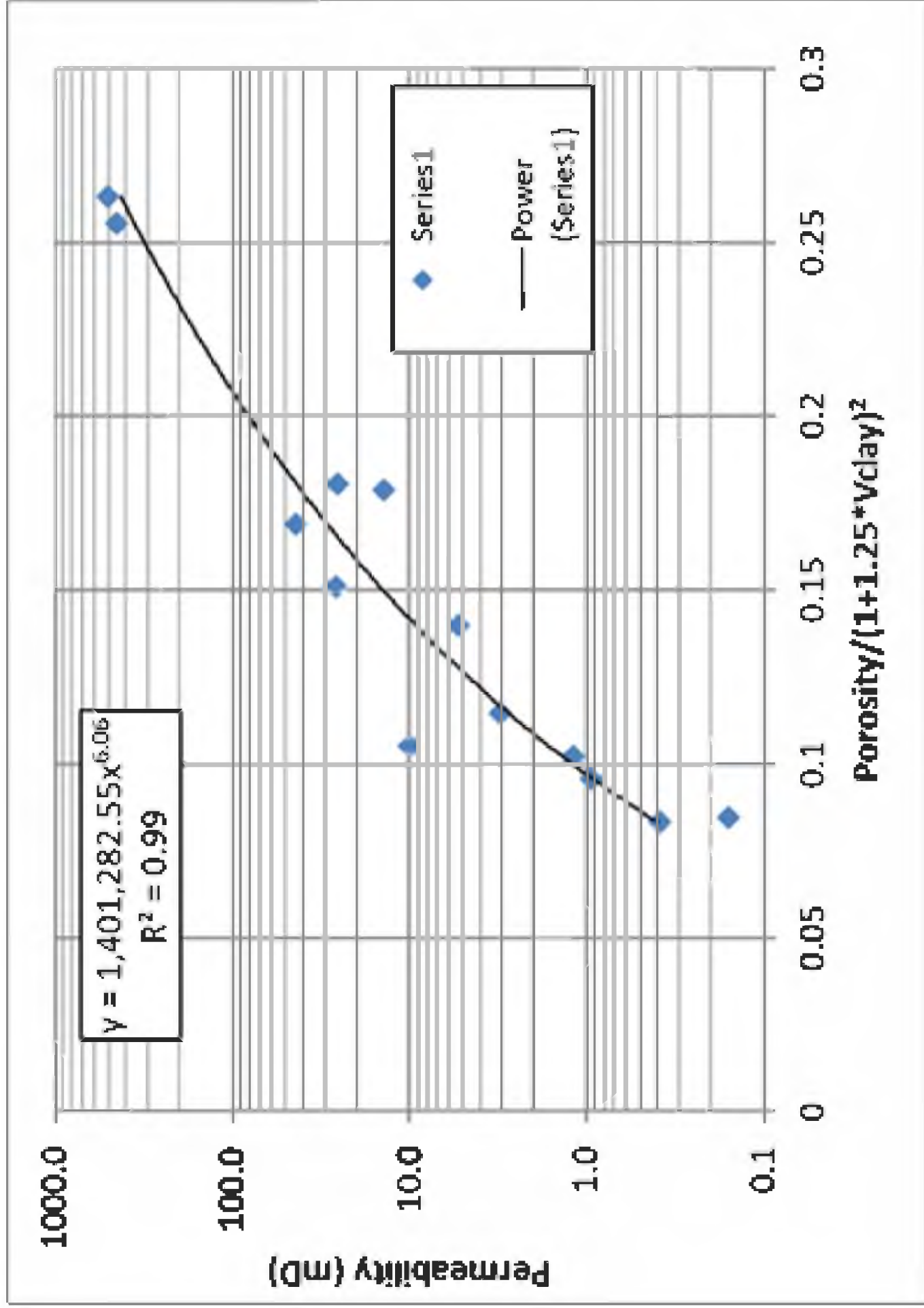


Figure 2.4-2. Permeability transform for Sacramento basin zones.

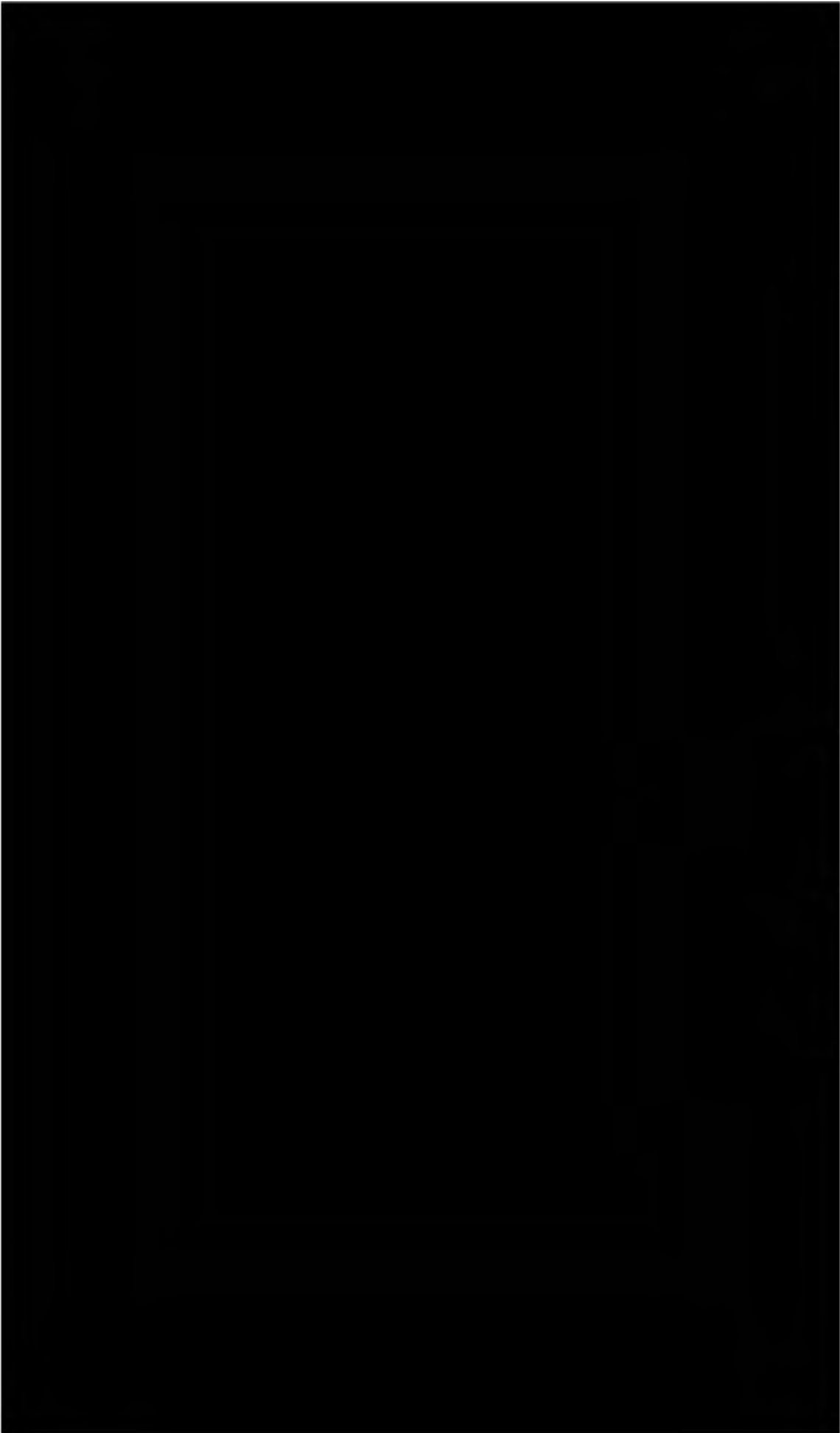


Figure 2.4-3. Porosity histogram for well [REDACTED]. In the histogram, [REDACTED]

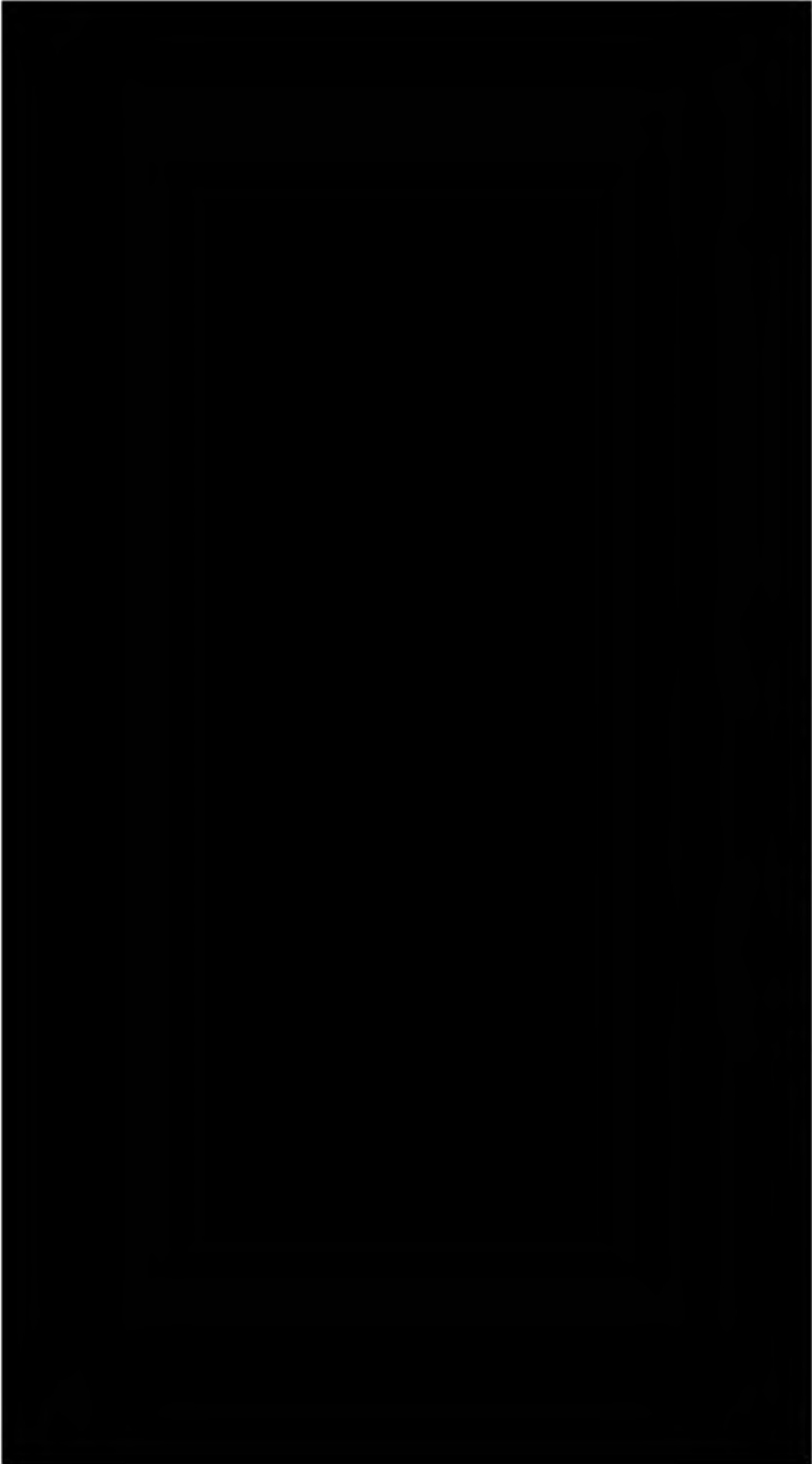


Figure 2.4-4. Permeability histogram for well [REDACTED]. In the histogram, [REDACTED]

[REDACTED]

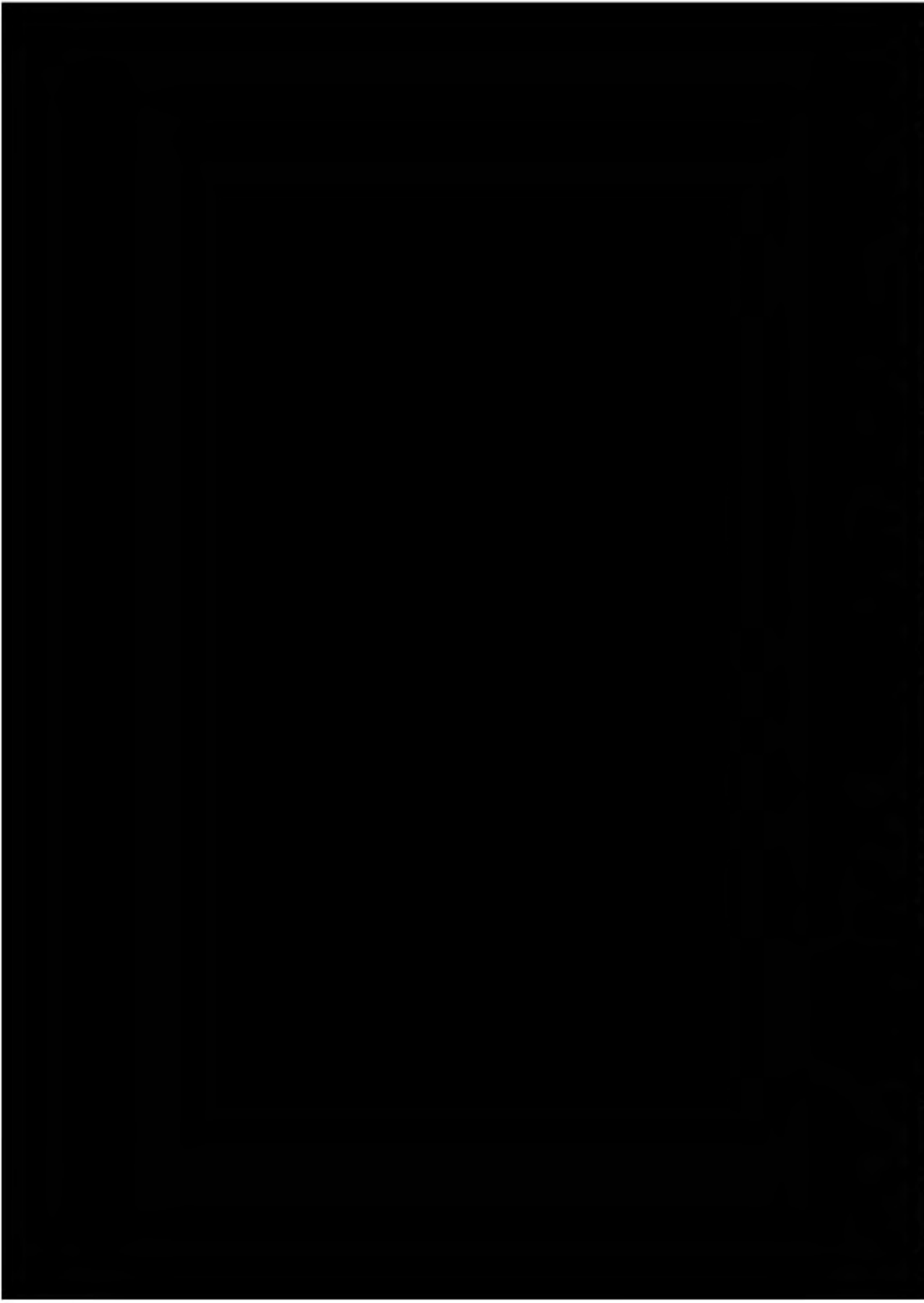


Figure 2.4-5. Log plot for well 2.4-5, showing the log curves used as inputs into calculations of day volume, porosity and permeability, and their outputs. Core data for porosity and permeability is shown for comparison to the log model. Track 1: Correlation and caliper logs. Track 2: Measured depth. Track 3: Vertical depth and vertical subsea depth. Track 4: Zones. Track 5: Resistivity. Track 6: Compressional sonic and density logs. Track 7: Volume of clay. Track 8: Porosity calculated from log curves and core porosity. Track 9: Permeability calculated using transform and core permeability.

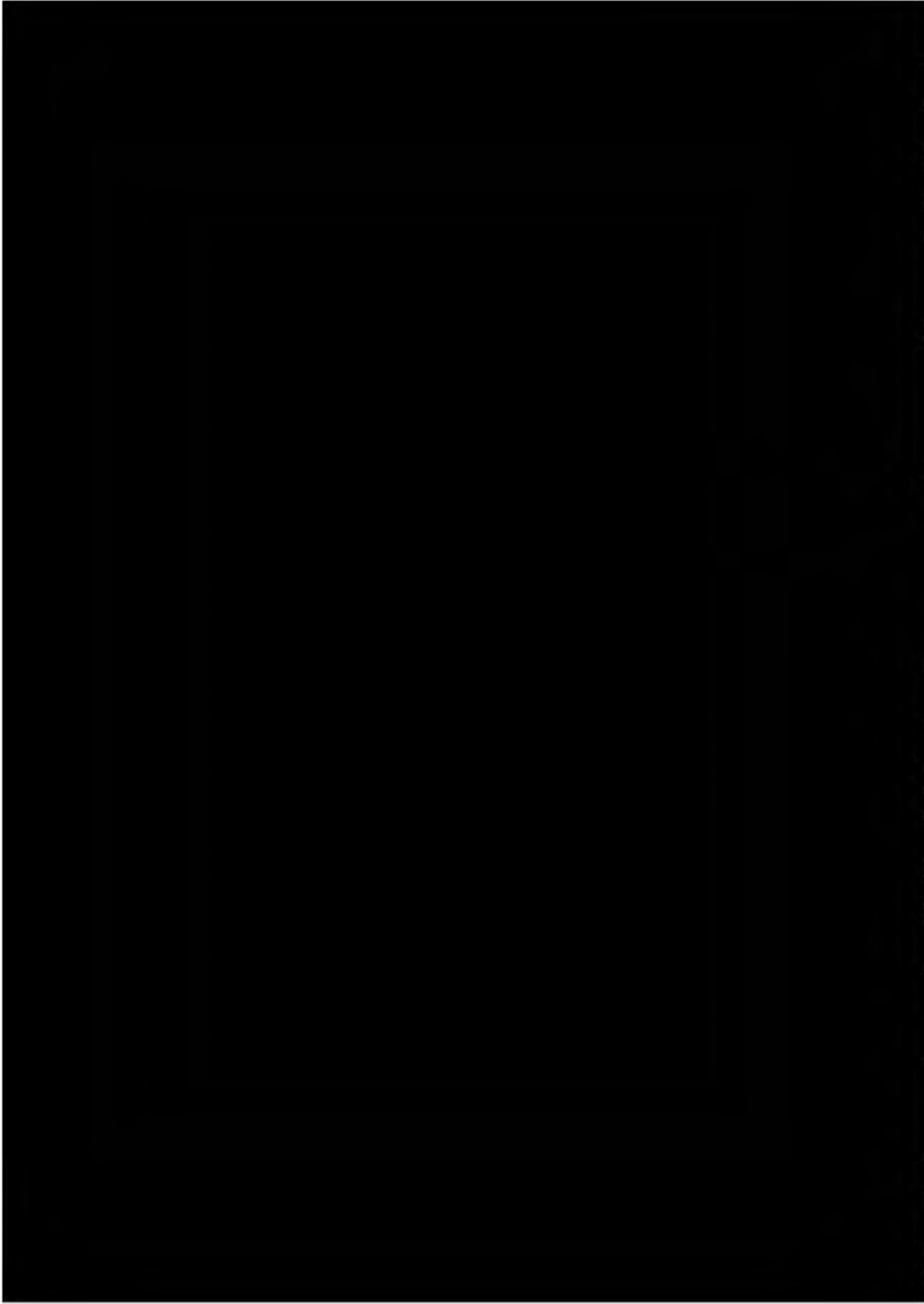


Figure 2.5-1: Unconfined compressive strength and ductility calculations for well [REDACTED]. The upper confining zone ductility is less than two, as are most of the [REDACTED]. Track 1: Correlation logs. Track 2: Measured depth. Track 3: Vertical depth and vertical subsea depth. Track 4: Zones. Track 5: Resistivity. Track 6: Density log. Track 7: Density and compressional sonic logs. Track 8: Volume of clay. Track 9: Porosity calculated from sonic and density. Track 10: Water saturation. Track 11: Permeability. Track 12: Caliper. Track 13: Overburden pressure and hydrostatic pore pressure. Track 14: UCS and UCS_NC. Track 15: Brittleness.

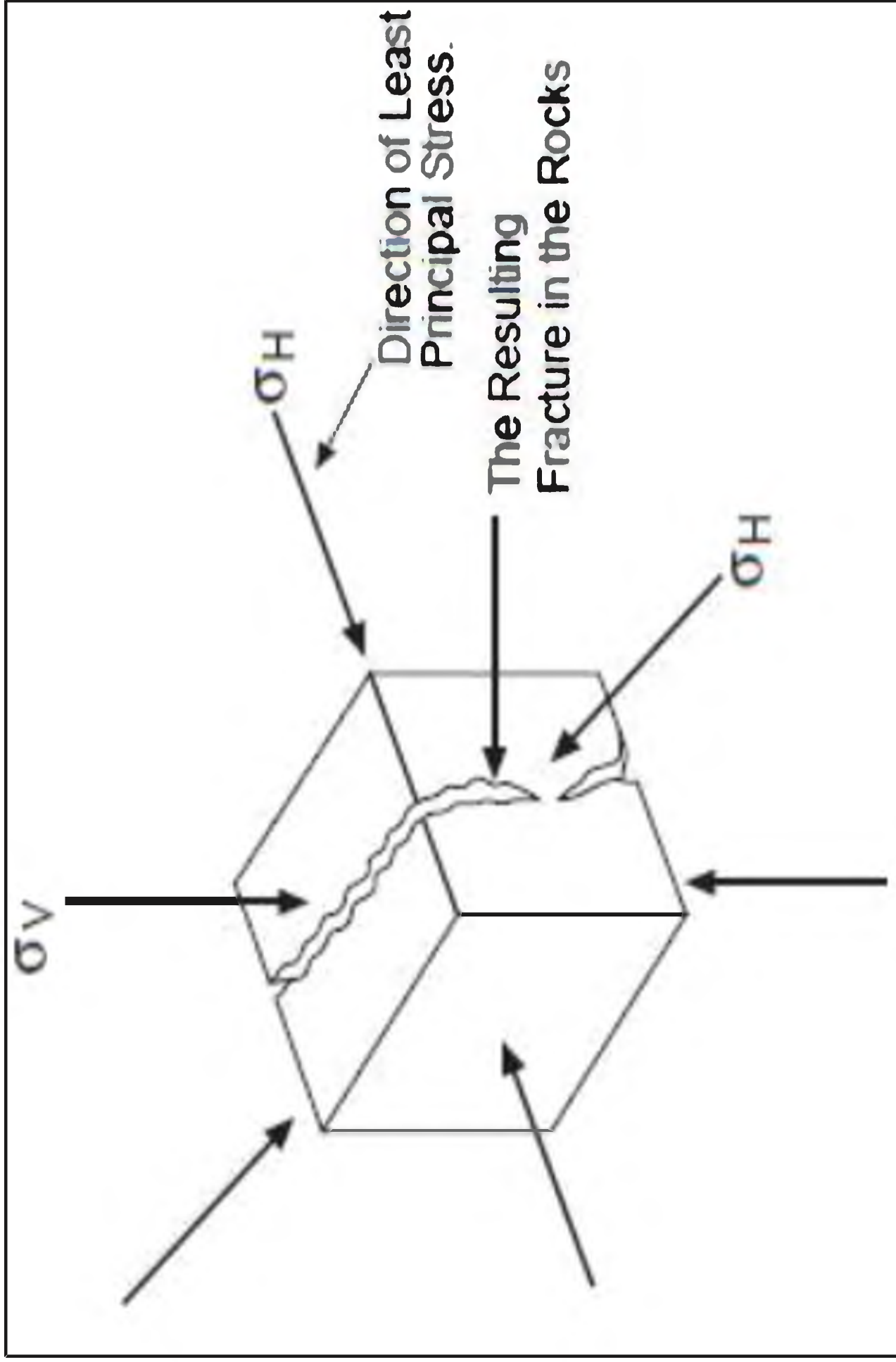


Figure 2.5-2: Stress diagram showing the three principal stresses and the fracturing that will occur perpendicular to the minimum principal stress.

[REDACTED]

[REDACTED]

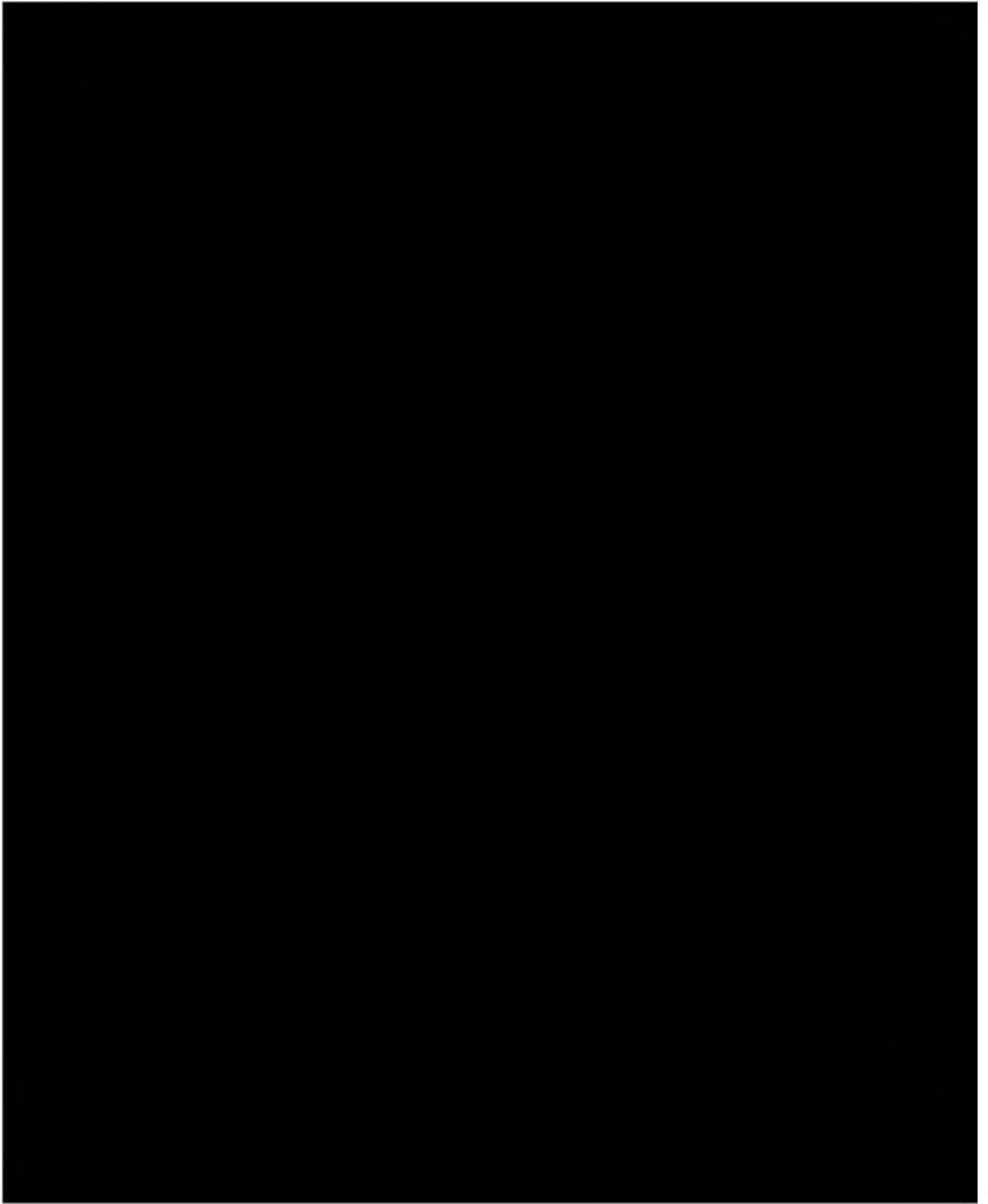


Figure 2.5-4: Location of wells with FIT data.

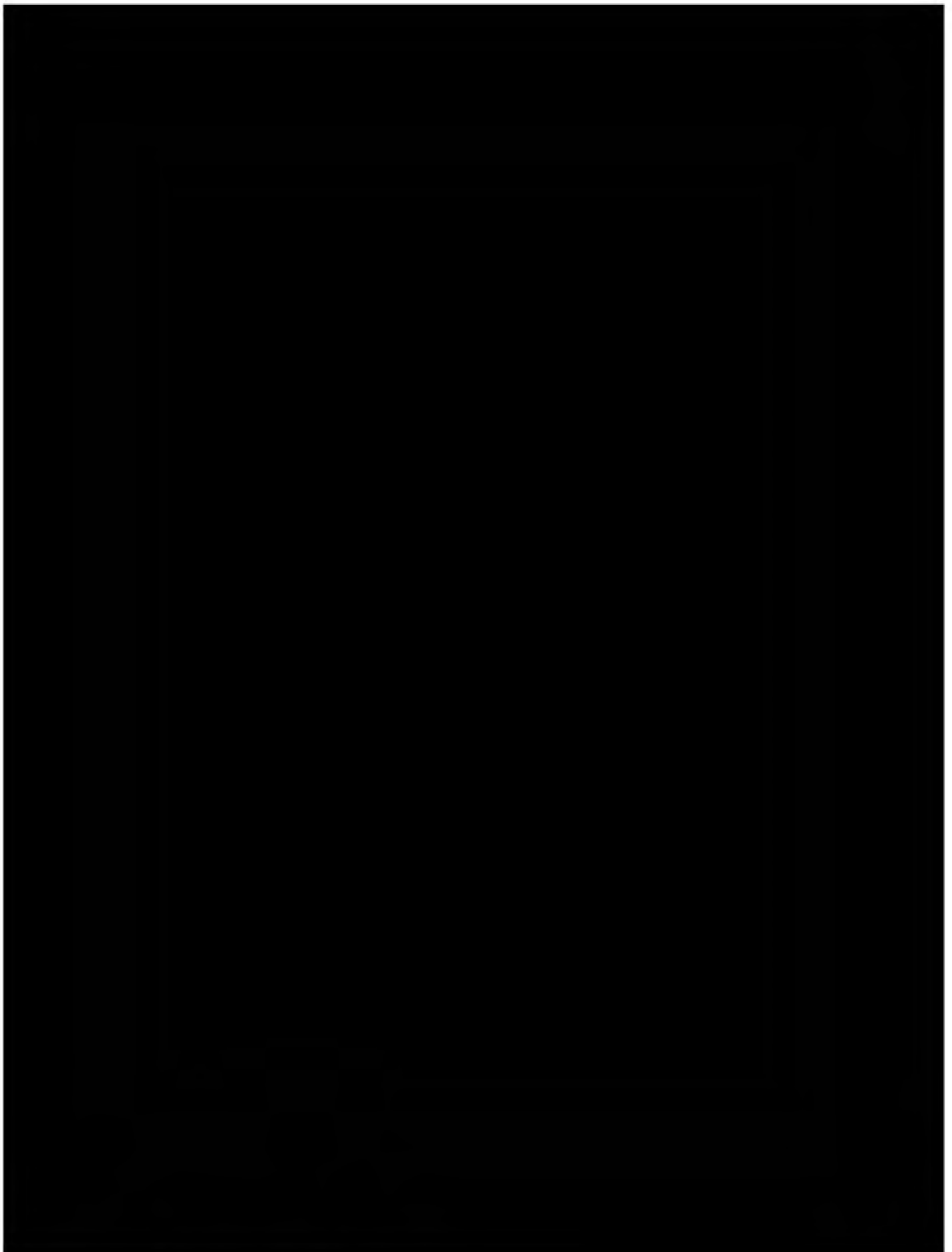


Figure 2.7-1 [REDACTED] Surface Geology, and Cross Section Index Map

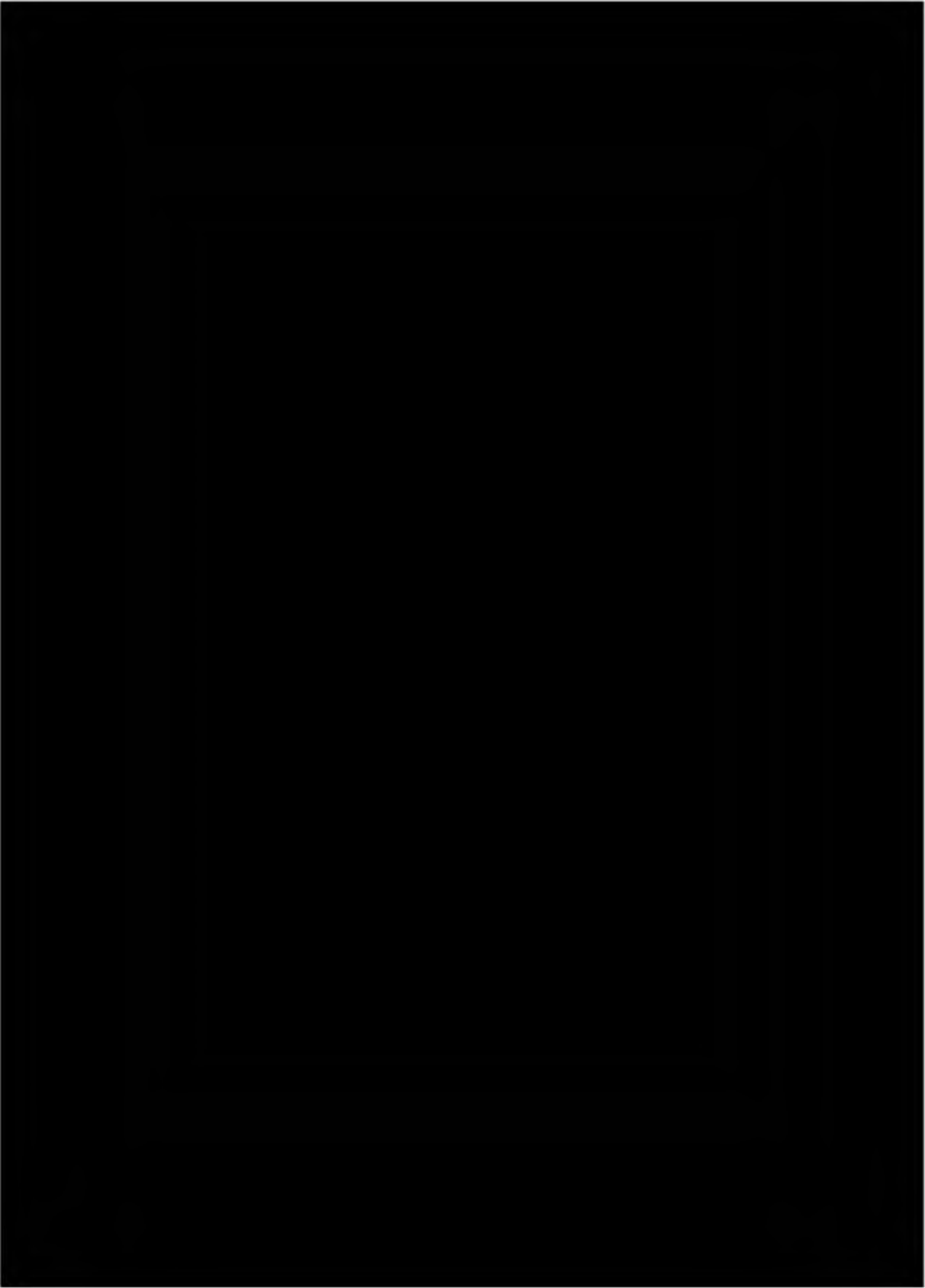
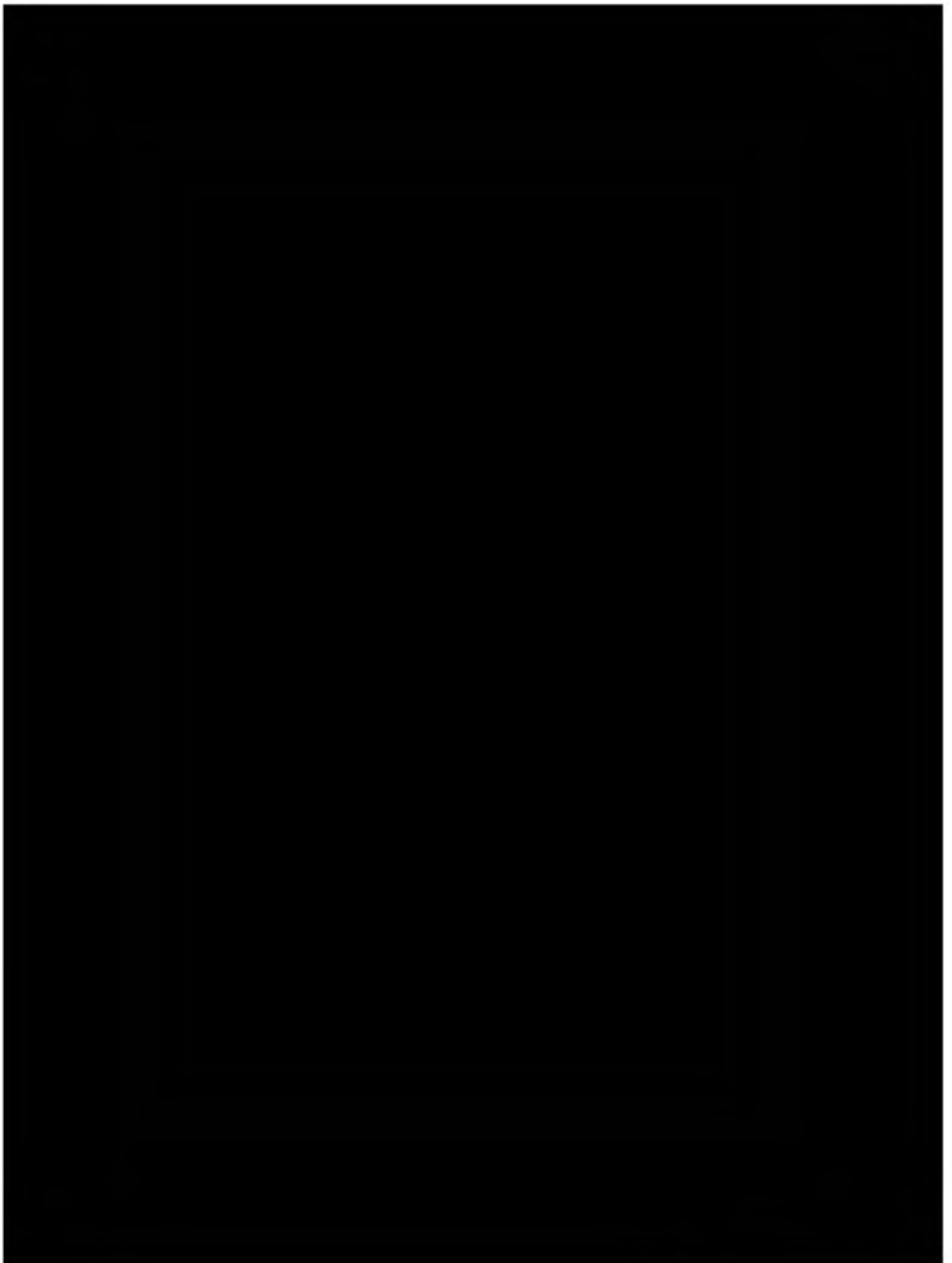


Figure 2.7-2 Geologic Map and Base of Fresh Water



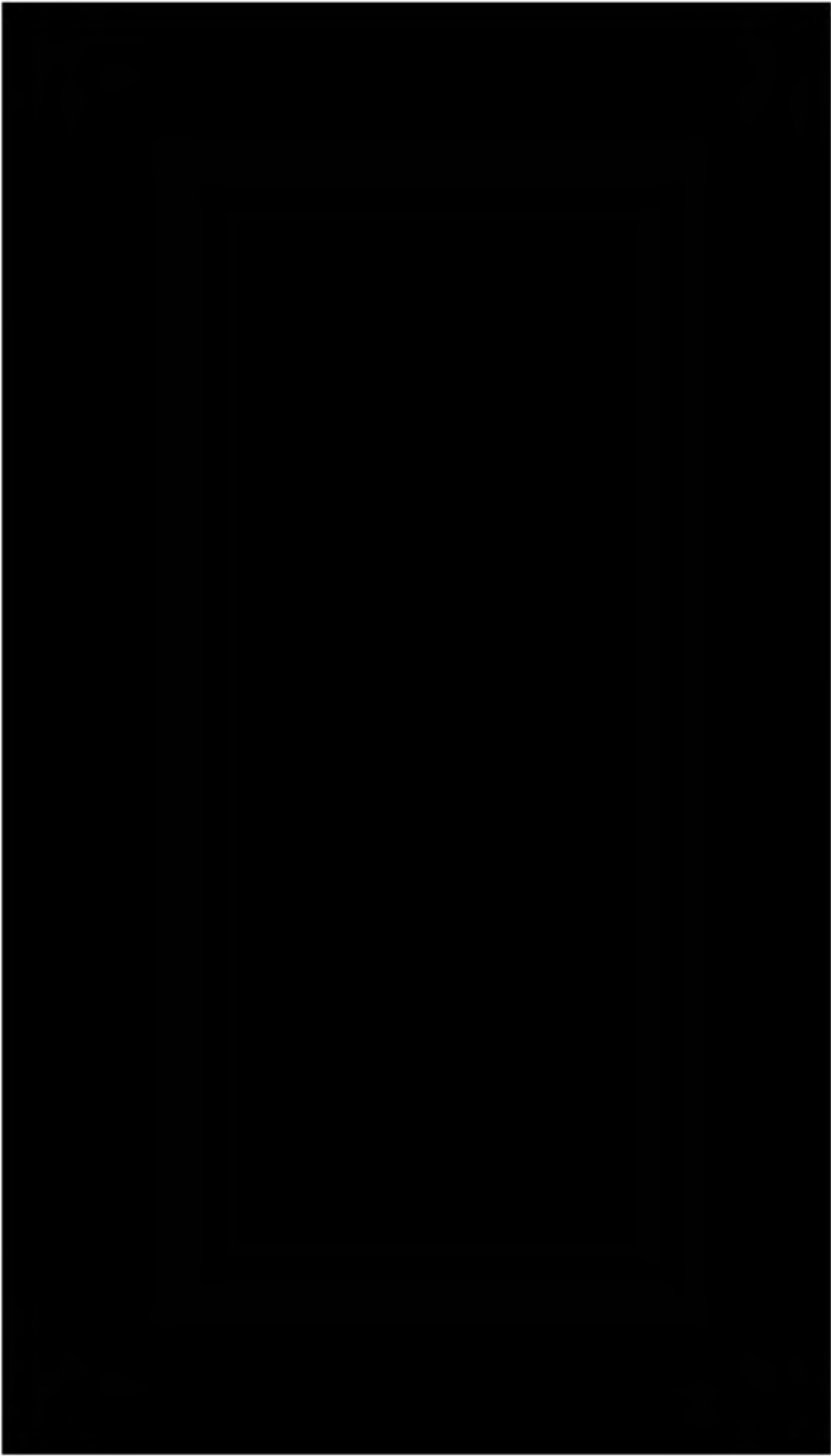


Figure 2.7-4 Geologic Cross Section B-B'

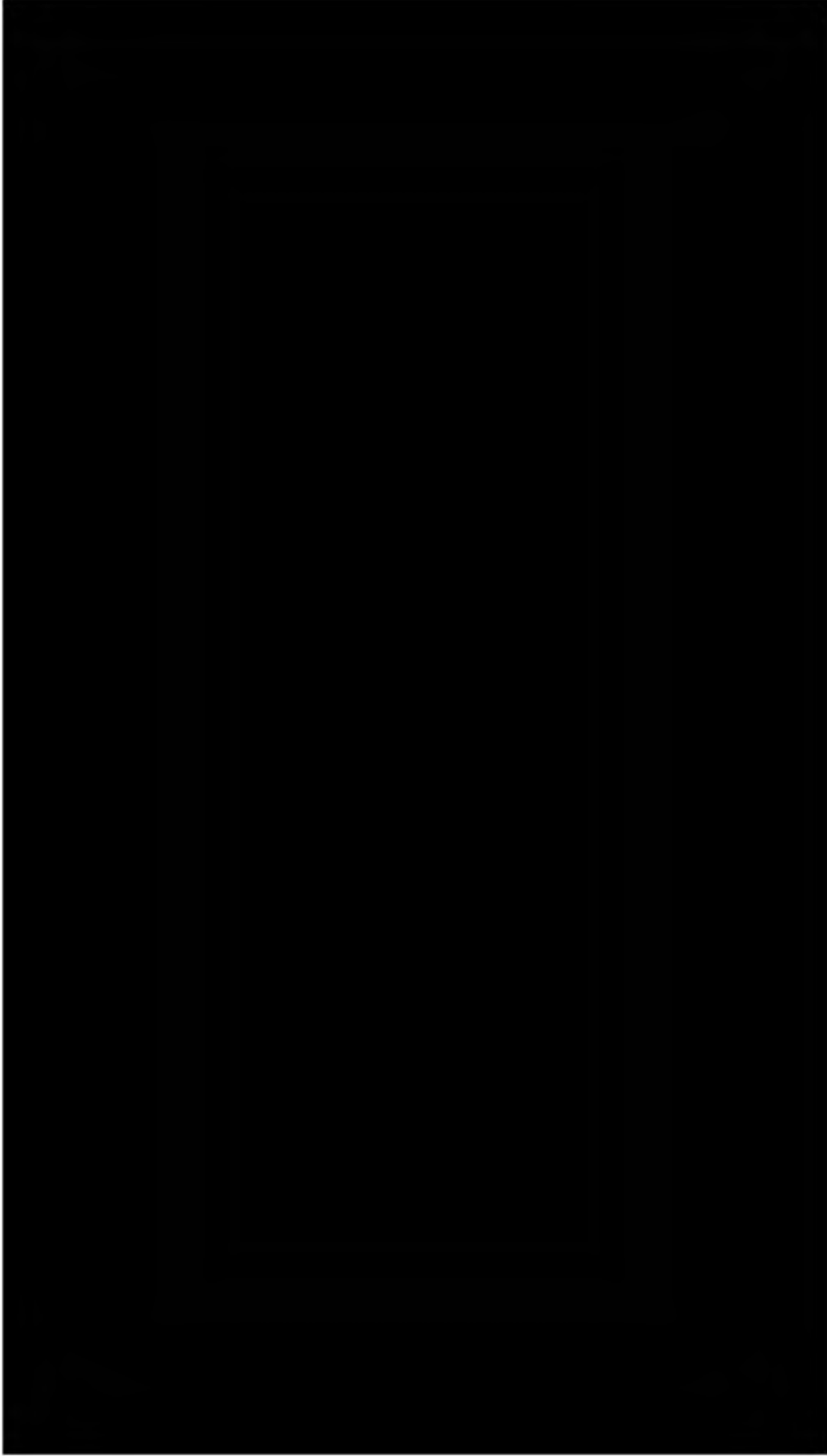


Figure 2.7-5 Geologic Cross Section C- C'

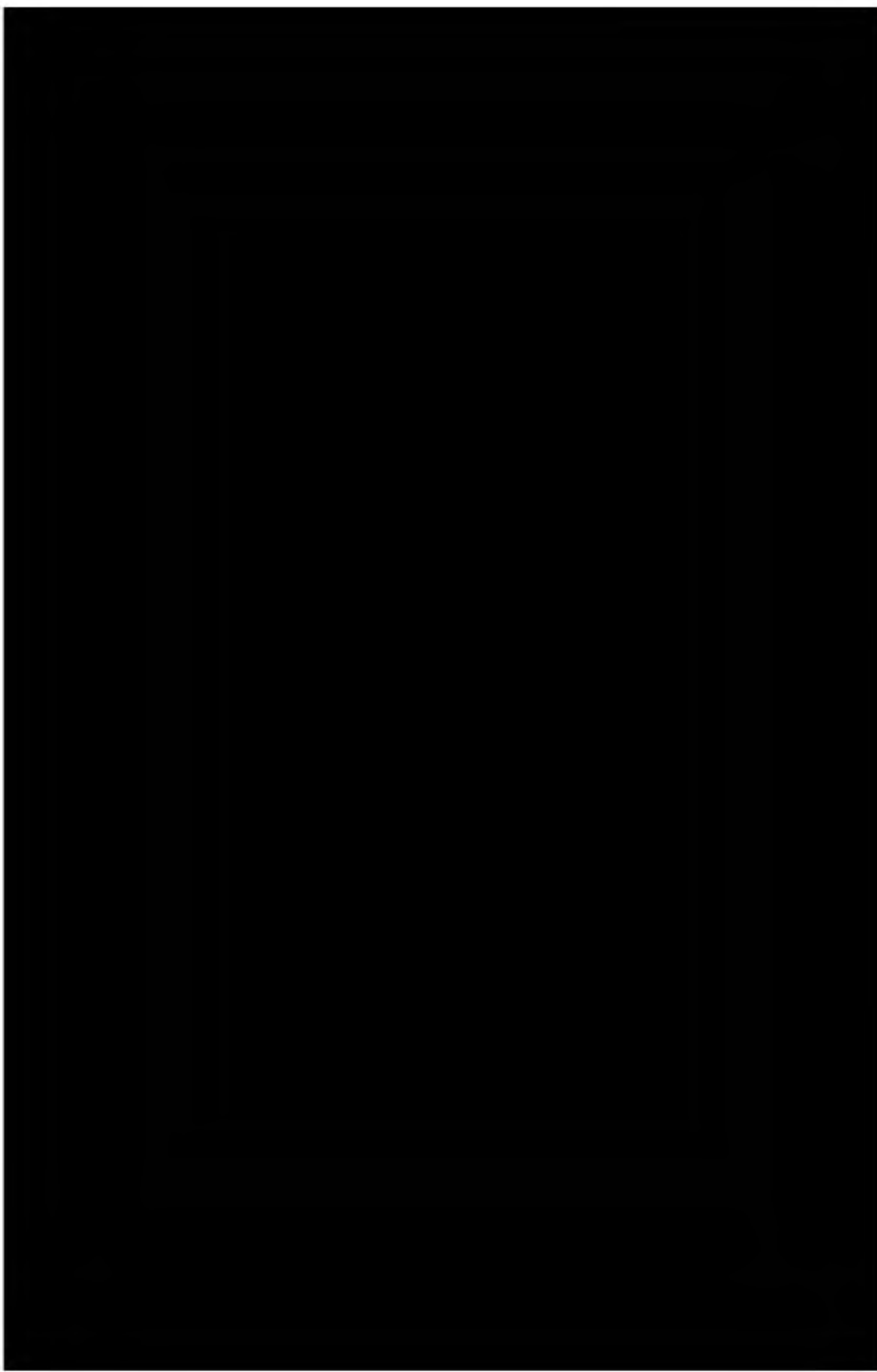


Figure 2.7-6 Principal Aquifer Schematic Profile

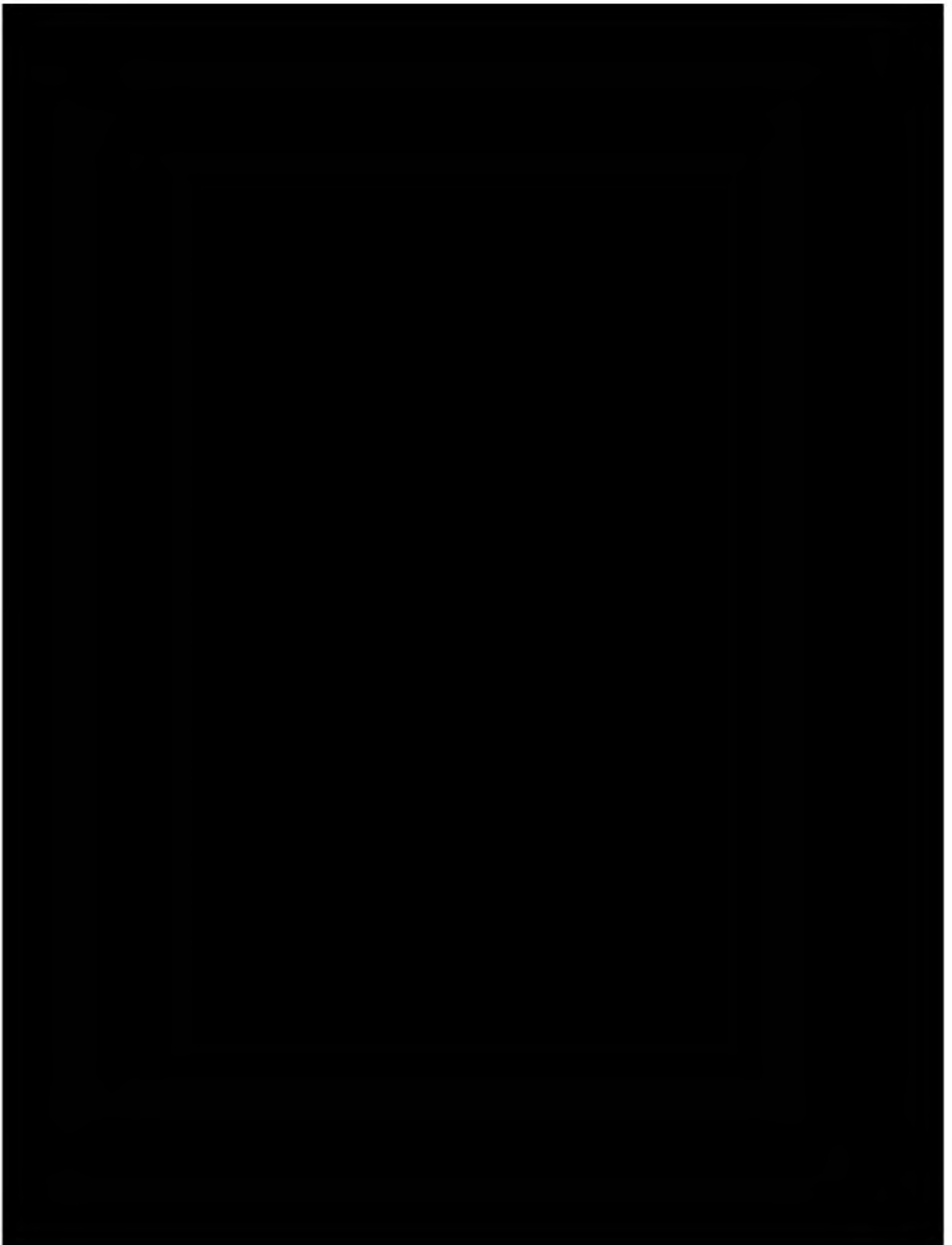


Figure 2.7-7 Upper Aquifer Groundwater Elevation- Fall 2019

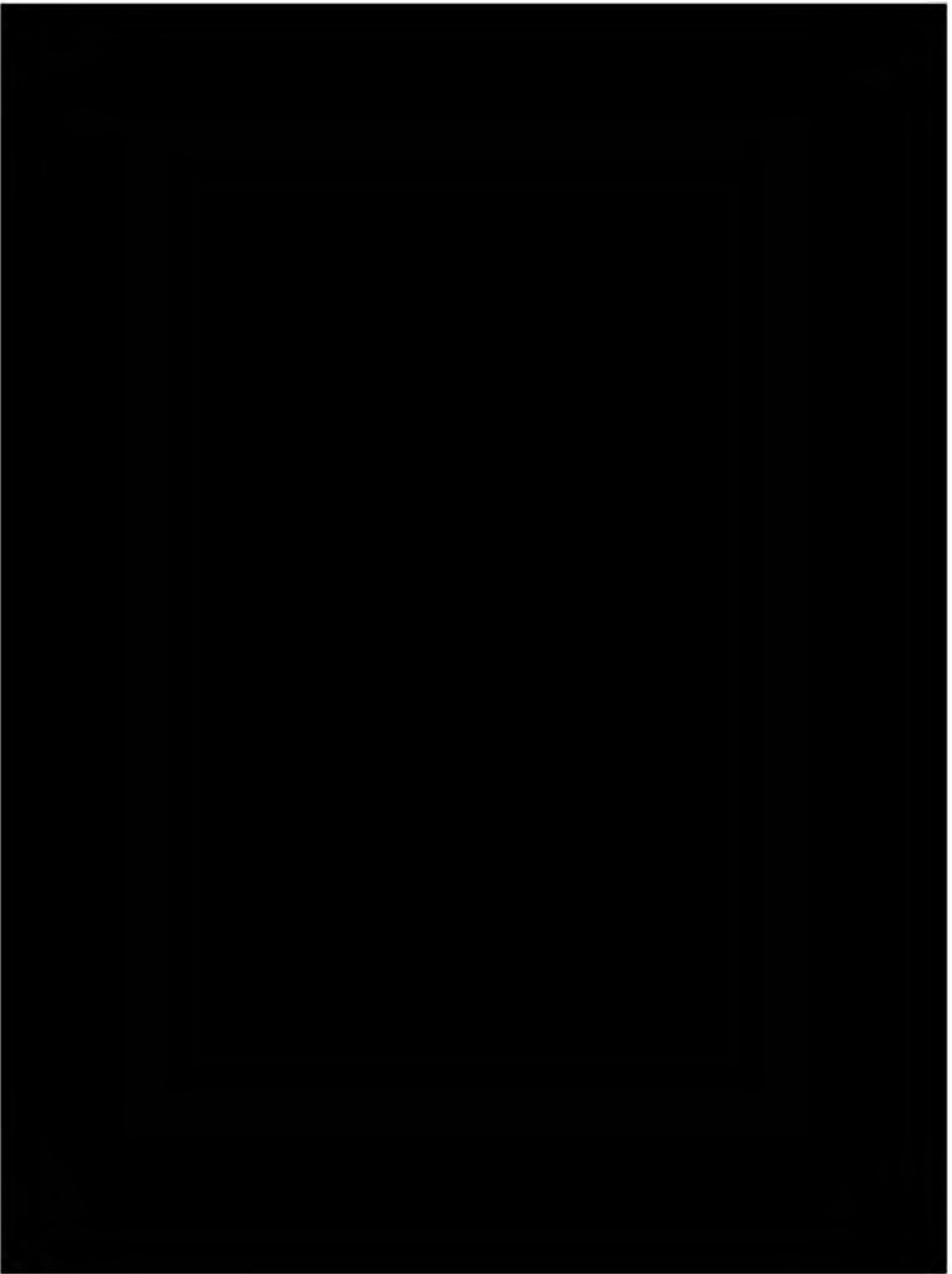


Figure 2.7-8 Lower Aquifer Groundwater Elevation- Spring 2019

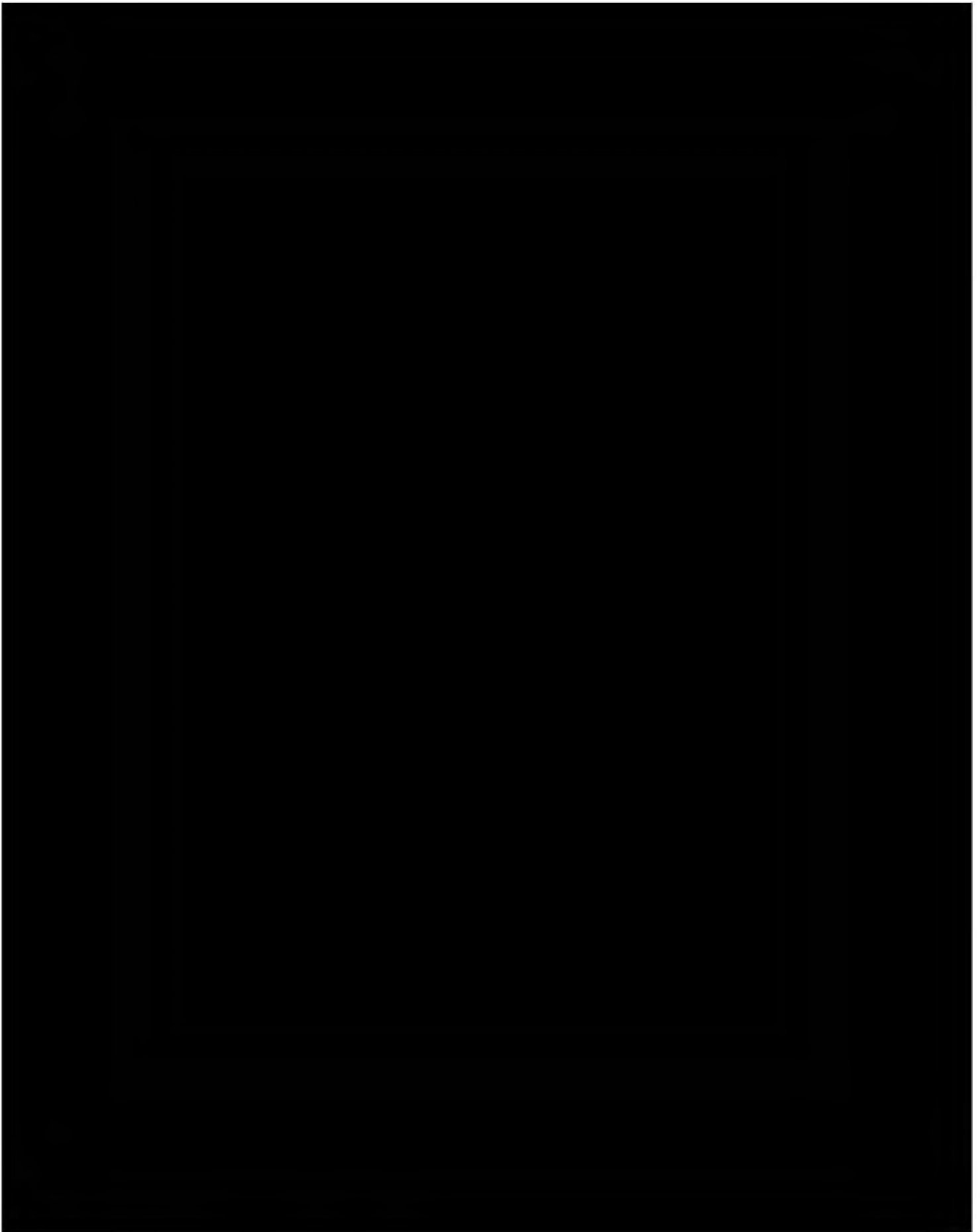


Figure 2.7-9 Water Well Location Map

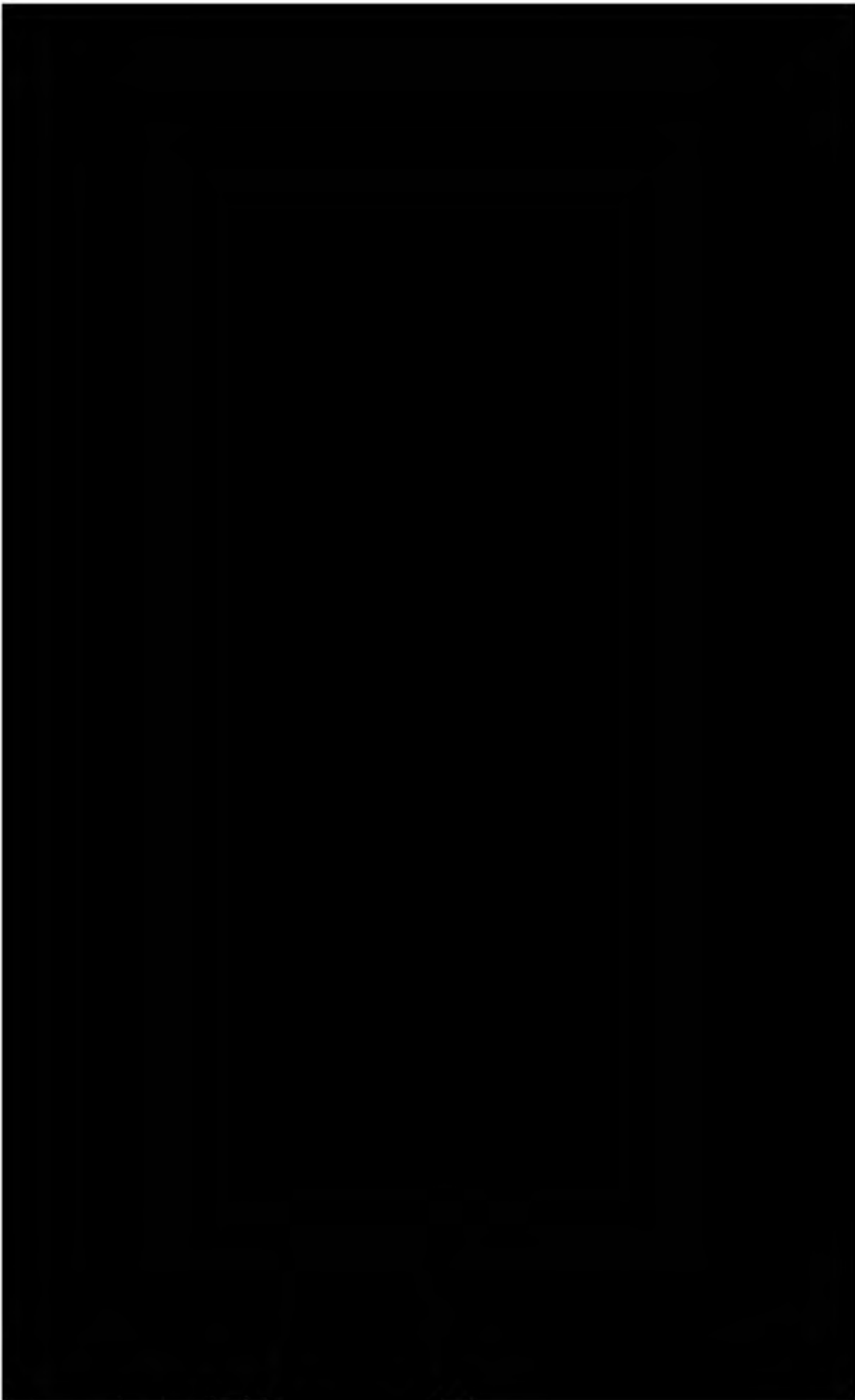


Figure 2.8-1: Water geochemistry for the [redacted] well.

Figure 2.8-2: Gas chromatography for the [REDACTED] well.

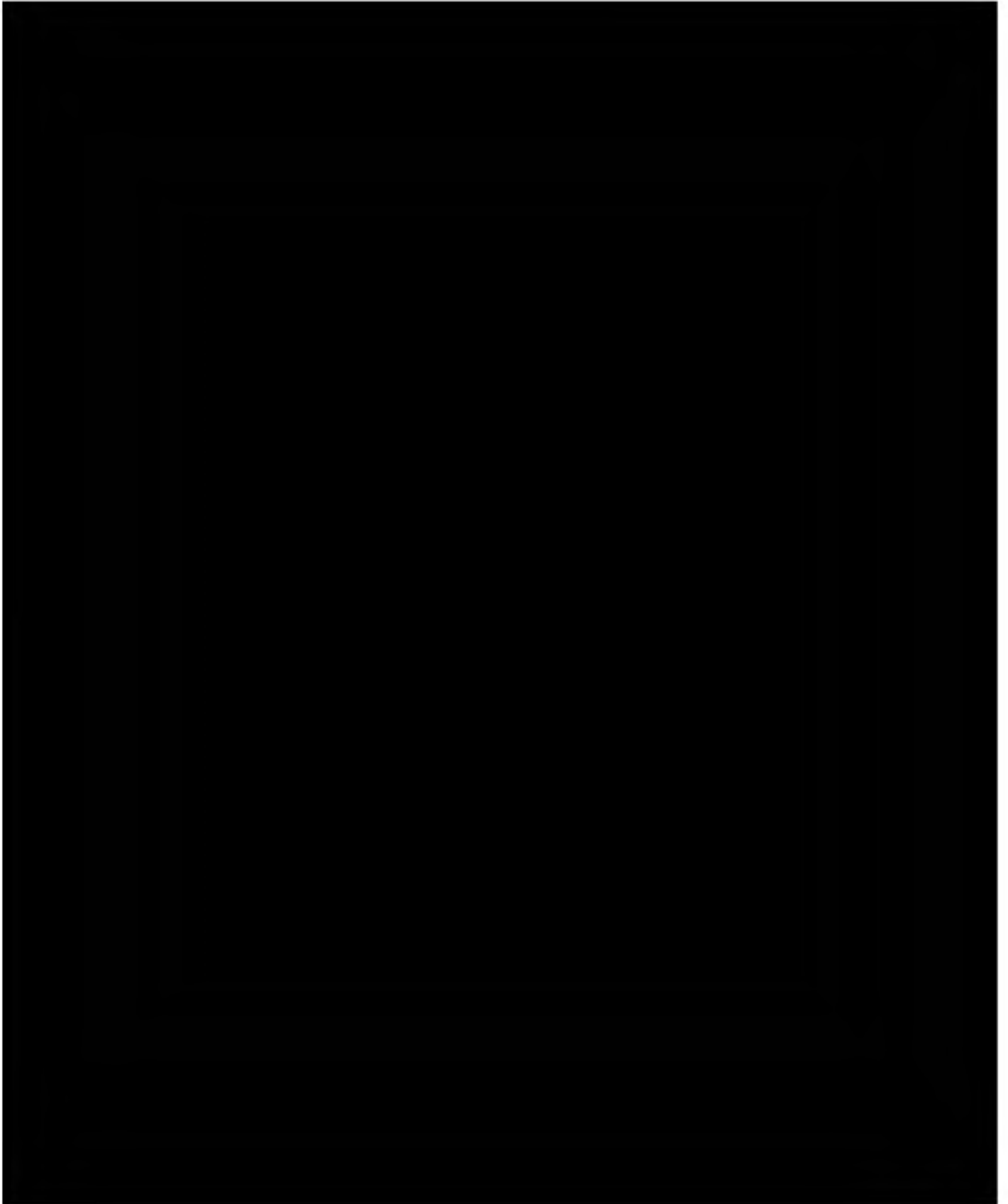


Figure 2.8-3: Location of wells with geochemistry data.

NARRATIVE REPORT - TABLES

Table 2.4-1: Formation mineralogy from X-ray diffraction in [REDACTED] and XRD and Fourier transform infrared spectroscopy (FTIR) in the [REDACTED] well.

[REDACTED]	
------------	--

Table 2.4-2: [REDACTED] gross thickness and depth within the AoR.

Zone	Property	Low	High	Mean
Upper Confining Zone [REDACTED]	Thickness (feet)	2,158	2,322	2,243
	Depth (feet TVD)	7,208	7,788	7,456
Reservoir [REDACTED]	Thickness (feet)	120	365	256
	Depth (feet TVD)	9,482	9,994	9,727

Table 2.6-1: Data from USGS earthquake catalog for faults in the region of CTV II.



Table 2.7-1- Water Supply Well Information

[REDACTED]	
------------	--